

**UCSF**

**UC San Francisco Electronic Theses and Dissertations**

**Title**

Therapeutic availability of a liposome encapsulated drug

**Permalink**

<https://escholarship.org/uc/item/9967k9qf>

**Author**

Raeder-Schikorr, Meggi,

**Publication Date**

1984

Peer reviewed|Thesis/dissertation

THERAPEUTIC AVAILABILITY OF A LIPOSOME ENCAPSULATED DRUG

by

MEGGI RAEDER-SCHIKORR  
PHARM.D., LUDWIG-MAXIMILIAN UNIVERSITÄT  
MÜNCHEN, W.-GERMANY, 1971

DISSERTATION

Submitted in partial satisfaction of the requirements for the degree of

DOCTOR OF PHILOSOPHY

in

PHARMACEUTICAL CHEMISTRY

in the

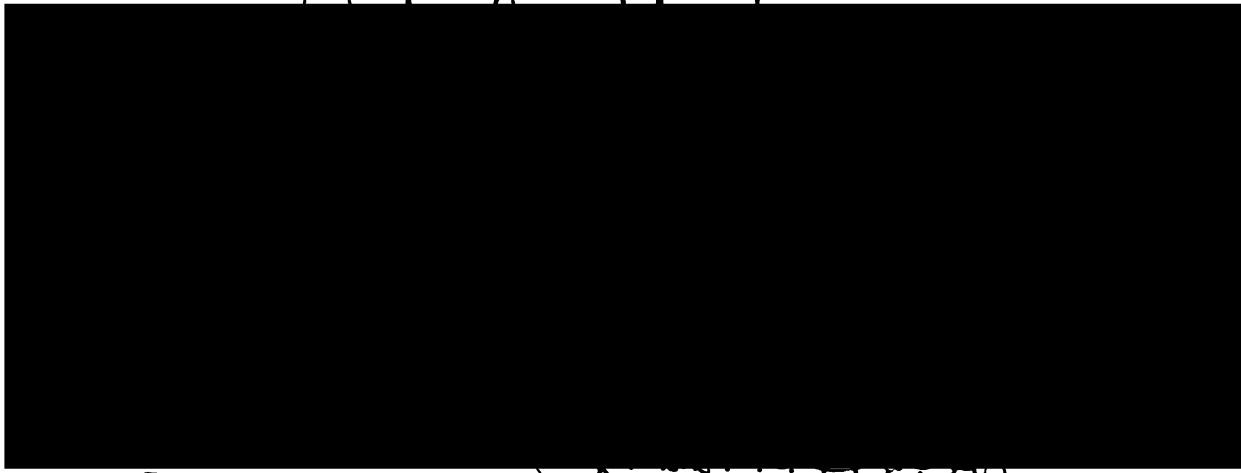
GRADUATE DIVISION

of the

UNIVERSITY OF CALIFORNIA

San Francisco

*[Handwritten signature]*



Date

MAR 25 1984

University Librarian

Degree Conferred: .....



"Wer mit dem Leben spielt  
kommt nie zurecht,  
wer sich nicht selbst befiehlt  
bleibt stets ein Knecht."

Goethe



To Michael

## Acknowledgements

To Professor Dr. Tony Hunt I wish to express my sincere gratitude for his initial recommendation of performing this research project, his constant guidance and continuous encouragement, patience and support, understanding and friendship throughout the course of my graduate work.

Special appreciation is extended to Professor Dr. Frank Scoka for his supportive discussions and his helpful - never failing - advise and reassurance.

I particularly like to recognize Professor Dr. Tom Tozer, who twice took responsibilities on very short notice. His helpful suggestions during the preparation of this thesis are highly appreciated.

The synthetic and analytical part of this investigation was supported by the skillful technical assistance of Diane Cheng which I like to acknowledge here. Thanks is also extended to all members of the Drug Delivery Group (Department of Pharmaceutical Chemistry, UCSF) for sharing the up's and down's commonly occuring in a graduate student's life, and for offering encouragement and friendship.

I wish to extend my appreciation to Dr. Hans Schreier for critically reading the manuscript and for his valuable and constructive suggestions as well as to Dr. G. McCasland for proof-reading the manuscript.

For financial support I am obliged to the University of California for providing Teaching and Research Assistantship, to the National Institute of Health for a stipend from the NIH Training Grant, as well as to the University Patent Fund for partial research funding.

My deepest thanks go to my husband Michael whose confidence and encouragement throughout all those years gave me more support than anything else.

Meggi Raeder-Schikorr  
December 1983

Table of Content

	<u>Page</u>
Acknowledgements	i
List of Figures	vii
List of Tables	ix
List of Abbreviations	xi
Abstract	xii
Chapter I: General Introduction	1
Purpose of this Study	1
Background Information	5
The Fate of Liposomes In Vivo	5
Liposome Interaction with the Physiologic Environment	6
Mechanisms of Liposome-Cell Interaction	8
Phagocytosis	9
Model Drugs in Liposome Research	11
The Experimental Drug: FdUMP	13
Cellular Events Prior to FdUMP-TS Complex Formation	14
Rate-Limiting Steps During FdUMP-TS Formation	18
The Liver	20
The Reticuloendothelial System (RES)	25
Organization of this Thesis	29

Chapter II: Evaluation of Thymidylate Synthetase in Non-Proliferating Mammalian Tissue	30
Introduction	30
Thymidylate Synthetase in Proliferating Tissue	31
Fluorinated Pyrimidines and Their Nucleotides	33
Mechanism of Thymidylate Synthetase Inhibition	35
Molecular Nature of the Covalent FdUMP- Cofactor-Enzyme Bonds	38
Thymidylate Synthetase in Rodent Tissue	39
Materials and Methods	41
Buffers and Solutions	41
Formation and Isolation of FdUMP-TS Complex	41
Preparation of Tissue Homogenates	42
Gel Exclusion Chromatography	43
Identification of FdUMP-TS	43
Molecular Weight Determination of FdUMP-TS	43
Dissociation Kinetics	44
In Vivo Quantitation of Thymidylate Synthetase	45
Radiopurity of <sup>3</sup> H-FdUMP	45
Measurements of Radioactive Markers	45
Results	47
Evaluation of the Cellularity of Rat Liver and Spleen Tissue	47
In Vitro Estimation of Thymidylate Synthetase	48
Evaluation of TS in the Rat Liver	49
Evaluation of TS Level in Isolated Liver Cells	55
Evaluation of TS in the Spleen	56

Molecular Weight Determination of FdUMP-TS Complex	56
Dissociation Kinetics	59
Comparison of the Amount of Enzyme Complex Formed In Vitro and In Vivo	59
Radiopurity of $^3\text{H}$ -FdUMP	63
Discussion	67
Chapter III: Cellular Availability of a Liposome Encapsulated Drug to Liver and Spleen	69
Introduction	69
Materials and Methods	71
Preparation of Liposomes	71
Dialysis	72
Column Chromatography	72
Quantitation of Lipid	73
Liposome Stability During Storage	74
Stability of Liposomes in Rat Plasma	76
FdUMP Stability after Encapsulation and Storage	76
FdUMP Stability in Physiological Fluids	76
In Vivo Experimental Set-Up	77
Identification of Radioactivity Eluting With the Void and the Salt Volume	78
Results	79
Stability of Liposomes	79
Leakage of Encapsulated Markers from Liposomes	79
FdUMP Stability after Encapsulation and Storage	81

FdUMP Stability in Physiologic Fluids	81
Disposition of Single-Labeled Liposomes	82
Disposition of Double-Labeled Liposomes	86
Therapeutic Availability of FdUMP	88
Identity of Non-Enzyme Bound Radioactivity in the Cell Cytosol	92
Presence of Intact Liposomes in the Void Volume	96
Incorporation of Tritiated Radioactivity into RNA	98
Discussion	99
Therapeutic Availability of FdUMP	102
Identity of Low Molecular Weight Radioactivity in the Cytosol	105
Stability of Liposomes	106
Stability of FdUMP in Physiologic Fluids	106
Chapter IV: Interactions of Liposomes with Hepatocytes and Non-Parenchymal Cells	108
Introduction	108
Background Information	109
Materials and Methods	113
Liver Preparation for Perfusion	113
Liver Cell Separation	115
Quantitation of Isolated Cells	116
Results	119
Cell Yield	119
Loss of Radiolabel During Cell Separation	119

Association of Liposome Markers with Hepatocytes and Non-Parenchymal Cells	121
Therapeutic Availability of FdUMP in Hepatocytes and Non-Parenchymal Cells	121
Discussion	128
Dissociation of Radiolabel During the Cell Separation	128
Uptake of Liposomes in Non-parenchymal Cells and Therapeutic Availability of the Drug	129
Liposome Interaction with Hepatocytes and Therapeutic Availability of the Drug	131
Proposed Mechanisms for the Uptake of Liposomes Encapsulated Material into Hepatocytes	132
Chapter V: Conclusions	139
Appendix: Synthesis of $^{32}\text{P}$ -FdUMP	145
List of References	169

List of Figures

<u>Figure</u>	<u>Page</u>	
I.1.	10	Scheme of Possible Liposome-Cell Interactions
I.2.	16	Partial Scheme of FdUMP Metabolism
I.3.	22	Diagram of a Liver Lobule
I.4.	23	Liver Plate
I.5.	24	Endothelial Fenestration
I.6.	26	Kupffer Cell
II.1.	32	Reaction Scheme for the Conversion of dUMP to dTMP
II.2.	34	Structure of 5-FU and FdUMP
II.3.	37	Structure of FdUMP-TS
II.4.	50	Biogel A 0.5m Column Chromatography
II.5.	58	Calibration Curve of Biogel A 0.5m
II.6.	62	Arrhenius Plot
II.7.	66	Radiopurity of $^3\text{H}$ -FdUMP
III.1.	75	Phosphate Assay Standard Curve
III.2.	80	Sephadex G-200 Elution Profile
III.3.	93	Biogel A 0.5m Chromatogram
III.4.	95	TLC - Low Molecular Weight Species in Liver and Spleen Cytosol
IV.1.	118	Standard Curve for Protein Assay
IV.2.	120	Distribution of Hepatocytes and Non-Parenchymal Cells in the Liver
IV.3.	124	Distribution of Radiolabel in Hepocytes and NPC



IV.4.	127	Distribution of TS and FdUMP-TS in Hepatocytes and NPC
A.1.	146	Reaction Scheme for the Conversion of FdUrd to FdUMP
A.2.	155	Calibration of a DEAE Anion Exchange Column
A.3.	156	DEAE Anion Exchange Chromatography
A.4.	158	Biobead SM 4 Chromatography
A.5.	159	Standard Curve for FdUMP Quantitation

List of Tables

<u>Table</u>	<u>Page</u>	
II.1.	52	Quantitation of TS In Vitro in Liver and Spleen Homogenates
II.2.	53	FdUMP-TS Complex per Organ
II.3.	54	FdUMP-TS Formation in the Presence of Increasing Substrate Concentration
II.4.	60	In Vitro Dissociation Rates of FdUMP-TS
II.5.	61	In Vivo Dissociation Rates of FdUMP-TS
II.6.	64	Quantitation of TS In Vivo in Liver
II.7.	65	Quantitation of TS In Vivo in Spleen
III.1.	84	Total Organ $^3\text{H}$ -Radioactivity in Liver
III.2.	85	Total Organ $^3\text{H}$ -Radioactivity in Spleen
III.3.	87	Total Organ Radioactivity in Liver after Dosing of Double-labeled Liposomes
III.4.	89	Total Organ Radioactivity in Spleen after Dosing of Double-Labeled Liposomes
III.5.	90	FdUMP-TS Complexes in Liver after Dosing of Single-Labeled Liposomes
III.6.	91	FdUMP-TS Complexes in Spleen after Dosing of Single-Labeled Liposomes
IV.1.	122	Association of $^3\text{H}$ and $^{14}\text{C}$ Label with Hepatocytes and NPC
IV.2.	123	Association of $^3\text{H}$ and $^{14}\text{C}$ Label with Equal Cell Mass of Hepatocytes and NPC
IV.3.	126	FdUMP-TS Complexes in Hepatocytes and NPC
V.1.	141	Comparison of Total Organ Radioactivity and Therapeutic Availability of FdUMP

- A.1. 163 Conversion of FdUrd to FdUMP Varying  
Thymidine Kinase and Incubation Time
- A.2. 164 Scaling-Down of the Reaction Conditions
- A.3. 165 Effect of Dilution on the Reaction Yield
- A.4. 166 Conversion of FdUrd to  $^{32}\text{P}$ -FdUMP  
Using  $^{32}\text{P}$ -ATP as Cofactor

List of Abbreviations

AUC	Area Under the Curve
ATP	Adenosine Triphosphate
a-T	alpha-Tocopherol
BSA	Bovine Serum Albumin
BW	Body Weight
Chol	Cholesterol
FdUMP	5-Fluoro-2'-deoxyuridine-5'-monophosphate
FdUMP-TS	FdUMP-thymidylate synthetase enzyme complex
FdUrd	5-Fluoro-2'-deoxyuridine
5-FU	5-Fluorouracil
HPS	Hanks Balanced Salt Solution
HEP-TS	Thymidylate Synthetase present in Hepatocytes
IgG	Immunoglobulin G
NPC	Non-Parenchymal Cells
NPC-TS	Thymidylate Synthetase present in NPC
PA	Phosphatidic Acid
PC	Phosphatidylcholine
RES	Reticuloendothelial System
TCA	Trichoroacetic Acid
TK	Thymidine Kinase
TLC	Thin Layer Chromatography
TS	Thymidylate Synthetase

Abstract

The effectiveness of liposomes as drug carriers was measured by quantitating therapeutic availability of a model drug to a specific intracellular target site in the rat liver and spleen. We have successfully used 5-fluoro-2'-deoxyuridine-5'-monophosphate (FdUMP) as the model drug. FdUMP neither partitions into nor is taken up by cells, however, once delivered intracellularly it acts as a suicide substrate for the enzyme thymidylate synthetase (TS). Therapeutic availability is defined as the fraction of the dose binding covalently to the target enzyme and was monitored by measuring the drug-enzyme complex, FdUMP-TS. In vitro and in vivo quantitation of thymidylate synthetase revealed enzyme levels of about  $10^{-12}$  mol/g of liver or spleen. Use of liposomes improved the therapeutic availability of FdUMP to the intracellular target in both organs by up to four-fold. However, total organ radioactivity overestimated therapeutic availability at all times. The time course of therapeutic availability neither parallels total organ levels nor can be predicted from them.

The mechanisms of liposome-mediated drug delivery were studied in the two major liver cell populations, non-parenchymal cells (NPC) and hepatocytes using double-labeled liposomes co-encapsulating the model drug FdUMP and an inert marker inulin. Surprisingly, both markers showed a similar distribution to non-parenchymal cells and hepatocytes. Delivery of marker material into NPC was accounted for in part by Kupffer cell phagocytosis. Various mechanisms for uptake by other cell types are discussed, including ones that do not involve Kupffer cell phagocytosis followed by cell-to-cell transfer of material into hepatocytes. Although the actual mechanism of the liposome-mediated delivery to hepatocytes was not identified, the idea that phagocytic removal of liposomes by Kupffer cells is the dominant mechanism for liposome clearance from the vasculature is challenged.

## Chapter I: General Introduction

### Purpose of this Study

Liposomes (phospholipid vesicles) have been extensively studied over the last decade as potential drug carriers. In the early sixties (Bangham, 1965) described these concentric multilamellar, bilayered structures while investigating the structure and functions of biological membranes. These model membrane systems - or liposomes - were initially used to study membrane permeability (Bangham, 1972), molecular motion within membranes (Kornberg, 1971; Jost, 1973; Stockton 1975), interactions of anesthetics with membranes (Papahadjopoulos, 1972), the immunologic properties of membranes (Kinsky, 1977; Alving, 1977) and lipid protein interactions (Kimelberg, 1976). Gregoriadis (1972) suggested their potential application as a transport system or drug carrier (for extensive reviews as regards this aspect see Kimelberg and Mayhew, 1978; Ryman, 1980; Yatwin, 1982; Schreier, 1982; Poste, 1983).

Speiser (1981) defined the term 'carrier', with regard to nanoparticles, as 'vesicular systems loaded with drug molecules' serving as 'reservoirs or compartments for drugs or other molecules'. Modifying and extending his definition, a drug carrier presents a different dosage form - in case of liposomes, a lipid vesicle containing an aqueous compartment between each bilayer - in which release

characteristics and tissue interaction can be predetermined by the physico-chemical properties of the carrier rather than the drug.

By utilizing a drug carrier, one goal is to improve the therapeutic index (TI) by increasing the pharmacological response. This can be accomplished by increasing the amount of drug or prolonging its presence at the target site, or by decreasing toxic side effects. Both are usually measured by secondary pharmacological responses.

The concept of using liposomes as carriers originated partly from their biodegradability and the possibility of manipulating their properties to suit special needs. Drug therapists had sought for a biodegradable carrier for many therapeutic substances. The carrier was expected to protect the entrapped substance against metabolism in the blood, to alter tissue distribution and to increase uptake into cells by mechanisms that are normally not available to small molecules. Since blood levels of carrier associated drugs are often monitored in most experimental conditions, distinguishing between these mechanisms in vivo is difficult. It has been shown that liposome encapsulation can alter the apparent pharmacokinetics and disposition properties of entrapped material (Juliano, 1975; Mayhew, 1979; Kimelberg, 1979; Roerdink, 1979; Abra 1981), and can enhance pharmacologic efficacy (Alving, 1978), indicating the potential of liposomes as a drug carrier system.

A variety of experimental procedures have been used to evaluate liposomes as drug carriers. It is important to note that, when different liposome markers are used, limits are automatically set for the liposomal properties that can be studied. The fate of a liposomal lipid does not readily allow predictions regarding the fate of the entrapped material and vice versa. Our objectives are concerned with hydrophilic compounds and, as a result, the fate of the aqueous compartment of liposomes becomes important. By entrapping commonly-used drugs into liposomes it is unfortunately not always clear if the change in pharmacologic response is brought about by a direct liposome mediated process, that is, by changing the mechanisms by which the drug reaches the target, or simply by changing the rate of delivery of the drug to the target site (e.g. prolonging circulatory half-life through slow release of the drug from liposomes). Therefore, the independent fate of released drug from the liposome cannot be differentiated from the fate of liposomally delivered drug.

Most drugs exert their pharmacologic response through a transient primary event (e.g. association with a receptor). Since in most cases this primary event cannot be measured directly, differentiation of the mechanisms governing how the drug was delivered is even more difficult.

In this investigation experiments were designed to allow differentiation between a liposome-mediated delivery



process and release of drug from liposomes in the vasculature. To investigate the mechanisms which may lead to intracellular delivery of entrapped material, a unique model drug was utilized as a diagnostic tool. The model drug does not exert its pharmacologic action in a transient (non-measurable) fashion, but allows a direct measurement of its bioactivity by monitoring the appearance of the drug at an intracellular target site. The model drug, 5-fluoro-2'-deoxyuridine-5'-monophosphate (FdUMP), a suicide substrate, when delivered intracellularly, forms a covalent complex with the enzyme thymidylate synthetase (TS) which can be isolated and quantified. This provides a direct measurement of therapeutic availability of the encapsulated drug. The therapeutic availability is defined here as the fraction of a dose covalently attached to the intracellular target. The number of drug-enzyme complexes formed per liver or spleen cell is also a measure of therapeutic availability. Maximum therapeutic availability can be reached when all available enzyme is successfully complexed with the substrate. Changes in therapeutic availability after administering the drug entrapped in liposomes are referenced to the therapeutic availability of free drug. It should be pointed out that the term 'therapeutic availability' should not be equated with the commonly used term 'bioavailability' which refers to the fraction of the administered dose reaching the

blood sampling site as opposed to a target site.

## Background Information

### The Fate of Liposomes In Vivo

The major portion of liposome research to date has been concerned with the in vivo fate of liposomes after i.v. injection, which is the most direct route for liposome-mediated delivery of therapeutic agents.

It has been observed that rapid clearance of liposomes from blood and their uptake by phagocytosis into cells of the reticuloendothelial system (RES) is analogous to the behavior of other colloidal particles such as colloidal carbon, latex beads, microspheres and microorganisms. The rate of clearance usually depends on size, charge and composition of the vesicles (Knight, 1981). Large multilamellar liposomes have been observed to be cleared more rapidly than small unilamellar ones (Juliano, 1975; Kimelberg, 1976). Furthermore, initially positively charged and neutral liposomes are cleared more slowly than those originally negatively charged (Gregoriadis, 1974), although there is evidence that all liposomes become negatively charged upon interaction with serum constituents (Black, 1976).

It has been suggested that recognition of liposomes may be a result of 'opsonization', which involves interaction of

the injected liposome with blood protein components. This implies that these surface-adsorbed compounds largely determine the clearance of administered liposomes (Tanaka, 1976).

The liver is the main site of liposome uptake. Greater than 50% of a liposome dose has been recovered from this tissue (Tyrell, 1976; Abra, 1981). Furthermore, liposomes are distributed in significant amounts to the spleen, and to a lesser extent to lung and bone marrow, all of them being part of the reticuloendothelial system (RES).

Attempts have been made to determine the cellular localization of liposomes in tissues, mainly in liver cells, both by morphological and biochemical methods (Gregoriadis, 1974; Freise, 1980; Rahman, 1982; Scherphof, 1983; Roerdink, 1981). Although strongly suggestive that liposomes are endocytosed by non-parenchymal liver cells in vivo these studies show some degree of uncertainty with respect to the cellular involvement of hepatocytes in liposome uptake (see also Chapter IV). Reticuloendothelial cells from other tissues, such as spleen, would be expected to take-up liposomes, at least in part, by endocytosis. However, these cells have not been studied on a cellular level.

#### Liposome Interaction with the Physiological Environment

When liposomes are administered in vivo a variety of interactions with the physiological environment can occur. First, the vesicles encounter the blood, where interaction

of plasma proteins with liposomes can cause leakage of encapsulated material (Black, 1976; Hunt, 1981; Senior, 1982). However, after an initial period of a relative high rate of loss of entrapped material, the increased permeability of the membrane seemed to be reversed. This has been attributed to a protein coat sealing the vesicles against further leakage. Initial induction of leakage can be reduced by a high cholesterol content (>33 mol%) in the liposomal membrane (Mauk, 1979; Kirby, 1980; Damen, 1981; Senior, 1982). The uptake of material leaked from the vesicle due to interaction with plasma proteins probably only accounts for a minor part of material released for vesicles with high cholesterol content (Gotfredsen, 1982).

Second, liposomes interact with various body tissues. The discussion here is limited to the liver, one organ of the reticuloendothelial system (RES), since liver sinusoidal cells have the strongest direct interaction with liposomes. The vesicles can adsorb to the cell surfaces of Kupffer and endothelial cells, which for the former cells can lead to phagocytic uptake of the vesicle. No or little phagocytic activity has been found in endothelial cells (Wisse, 1977; Roerdink, 1981). However, adsorption of the vesicles to their surface might lead to membrane permeability changes followed by release of entrapped material into the sinusoid. This surface mediated leakage of liposome content may be reduced by high cholesterol content (Fraley, 1981). How-

ever, if a relative high local concentration of free drug or model substance occurs, the material can either be flushed away by the bloodstream or taken up by endocytosis into cells to which the vesicles were initially adsorbed, or into cells in the vicinity (Papahadjopoulos, 1974).

#### Mechanisms of Liposome-Cell Interaction

The mechanisms of liposome-cell interaction have been largely addressed in vitro. Four basic types of liposome-cell interactions have been proposed (Kimelberg and Mayhew, 1978):

- Stable adsorption, which is the association of intact liposomes with the cell surface, without internalization. The adsorption may be of nonspecific nature (e.g. electrostatic or hydrophobic forces) or mediated through cell surface components (e.g. surface receptors).
- Phagocytosis or endocytosis, leading to internalization of vesicles into phagocytic or endocytic vesicles most likely followed by interaction of these vesicles with the lysosomal apparatus (Dijkstra, 1982).
- Fusion of lipid membranes of liposomes with the plasma membrane, resulting in a direct delivery of the vesicle content to the cytoplasmic space (Szoka, 1980,1981).

- Lipid exchange, reflecting the transfer of lipid constituents from the liposome bilayer membrane to the plasma membrane. Lipid transfer is a complex mechanism probably involving plasma lipoprotein as an intermediate step (Damen, 1981; Scherphof, 1982).

A schematic representation of the above mechanisms is given in Figure I.1.

The occurrence of a given mechanism in vivo is often difficult to demonstrate since these mechanisms are not mutually exclusive. However, fusion is most likely not a relevant mechanism for liposome-cell interaction in mammalian cells in vivo, since it has only been observed under special conditions in vitro (Szoka, 1980,1981; Straubinger, 1983).

A more detailed description of liposome-cell interactions is provided in an excellent review by Pagano and Weinstein (1978).

### Phagocytosis

Phagocytosis describes a process whereby particulate matter in close contact with the cell is engulfed by the cell membrane. Intracellularly, the so-called phagosome fuses with a primary lysosome to form a secondary lysosome. If liposomes are taken-up by such a mechanism, the lipid membrane is presumably degraded by phospholipases present in

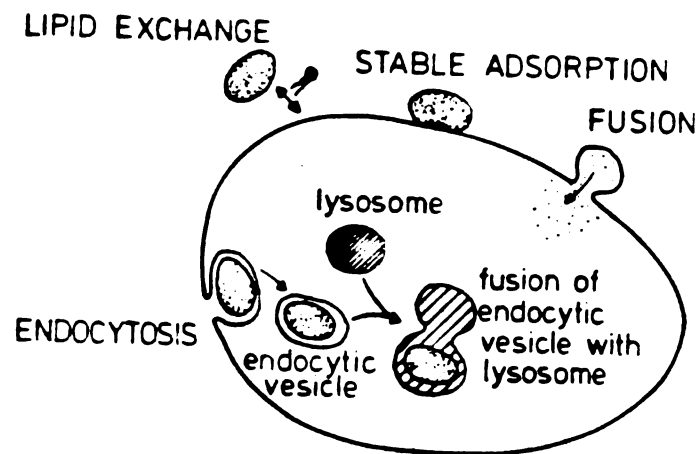


**Figure I.1.** A scheme of possible liposome-cell interactions (taken with permission from Dijkstra, 1983)

the secondary lysosome. Exposure of encapsulated material to lysosomal enzymes then can lead to:

- degradation / metabolism, followed by
- release into the cytosol, or
- extrusion from the cell leading to elimination or reabsorption.

Substances which are resistant to lysosomal degradation remain sequestered in the cell (see also review on RES, presented in this chapter).

#### Model Drugs in Liposome Research

A variety of model drugs and marker substances have been employed in liposome research depending on the specific research aims:

- Active drugs have been encapsulated and their pharmacological response monitored in comparison to free drug.
- Inert marker materials (i.e. inulin, sucrose, I-polyvinylpyrrolidone) and fluorescent substances have been encapsulated. Their tissue distribution has been monitored in order to evaluate the mechanistic events in liposomal drug delivery.

Most pharmacologic-active compounds that have been entrapped in liposomes have physical properties that preclude their use as accurate indicators of delivery mechan-



isms, because the compounds used are often either capable of entering and leaving the target cells on their own, or are metabolized to compounds which can permeate membranes. On the other hand, the localization of inert markers with respect to intracellular or extracellular localization cannot easily be differentiated, although organ plateau levels of a marker such as inulin, especially in the liver, indicate cellular transfer via liposomes (Bosworth, 1980; Abra, 1980,1981). Such findings suggest cellular availability of the marker, but say nothing directly about therapeutic availability, as defined in this study, due to the very nature of the inert marker substances.

Therefore, specific emphasis in this work is put on the therapeutic availability of a liposome encapsulated model drug whose effect is monitored not by its pharmacologic action or response, but rather by its binding to an intracellular macromolecular constituent which can be isolated and analyzed quantitatively. The model drug was expected to exhibit bioactivity which provides additional and crucial criteria in our model system when assessing the potential of liposomes as drug carriers. The goal was to find a marker which satisfied the following criteria. The model drug should:

- neither partition into nor be taken up by cells,
- have a short half-life ( $t_{1/2}$ ) in the blood and be rapidly excreted from the circulation, when no longer

encapsulated in liposomes (free), and

- be bioactive once introduced into cells by means of a liposome-mediated process.

#### The Experimental Drug: FdUMP

5-Fluoro-2'-deoxyuridine-5'-monophosphate (FdUMP) was chosen as the model drug because it reasonably satisfies the criteria above:

- Due to its polar nature it does not partition across cell membranes nor is it taken up into cells,
- the circulatory  $t_{1/2}$  in rats is approximately 10 minutes with rapid urinary excretion (Myers, 1976).
- FdUMP is a suicide substrate for the enzyme thymidylate synthetase (TS); it forms a covalent stable enzyme complex  $N^5, N^{10}$ -methylenetetrahydrofolate-FdUMP-TS. The molecular nature of this enzyme complex is described in detail in Chapter II.

Thymidylate synthetase is therefore our intracellular target and the formation of the FdUMP-TS complex will be taken as direct evidence for the successful delivery of the entrapped drug to the target site, and thus for therapeutic availability.

### Cellular Events Prior to FdUMP-TS Complex Formation

When FdUMP is administered in vivo either in its free form or encapsulated in liposomes, a variety of consecutive steps must occur prior to binding of the drug to the enzyme thymidylate synthetase.

Considering the application of free FdUMP first, it is necessary for the nucleotide to be dephosphorylated extracellularly before it can permeate the cell membrane. FdUMP itself does not diffuse across cell membranes due to its negative charge and the absence of any known transport mechanism. However, once hydrolyzed to the nucleoside 5-fluoro-2'-deoxyuridine (FdUrd) by alkaline phosphatase - this enzyme has been located at the hepatic cell surface (Jung, 1982) - , FdUrd in turn can be transported across the plasma membrane by a carrier-mediated process. This carrier protein has been studied in a variety of cells including HeLa cells and erythrocytes (Paterson, 1980). This carrier protein facilitates both the influx and efflux of nucleosides (Berlin, 1975; Cass, 1979; Paterson, 1980; Shohami, 1980). Reaching the cytoplasm, the nucleoside can enter both the anabolic and the catabolic pathways.

Anabolically, FdUrd will be rephosphorylated to FdUMP by the enzyme thymidine kinase, utilizing adenosine triphosphate (ATP) as a cofactor. Only then can FdUMP form the covalent enzyme complex, FdUMP-TS.

If FdUrd enters the catabolic pathway the enzyme nucleoside phosphorylase converts the nucleoside to the pyrimidine base 5-fluorouracil (5-FU). 5-FU can be further metabolized to fluorodihydrouracil, then after ring opening to fluoroureidopropionic acid, give the final metabolic products, alpha-fluoro-beta-alanine and urea, with the radiolabel retained in the former product. Through an alternative pathway, 5-FU enters the ribose nucleotide pool, interacting with phosphoribosyl transferase (PRT) to give fluorouridine monophosphate (FUMP) which, after conversion to fluorouridine diphosphate (FUDP) and fluorouridine triphosphate (FUTP), can be incorporated into RNA in place of uridine triphosphate (UTP) (Figure I.2.).

All of these anabolic and catabolic conversions have been observed in healthy animal and animal tumor models after application of the nucleoside FdUrd (Armstrong, 1980,1981). The use of FdUMP was not considered advantageous for metabolic studies or for the evaluation of the antineoplastic efficacy of fluoropyrimidines since the nucleotide has to be converted to the nucleoside extracellularly to be rendered able to permeate the cell membranes as described above. Moreover, the nucleotide is rapidly excreted in urine, as is FdUrd.

The following series of events must occur prior to drug enzyme binding and must be taken into consideration when FdUMP is administered within liposomes. All the above path-

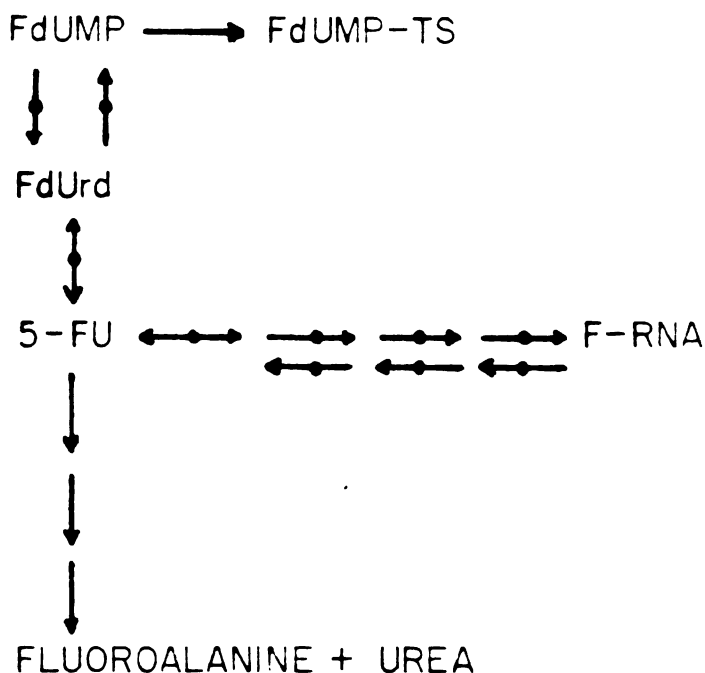


Figure I.2. A partial scheme of anabolic and catabolic conversions, relevant to this investigation, of 5-fluoro-2'-deoxyuridine-5'-monophosphate (FdUMP) in the cell cytosol. The abbreviations used are:

FdUMP, 5-fluorodeoxyuridine monophosphate;  
 FdUMP-TS, FdUMP-thymidylate synthetase complex;  
 FdUrd, 5-fluoro-2'-deoxyuridine;  
 5-FU, 5-fluorouracil;  
 F-RNA, 5-FU incorporated into RNA.

The symbols are:  
 —●→ enzymatic reaction  
 —→ non-enzymatic reaction  
 ↔ the same enzyme catalyzes the forward and reverse reaction.

ways apply to entrapped drug after its leakage from the vesicles into the vasculature.

When liposomes are exposed to physiologic media, increased permeability to small drug molecules has been observed even with very stable vesicles (high cholesterol content). The leakage of FdUMP from vesicles and the exposure of the drug to alkaline phosphatases on the surface of hepatic cells can induce extracellular hydrolysis to FdUrd. Since the radiolabel on the FdUMP is at the 6-position of the pyrimidine ring, uptake of extracellularly released and hydrolyzed FdUMP cannot be differentiated from liposome-delivered FdUMP, because in both cases radiolabeled FdUMP-TS complex is formed intracellularly.

When intact liposomes are taken up by a phagocytic mechanism, it is expected that the liposomal membranes will be degraded intralysosomally. In this environment, FdUMP will be hydrolyzed by lysosomal acid phosphatases. The hydrolysis product, FdUrd, was confirmed by incubating the drug with lysosomal enzymes in vitro (see Chapter III). Although little is known about the permeability of lysosomal membranes (Bundgaard, 1980), it is not unreasonable to assume that FdUrd may be transported across the lysosomal membrane by simple diffusion (DeDuve, 1978), or by the same carrier protein which exists in the plasma membrane (Docherty, 1983; Steinmann, 1983). A similar situation was reported by Gordon (1973). A plasma membrane enzyme, 5-

nucleotidase, was located in the secondary lysosomal membrane after phagocytosis of latex beads into macrophages.

Once FdUrd reaches the cytosol, anabolic and catabolic reactions should occur leading to FdUMP-TS formation and degradation of the drug, respectively. Since non-parenchymal cells (NPC) are less metabolically active than hepatocytes, FdUrd can be extruded from the cell by the same carrier protein which facilitates its influx (C.C.Wang, personal communication).

There are, however, several problems associated with the use of FdUMP for the evaluation of therapeutic availability of an encapsulated drug from a drug carrier. Extracellular hydrolysis of FdUMP to FdUrd enables the initially nonpermeating model drug to permeate the cell membrane. The intracellular target enzyme is present only in a limited amount, so that simultaneously with binding of the drug to the target enzyme, extrusion from NPC and rapid metabolic degradation in hepatocytes may occur.

#### Rate-Limiting Steps During FdUMP-TS Formation

Any of the above processes may be saturable. From studies on the nucleoside transport mechanism in HeLa cells where the  $K_M$  and  $V_{max}$  are reported to be 3.9  $\mu\text{M}$  and 95  $\text{pmol}/\text{min}/10^6$  cells, respectively (Paterson, 1977), it is probably fair to suggest that when nmol quantities per animal of FdUMP are administered, the nucleoside transport

will not be saturated. This assumes a comparable transport capacity in the rat tissues. Similarly, no saturation should occur for the hepatic alkaline phosphatase (Jung, 1982).

Since ATP is needed for the formation of FdUMP by thymidine kinase, low levels of ATP might be rate-limiting rather than low levels of TS. A cofactor, N<sup>5</sup>,N<sup>10</sup>-methylene-tetrahydrofolic acid (CH<sub>2</sub>-H<sub>4</sub>-folate), is necessary for the FdUMP-TS complex formation. However, Priest (1980) reports sufficient cofactor in the mouse liver cytosol, high enough to ensure complete inhibition of the enzyme thymidylate synthetase in vitro through FdUMP-TS complex formation.

The enzyme nucleoside phosphorylase converts FdUrd to 5-FU intracellularly. Armstrong (1980) reported a K<sub>M</sub> of 278 uM and a V<sub>max</sub> of 13 nmol/min per mg protein for the mouse Ehrlich ascites tumor enzyme.

Since most of the initial conversion steps can occur in parallel, it is not known what ultimately governs the fraction of drug being shuttled along the anabolic or catabolic routes. However, after encapsulation of nmol quantities of FdUMP into liposomes it appears that none of the enzymatic conversions prior to FdUMP-TS formation will be rate-limiting.



### The Liver

A review of the liver and the reticuloendothelial system (RES) is presented next since the role of the RES in clearing foreign particles from the circulation cannot be overlooked with respect to the evaluation of the effectiveness of a liposomal drug carrier. Liposomes are foreign particles and therefore assumed to be subject to phagocytosis by the Kupffer cells in the liver (Dijkstra, 1982) and the macrophages of the spleen.

The liver is an organ with a multitude of functions (Jones, 1977) and with the capability to regenerate (in the rat). In addition to bile secretion, which is required for emulsification of dietary fats prior to digestion, the liver takes up digested food from the blood and stores carbohydrates (glycogen), proteins, vitamins and certain lipids. These stored substances may be utilized by the hepatocyte or released into the blood either unbound (e.g., glucose) or in association with a carrier (e.g., triglycerides contained in lipoproteins). Certain substances are synthesized by the liver in response to the demands of the body, such as albumin and other plasma proteins, glucose, fatty acids, cholesterol and phospholipids. The liver has a high capacity to metabolize, detoxify and inactivate exogenous agents such as drugs, and endogenous compounds such as steroids and hormones.

Evaluation of the liver by light microscopy or by transmission or scanning electron microscopy demonstrates that the liver consists of hexagonal lobules which are composed of continuous systems of communicating parenchymal plates (Figure I.3. and I.4.). The parenchymal cells or hepatocytes throughout a lobule are interconnected and subdivided by sinusoids. Each sinusoid opens directly into the central vein.

The liver is a highly vascularized organ which receives blood from both the portal vein (75%) and hepatic artery (25%). The sinusoids differ from typical capillaries in two basic aspects: they are larger and more variable in size, and their walls are lined by two distinct cell types: endothelial cells and Kupffer cells. The endothelial cells generally have a flattened profile and only the nuclei of the individual cells protrude into the sinusoidal lumen. These cells are characterized by numerous pinocytotic vesicles. Although the endothelial lining of the sinusoids is continuous, fenestrae of various sizes in the endothelial cells allow for the exchange of material between the blood and the hepatocytes across the space of Disse (Figure I.5.) (Wisse, 1970).

The endothelial lining does not function as a barrier since hepatocyte microvilli protrude through the fenestrae into the sinusoidal lumen. Furthermore, the fenestrae offer no resistance to macromolecules such as very low density

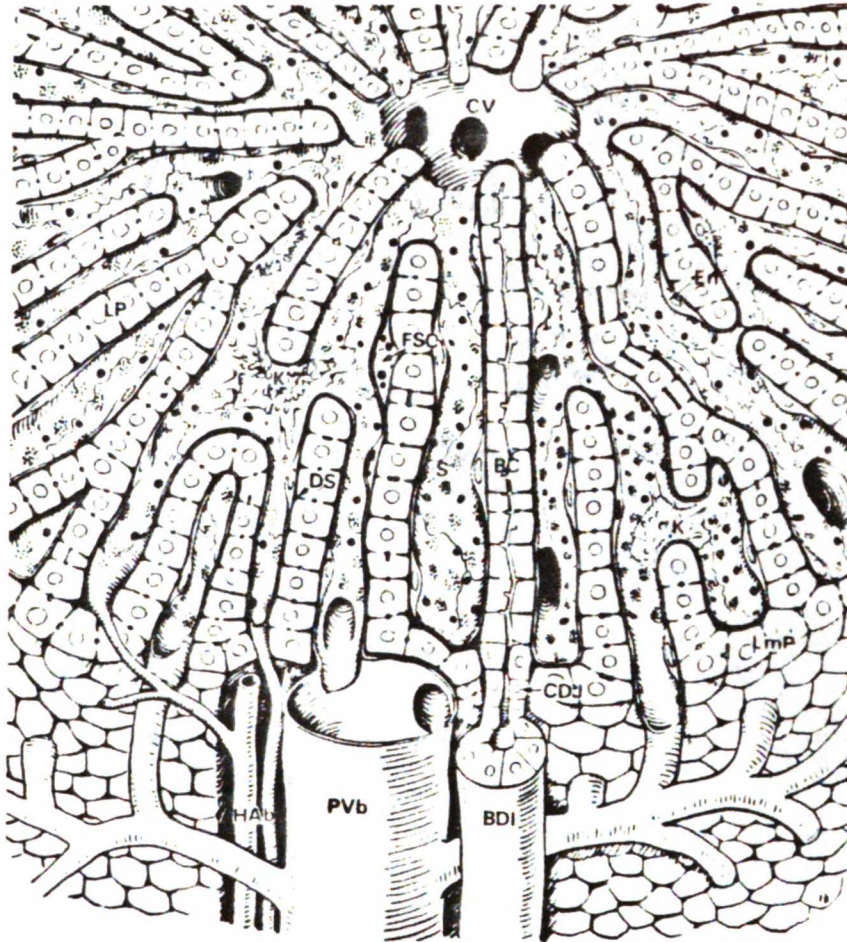


Figure 1.3. This schematic diagram shows the three-dimensional structure of the hepatic lobule. CV: central vein; K: Kupffer cell; FSC: fat-storing cell; BC: bile canaliculus; En: endothelial cell; S: sinusoid populated with large and small fenestrae; DS: space of Disse; HAB: hepatic artery; PVb: portal vein branch; CDJ: canalicular-ductular junction; BDI: bile ductule; LP: liver plate (taken with permission from Motta, 1978).

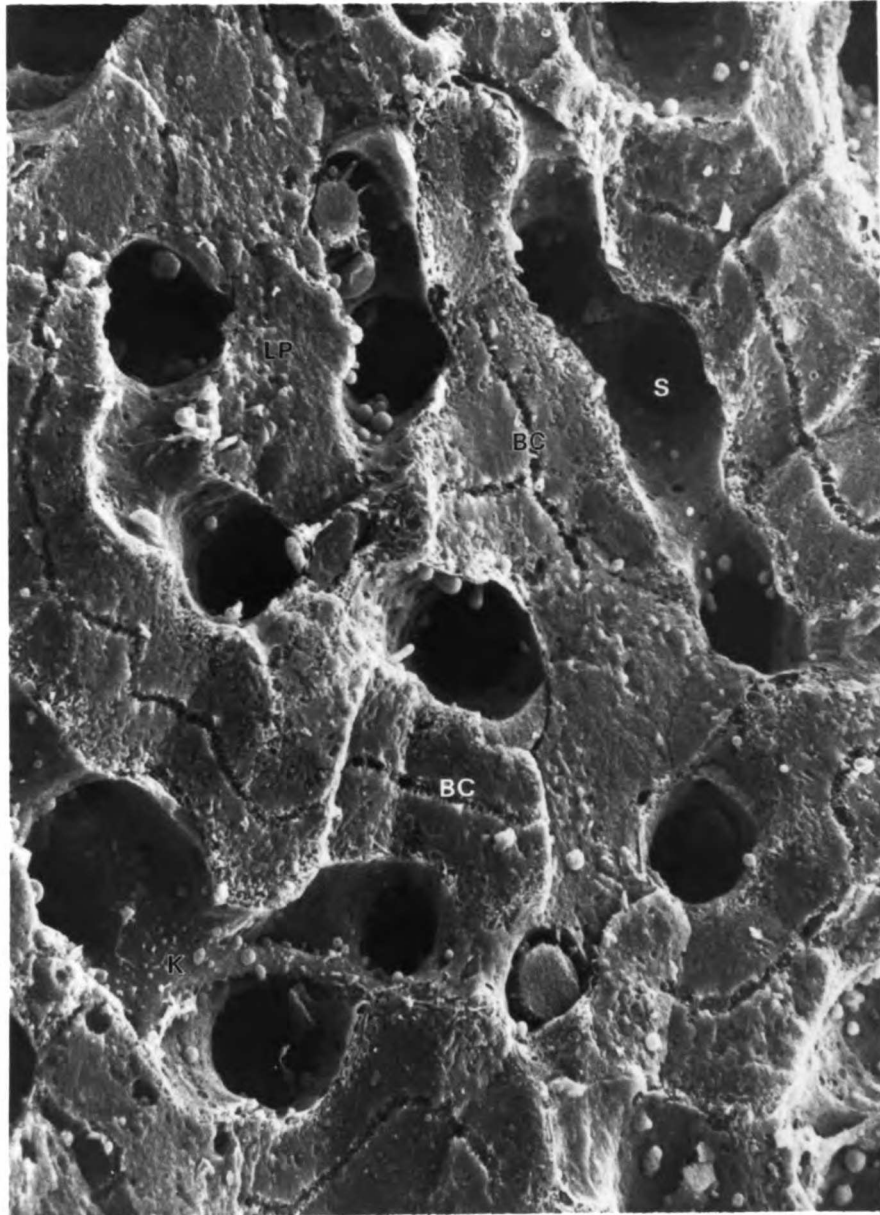


Figure I.4. This scanning electron micrograph shows that the liver lobule is formed by a continuous wall made of one cell thick liver plates (LP). The cellular walls form a continuous system of tunnels in which a network of sinusoids (S) is suspended. BC: bile canaliculi; K: Kupffer cell (taken with permission from Motta, 1978).

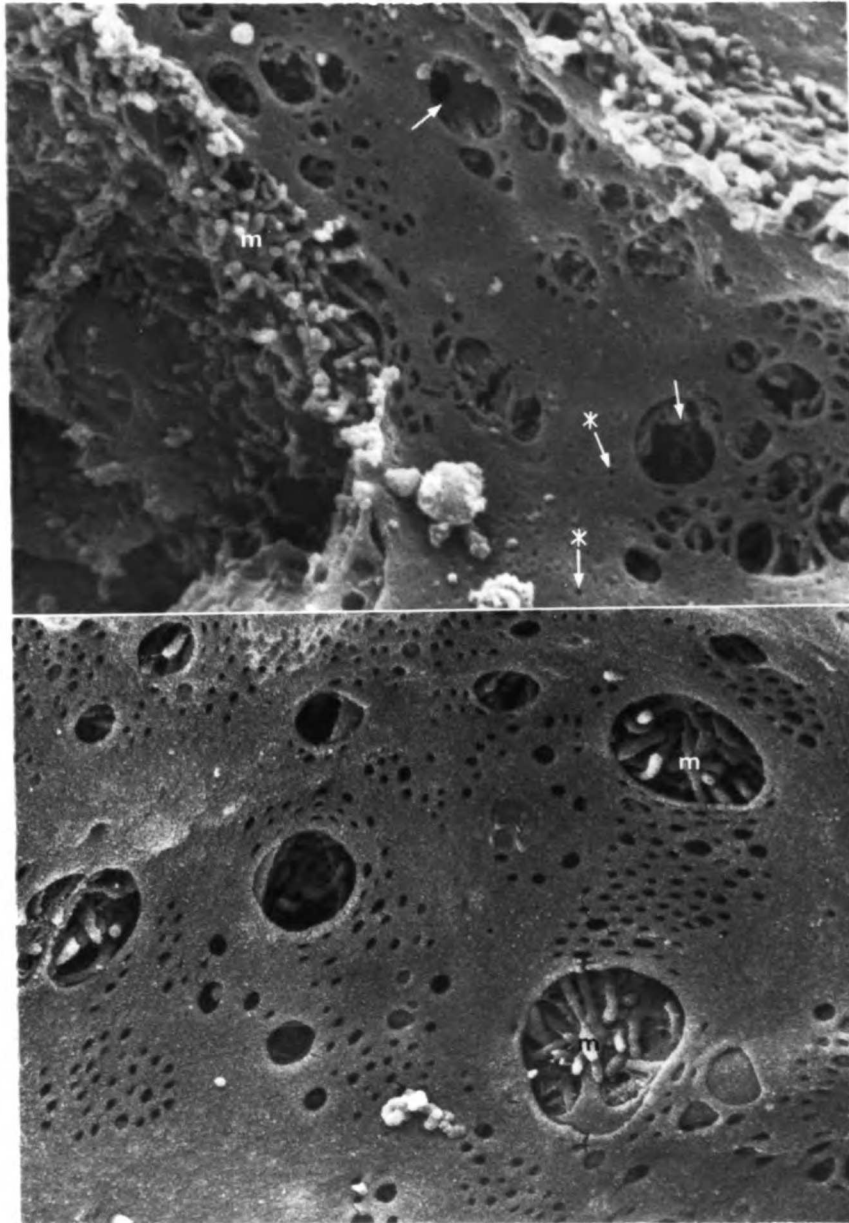


Figure I.5. The endothelial luminal surface shows small and large fenestrae. Microvilli (m) are evident through the large gaps (arrows) and on the adjacent hepatocytic surface (taken with permission from Motta, 1978).

lipoproteins (VLDL) which gain access to the sinusoids after being synthesized by hepatocytes.

Within the space of Disse, fat-storing cells and bundles of collagen are found. The collagen serves as a supporting network for the interconnecting plates of liver cells.

Kupffer cells are frequently observed spanning the sinusoids. These cells are large with an irregular surface characterized by folds and ruffles (Figure I.6.). Kupffer cells are phagocytically active and their cytoplasm contains many phagocytic vacuoles.

#### • The Reticuloendothelial System (RES)

The RES is a cellular system made up by a variety of widely distributed cells which share certain characteristics:

- phagocytic activity,
- adherence to glass surfaces,
- possession of a ruffled and 'sticky' outer membrane, and
- many lysosomes containing a variety of enzymes. Moreover, these cells show the ability to synthesize additional enzyme-containing lysosomes upon stimulation.



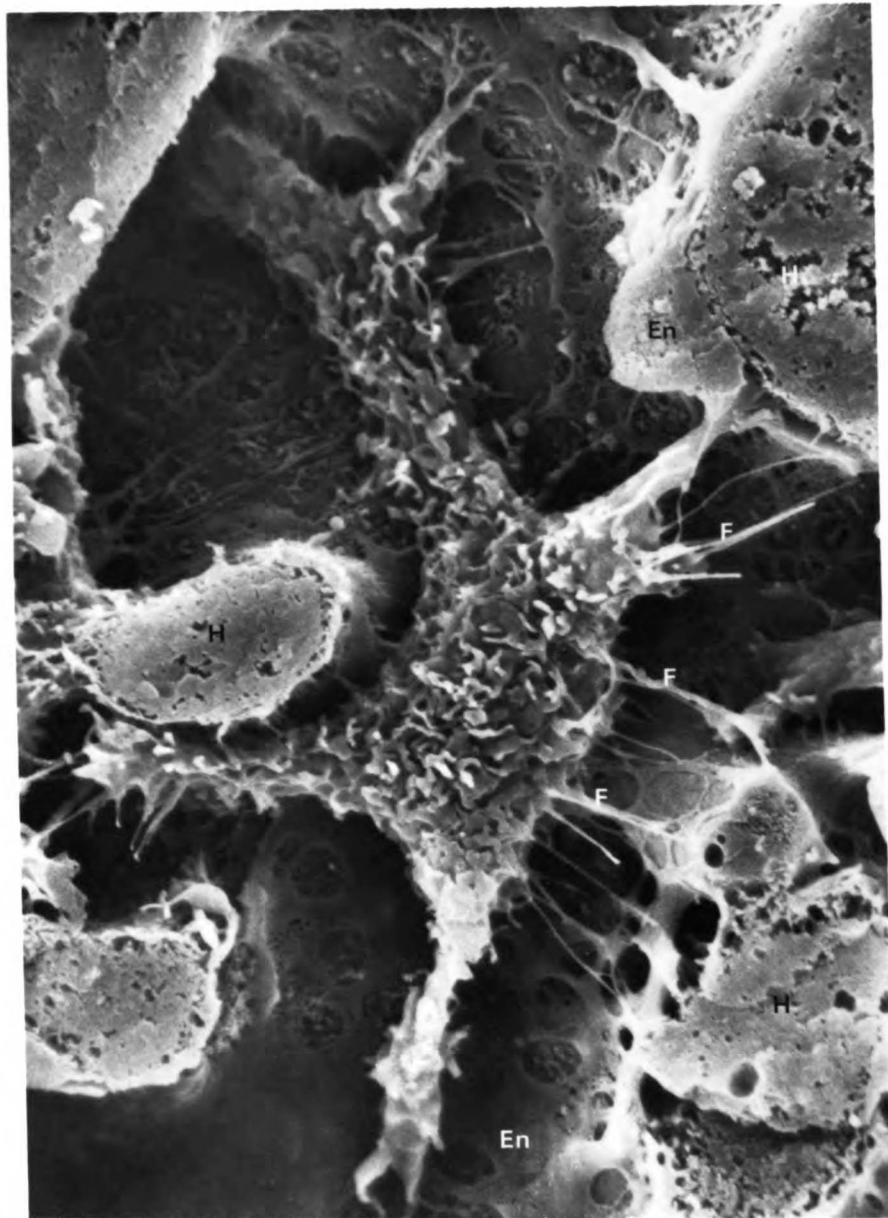


Figure I.6. The Kupffer cell is located in the lumen of the sinusoid showing a typical star shape. Its surface is covered by a number of microvilli, ruffles and invaginations. The Kupffer cell is attached to the largely fenestrated endothelial wall. H: hepatocyte; En: endothelial cell. (taken with permission from Motta, 1978)

The parent organ for the RES for all tissue macrophages is the bone marrow. Marrow promonocytes provide the blood monocytes which in turn migrate into the organs and tissues of the RES, to become the tissue macrophages. These tissue macrophages become histiocytes in connective tissues, Kupffer cells in the liver, alveolar macrophages in the lung, macrophages in the spleen. They are present in the bone marrow and lymph nodes as well as in the peritoneal and other serous cavities (McIntyre, 1972).

Phagocytosis describes the process when particulate or colloidal matter is engulfed by reticuloendothelial cells. After fusion with and formation of a secondary lysosome, the material:

- is completely digested by the lysosomal enzymes, if biodegradable, or
- remains surrounded by a membrane and sequestered in the cell, if resistant to lysosomal degradation.

The anatomical location of the reticuloendothelial cells ensures that all blood and lymph is constantly screened for foreign particles and foreign proteins (Bencerraf, 1958; Biozzi, 1968; Saba, 1970). In the lung, the filter effect is directed towards particles in the inspired air. Moreover, effete autologous tissue debris is effectively removed from the body by the RES (Boyden, 1963). The spleen macrophages are specifically active towards aged erythrocytes, simultaneously serving a conservatory function



### Organization of this Thesis

In order to verify sufficient amounts of the target enzyme thymidylate synthetase (TS) in the rat liver and spleen for the purpose of the evaluation of liposome-mediated drug delivery, a quantitative evaluation of the enzyme thymidylate synthetase present in these organs is described in Chapter II.

Chapter III gives an account of in vivo studies using single- and double-labeled liposomes containing the experimental drug FdUMP alone or in conjunction with the inert marker inulin. This serves to show that the model drug has a changed therapeutic availability in the liver as well as in the spleen after encapsulation into liposomes. The delivery modes were investigated using the double-labeled liposomes.

Chapter IV describes the studies evaluating the liposome drug delivery to the two major cell types in the liver, hepatocytes and non-parenchymal cells (NPC). Main emphasis is placed on investigating the involvement of hepatocytes in the liposome-mediated drug uptake and the distribution of the model drug as well as the inert marker in the two cell populations.

The conclusions of the last two chapters, Chapter III and IV, are presented in Chapter V.

Chapter II: Evaluation of Thymidylate Synthetase (TS) in Non-Proliferating Mammalian Tissue

Introduction

The main body of knowledge on thymidylate synthetase (TS)(EC 2.1.1.45) has been collected by studying the enzyme in proliferating tissues. Such tissues are the target in cancer chemotherapy and offer the advantage of elevated levels of thymidylate synthetase suitable for investigating enzyme and substrate interactions on a molecular basis. A literature review of the existing knowledge about TS is presented in the next section.

There is little known about thymidylate synthetase in adult mammalian tissue. Before being able to utilize this enzyme as a target for measuring the intracellular availability of liposome encapsulated agents, it became apparent that it was necessary to determine whether or not TS is present in the rat liver and spleen in sufficient amounts. Following available experimental procedures (Washtien, 1979; Tryfiates, 1980; Priest, 1981) the evaluation of the enzyme thymidylate synthetase was carried out in vitro by incubating liver and spleen homogenates with the radiolabeled substrate, and in vivo by administering 5-fluoro-2'-deoxyuridine (FdUrd).

### Thymidylate Synthetase In Proliferating Tissue

Thymidylate synthetase is an important enzyme in the biosynthesis of DNA because it is responsible for the only de novo source for thymidylate, a necessary building block of DNA. The enzyme converts deoxyuridine monophosphate (dUrd) in a unique two-step process to deoxythymidine monophosphate (dTMP), utilizing  $N^5, N^{10}$ -methylene tetrahydrofolate ( $CH_2-H_4$ -folate) as a cofactor for the transfer of a one carbon unit on to the 5 position of the uridine (see reaction scheme, Figure II.1.). This reaction is unique (i) because it involves a modification of the pyrimidine base: the methylation of uridilate in the 5 position and (ii) all other deoxyribose nucleotide constituents are formed by reduction of the ribose nucleotides at the diphosphate level by ribose diphosphate reductase, whereas thymidylate first appears at the monophosphate level (Lehninger, 1975).

The activity of thymidylate synthetase, which is required only during DNA synthesis, is substantially elevated in proliferating tissues, whereas little activity can be detected in normal tissue. Its regulation seems to be linked to the cellular demand for increased DNA synthesis. Additional enzyme is synthesized as DNA synthesis increases (Danenberg, 1977). Thus, thymidylate synthetase has become a target for new cancer chemotherapeutic agents.

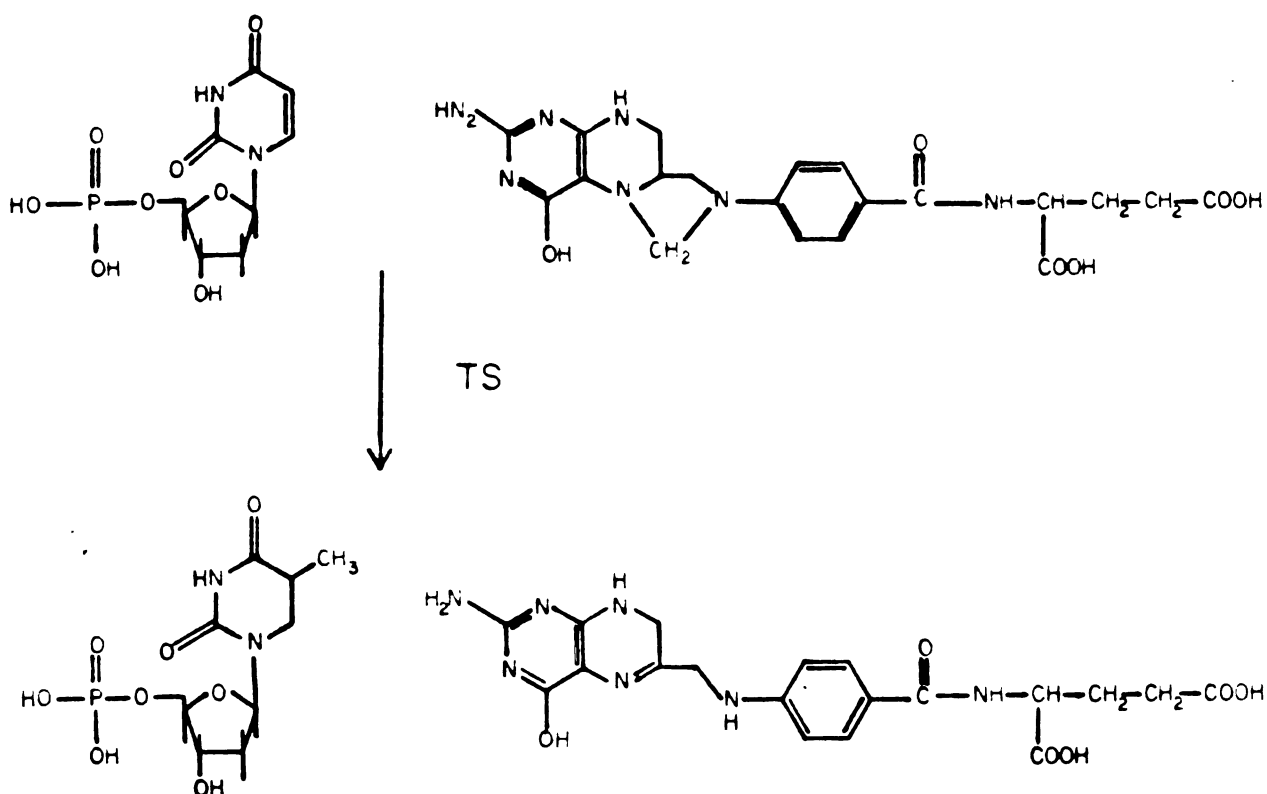


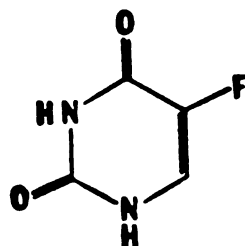
Figure II.1. The reaction scheme for the naturally occurring conversion of 2'-deoxyuridine-5'-monophosphate (dUMP) to 2'-deoxythymidine-5'-monophosphate (dTMP) catalyzed by thymidylate synthetase (TS) utilizing N<sup>5</sup>,N<sup>10</sup>-methylenetetrahydrofolic acid (5,10-CH<sub>2</sub>H<sub>4</sub>-folate) as cofactor.

### Fluorinated Pyrimidines and Their Nucleotides

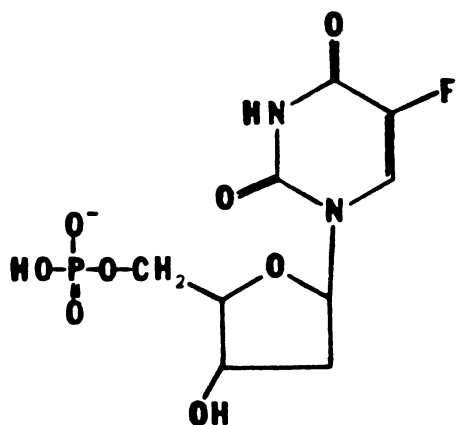
The synthesis of fluorinated pyrimidines is an example for a series of drugs being rationally designed according to specific biochemical predictions. They were synthesized and introduced by Heidelberger (1957) after the observation was made that uracil was incorporated to a greater extent into tumor tissues than into slowly proliferating normal tissues (Rutman, 1954). Because of the apparently special role of uracil in tumor metabolism, a uracil analog, 5-fluorouracil, was designed as an antimetabolite (Figure II.2.). Since thymidylate, a 5-methyl analog of uracil, is essential for operational DNA, it was predicted that blocking the 5 position on the pyrimidine ring with the C-F bond would inhibit the methylation and consequently decrease DNA biosynthesis due to lack of thymidylate. Furthermore, it was postulated that 5-fluorouracil would exert little toxicity on normal nonproliferating tissues, yet some toxicity was expected for normal tissues with high cellular turnover such as intestinal mucosa and bone marrow. All these predictions were substantiated in experimental studies (Heidelberger, 1975).

Similar predictions have been offered for 5-fluorouracil (Danenberq, 1958) and 5-iodo-2'-deoxyuridine (Goz, 1970).

Moreover, when the tumor-inhibitory properties of such fluorinated pyrimidines were studied, it was found that the deoxynucleoside exhibited the largest growth-inhibitory



5-FU



FdUMP

Figure II.2. Structure of the antimetabolites:  
5-fluorouracil and 5-fluoro-2'-deoxyuridine-  
5'-monophosphate.

effect (Heidelberger, 1958).

#### Mechanism of Thymidylate Synthetase Inhibition

After these initial findings, the mechanism of inhibition of DNA synthesis was widely studied. It was shown that the effect at the enzymatic level was due to a powerful inhibition of the enzyme thymidylate synthetase by the nucleotide 5-fluoro-2'-deoxyuridine-5'-monophosphate (FdUMP) (Figure II.2.) (Cohen, 1958).

When competitive inhibition studies with FdUMP and deoxyuridine monophosphate (dUMP) were carried out it was found that preincubation with FdUMP abolished the competitive inhibition. The mechanistic model which subsequently evolved was one of a two-step process for tightly binding inhibitors, the initial step being competition for the enzyme binding site between the substrate and inhibitor. Binding of the inhibitor FdUMP then leads to an irreversible (covalent) enzyme complex which is formed at a rate proportional to the concentration of the inhibitor (Myers, 1975; Aldridge, 1972).

Characterizing the tightly bound enzyme-FdUMP complex was possible only after radiolabeled FdUMP became available. Studies were difficult because of the rather low enzyme level present in bacteria and, even more so, in animal tissue. Only the isolation of a methotrexate resistant strain of Lactobacillus casei having elevated thymidylate

synthetase levels made purification of the enzyme feasible (Dunlap, 1971). Subsequent studies using thymidylate synthetase isolated from both Lactobacillus casei (Santi, 1972) and Ehrlich ascites tumors (Langenbach, 1972) produced results that were indicative of a covalent bond between FdUMP and the enzyme. The necessity of the cofactor  $N^5, N^{10}$ -methylenetetrahydrofolate for forming the covalent complex was confirmed by the same workers.

Evidence to date is consistent with the structure shown in Figure II.3. The enzyme is covalently bound to the 6-position on the pyrimidine ring. The cofactor is attached to the 5-position on the pyrimidine ring via a methylene bridge to the  $N^5$  of the  $N^5, N^{10}$ -methylenetetrahydrofolic acid. (Langenbach, 1972; Danenberg, 1974; Sommer, 1974; James, 1976).

In spite of the stability of the enzyme-FdUMP-cofactor complex, the covalent bond is of 'pseudo-irreversible' nature. That is, the covalent complex can be hydrolyzed to give the starting materials. Such reversibility had already been noticed in dialysis experiments on the enzyme complex (Reyes, 1965). A quantitative study of the reversibility phenomenon using labeled  $^3\text{H}$ -FdUMP-TS complex showed temperature-dependent first-order dissociation kinetics independent of the FdUMP concentration (Santi, 1974). From these binding studies a dissociation constant of FdUMP from the complex (ratio of  $k_{\text{off}}/k_{\text{on}}$ ) was obtained:  $5 \times 10^{-11} \text{ M}$ ,



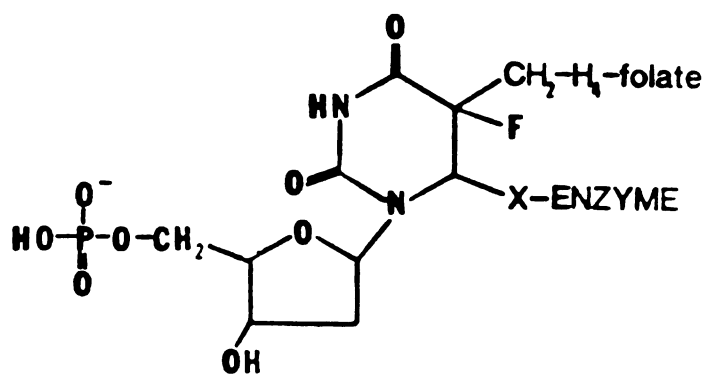


Figure II.3. Structure of the enzyme complex FdUMP-TS showing the attachment of the cofactor methylenetetrahydrofolic acid ( $\text{CH}_2\text{-H}_4\text{-folate}$ ) in 5-position and the covalent linkage of the enzyme thymidylate synthetase (TS) in 6-position.

heavily favoring the forward reaction.

Molecular Nature of the Covalent FdUMP-Cofactor-Enzyme Bonds

Considerable effort has gone into verifying the structure of the ternary enzyme complex. Early evidence showed that both  $^3\text{H}$ -FdUMP and  $\text{N}^5, \text{N}^{10}$ -methylenetetrahydrofolate were complexed with the enzyme. A peptide formed by trypsin cleavage of the protein contained both isotopes in the same peptide fragment (Danenberg, 1974). Using the cofactor analogs 5-methyl- and 10-methyltetrahydrofolate the necessity of the reactive methylene group could be demonstrated. The analogs were able to initiate the interaction between FdUMP and the enzyme, yet the complex was unstable under conditions which denature proteins. Therefore the binding was believed not to be covalent (Danenberg, 1974). However, a NMR (James, 1976) study on a pronase-generated peptide revealed the most convincing evidence for the methylene bridged structure covalently linking the pyrimidine ring to the cofactor at the 5 position.

Defining the covalent attachment between the pyrimidine ring and the active site of the enzyme proved to be difficult. The enzymatic reaction apparently was initiated by nucleophilic attack of the enzyme on the 6 position of the 5,6 double bond on the pyrimidine ring. Yet, the identity of the nucleophilic product has been controversial. It

appeared that a sulfhydryl group was essential at the catalytic site (Wataya, 1972; Danenberg, 1974, 1976). However, the specific amino acid that acts as the pyrimidine binding nucleophile has yet to be identified.

#### Thymidylate Synthetase in Rodent Tissue

Little is known about this enzyme in adult mammalian tissue, a fact which is not too surprising. Because thymidylate synthetase exclusively serves in DNA synthesis, its levels are expected to be very low in non-proliferating adult tissues.

In the earliest attempt (Maley, 1961) to measure TS activity in normal rat liver, no measurable TS activity could be detected (n=6). However, in 1969 Labow and coworkers measured the specific activity of rat liver TS to be 0.09 - 0.14 nmol dTMP/min/mg protein (n=10) with a more than a ten-fold increase when measured 12 hours after partial hepatectomy (Labow, 1969). The large variation in thymidylate synthetase basal level was due to 3 animals in which no enzyme activity could be detected. The increase after partial hepatectomy was not surprising since the rat liver can regenerate to its original size within 3-5 days. During this time new cells are produced and consequently increased DNA synthesis occurs with a concomitant necessity of the enzyme TS.

Recently thymidylate synthetase has been purified from neonatal mouse liver homogenates and the specific activity was reported as 1.4 units/mg protein in the crude homogenate (Priest, 1981). Through ammonium sulfate precipitation followed by anion exchange chromatography and affinity chromatography, it was possible to highly purify the enzyme (714 fold), although not to homogeneity. Its molecular weight was determined in the native and SDS denaturated form by gel electrophoresis. The enzyme was found to exist in a dimeric form with two equal subunits having molecular weights of about 35,000 D.

In this chapter, thymidylate synthetase originating from rat liver and spleen was evaluated after binding of the radiolabeled substrate FdUMP to the enzyme and isolating the covalent enzyme complex in order to quantify the available and functioning TS. This was necessary to assure sufficient enzyme levels in the rat liver and spleen prior to the evaluation of the therapeutic availability of the model drug FdUMP, after encapsulation in liposomes, as described in Chapter III.

## Materials and Methods

### Buffers and Solutions

The following buffers and solutions were used throughout the experimental work.

Tissue Homogenizing Buffer: In early experiments 20 mM phosphate : 10 mM 2-mercaptoethanol (pH 7.4) was employed in the formation and isolation of FdUMP-TS complex. Since phosphates in the buffer solution may interfere with the phosphate binding site on the TS enzyme, later experiments utilized 50 mM Tris-HCl (pH 7.4) : 1 mM EDTA : 10 mM 2-mercaptoethanol (=Buffer T).

Solvent for TLC: The following solvent system was used for TLC of nucleosides and nucleotides on cellulose plastic sheets (Eastman Kodak No 6064) (Ciardi, 1968):

Solvent A:	1 M ammonium acetate	30 ml
	95% ethanol	75 ml.

### Formation and Isolation of FdUMP-TS Complex In Vitro

Estimation of the available TS in rat liver and spleen as well as in the two major liver cell populations, hepatocytes and non-parenchymal cells (NPC), was carried out by incubating tissue homogenates with  $^3\text{H}$ -FdUMP and isolating the FdUMP-TS complex from the tissue cytosol by gel exclu-

sion chromatography.

#### Preparation of Tissue Homogenates

Sprague Dawley rats weighing between 215-530 g were anesthetized with ether. The liver and spleen were surgically removed, washed in saline and weighed. The tissue was immediately minced and homogenized in a Potter Elvehjem Tissue Grinder using an equal volume Buffer T containing 10% glycerol and 80-640 pmol FdUMP. Approximately 5 umole folinic acid, a precursor of the necessary cofactor methylenetetrahydrofolate, was added to the incubating mixture followed by incubation on ice for 2 hours. An aliquot of the homogenate (200 ul) was bleached with 2 volumes of 0.1 N KOH and tertiary butyl hydroperoxide, and counted for total radioactivity.

In case of the in vitro estimation of FdUMP-TS in hepatocytes and non-parenchymal cells, liver perfusion and cell separation preceded the preparation of the cell homogenate (see Chapter IV for details). The isolated cells were sonicated 3 times for 30 seconds with 1 minute cooling-periods in an ice bath. Incubation with FdUMP followed as described above.

At the end of the incubation time the cell cytosol was obtained by centrifugation at 15500 RPM = 27000g (Sorvall SS34) at 4°C for 1.5 hours. The clear cell cytosol was

immediately removed from the cell debris and stored on ice.

#### Gel Exclusion Chromatography

In the initial experiments Sephadex G-25-150 was employed (Washtien and Santi 1979), but was replaced by Biogel A 0.5m in later studies. Both gels were prepared as described in Chapter III, equilibrated and eluted with Buffer T. An aliquot of the cell cytosol (1-2ml) was applied on the column (1.5x27 cm, Sephadex G-25; 1.5x50 cm, Biogel A 0.5m), the eluent was fractionated with an automatic fraction collector (LKB, Model 2112 Redirac), and the radioactivity in each fraction was counted after the addition of scintillant.

#### Identification of FdUMP-TS

To verify the identity of the complex as FdUMP-TS, the molecular weight was first estimated using gel exclusion chromatography. Second, the dissociation kinetics of the enzyme complex were studied at different temperatures.

#### Molecular Weight Determination of FdUMP-TS

Biogel A 0.5m (exclusion limits 500,000-10,000 D) was employed. A 1.5x50 cm column was calibrated using ferritin (MW 450,000), rabbit antimouse IgG (MW 155,000), bovine serum albumin (BSA) (MW 67,000) and potassium dichromate (MW

294) as molecular standards. The elution volume of ferritin, IgG, albumin and potassium dichromate was each determined by monitoring the UV absorbance at 280 nm in a flow through UV cell which was in-line between the column and the fraction collector. The IgG was tagged with a fluorophore and the fluorescence was measured. A calibration curve was prepared by plotting the elution volume versus the log of molecular weight.

#### Dissociation Kinetics

It has previously been demonstrated that FdUMP can be released from the enzyme complex (Santi, 1974). The release rates accelerate with increasing temperature. Therefore, the FdUMP-TS complex was incubated at 0, 23, 37 and 65°C for times ranging from 1 month to 15 minutes, respectively. At intervals 300  $\mu$ l aliquots were precipitated with 1 ml ice cold 20% trichloroacetic acid (TCA), the sample was spun at 12,000 g (Eppendorf) for 3 minutes and the TCA soluble radioactivity in the supernatant was counted. Total radioactivity (control values) was obtained by substituting TCA with water. All samples were analyzed in duplicate. Semilogarithmic plots of the amount precipitated versus time were linear.



### In Vivo Quantitation of Thymidylate Synthetase

FdUrd (15 nmol;  $^3\text{H}$ -FdUrd 20 mCi/mmol) was administered to rats via tail vein injection and the animals were sacrificed after 2, 5 and 24 hours as detailed in Chapter III. The liver was removed and the cell cytosol was chromatographed as described above.

### Radiopurity of $^3\text{H}$ -Fluorodeoxyuridine Monophosphate

The commercially-available  $^3\text{H}$ -FdUMP was routinely checked for radiopurity by thin layer chromatography (TLC).

An aqueous solution of  $^3\text{H}$ -FdUMP (0.5 uCi) plus cold carrier (10 ul, 40mM) were spotted onto cellulose plastic TLC sheets (Kodak) which were then developed in solvent A. The  $R_F$  value of the cold carrier FdUMP can be recorded directly after viewing the plates. The developed TLC plates were cut into 0.5 cm strips, the cellulose suspended into 1 ml water by sonication and the radioactivity counted after addition of the scintillant PCS (Amersham).

### Measurements of Radioactive Markers

Direct Counting. Markers in aqueous media (i.e. HEPES buffered saline, Buffer T) were combined with PCS scintillation counting fluid (Amersham) at a final concentration of 10% aqueous medium and placed into 22 ml screw-cap glass counting vials. Miscibility was checked visually. Counting

was done in a Beckman LS 7800 scintillation counter (Beckman Instruments, Palo Alto, Ca.) in the external standard channel ratio mode. To correct for variable quenching, a quench curve was prepared: constant amounts of isotope were put in several vials along with scintillation fluid PCS and increasing amounts of chloroform as quenching agent. Each sample was evaluated using an external standard. The efficiency was recorded and the resulting quench curve was stored in the computer memory. Each experimental sample was then corrected for quench accordingly.

Counting After Tissue Bleaching. Tissue homogenates (0.1-0.2 ml) had to be decolorized prior to counting to avoid extensive quenching. To an aliquot of homogenate, twice the volume of 0.1 N KOH and tertiary butyl hydroperoxide were added. After thorough mixing, the samples were left standing for at least 6 hours or until they showed a faded white-yellow color. After the addition of the scintillant PCS the sample was counted.

## Results

### Evaluation of the Cellularity of Rat Liver and Spleen Tissue

Little information on the quantitative cellularity of liver tissue is available from the literature. Since the evaluation of the enzyme was based on drug-enzyme complexes formed per liver or spleen cell, the literature was reviewed for corresponding data.

Weibel (1969) reports:  $169 \times 10^6$  hepatocytes/ml liver,  $92 \times 10^6$  non-parenchymal cells/ml liver, and a liver density of 1.06g/ml. These data were derived from 8-9 weeks old rats (average body weight 173g). Recalculation gives  $249 \times 10^6$  cells/g liver.

Berg (1978) reports  $756 \times 10^6$  hepatocytes and  $299 \times 10^6$  Kupffer cells in the rat liver obtained through cell separation, representing 91.5% of the original hepatocytes and Kupffer cells (based on protein measurements). A third of the non-parenchymal cells are Kupffer cells, so the following calculation can be carried out:

$$\frac{[756 + (3 \times 299)] \times 10^6 \text{ cells/200g BW}}{0.915} = 1806 \times 10^6 \text{ cells/200g BW}$$

The rat liver amounts to 3.5% of body weight (BW), therefore the above figure corresponds to  $240 \times 10^6$  cells/g liver.

Jandle (1965) reported  $3.2 \times 10^9$  liver cells for rats with an average body weight of 407 g and an average liver weight of 14.4 g. From his report  $222 \times 10^6$  cells/g liver can be calculated.

Since these three reports differ little in their total number of liver cells and considering the difficulty of the measurements,  $250 \times 10^6$  cells/g liver will be assumed as the basis for all subsequent calculations. The quantitation of isolated cells will be based on the hemocytometer counts or protein measurements.

The spleen cellularity has also been re-evaluated. Jandle (1965) reported  $1.9 \times 10^9$  cells/0.808g spleen obtained from rats with an average body weight of 407g (range 310-510g)(n=55). The resulting  $2.35 \times 10^9$  cells/g spleen will be used in our calculations.

#### In Vitro Estimation of TS

To evaluate the availability of the enzyme thymidylate synthetase in rat liver and spleen, as well as in the two major liver cell populations, hepatocytes and non-parenchymal cells, tissue homogenates were incubated with  $^3\text{H}$ -FdUMP and the enzyme complex FdUMP-TS was isolated from the cell cytosol by gel exclusion chromatography.

### Evaluation of TS Level in the Rat Liver

A typical radioactivity versus elution-volume profile obtained through gel exclusion chromatography on Biogel A 0.5m is shown on Figure II.4. The two major peaks were the macromolecular bound radioactivity, which represented FdUMP-TS complex eluting at fractions #19-24, and radioactivity eluting with the salt peak (fractions #37-45), which included molecular weight species smaller than 10,000 D. In a few cases some radiolabeled material eluted at fractions #15-18. This elution volume corresponded to the void volume of the Biogel A 0.5m column and therefore represented high molecular weight species. This material absorbed UV light at 254 nm. When these fractions (#15-18) were analyzed for protein, the amount measured was one-third of the total protein present in the cytosol. However, the radioactivity associated with this protein was readily dissociated upon precipitation with TCA, therefore indicating an association in a nonspecific manner. In contrast, when TCA was added to fractions #19-24, more than 80% of the radioactivity coprecipitated with the protein, indicating the presence of a covalent substrate-enzyme complex.

Evaluation of the nature of the radioactivity eluting with the salt peak revealed that, although protein was present in these fractions, all the radioactivity was acid soluble. Analysing these fractions by TLC indicated the absence of FdUMP and FdUrd. The  $R_F$  values suggested the

## BIOGEL A 0.5 m COLUMN CHROMATOGRAPHY

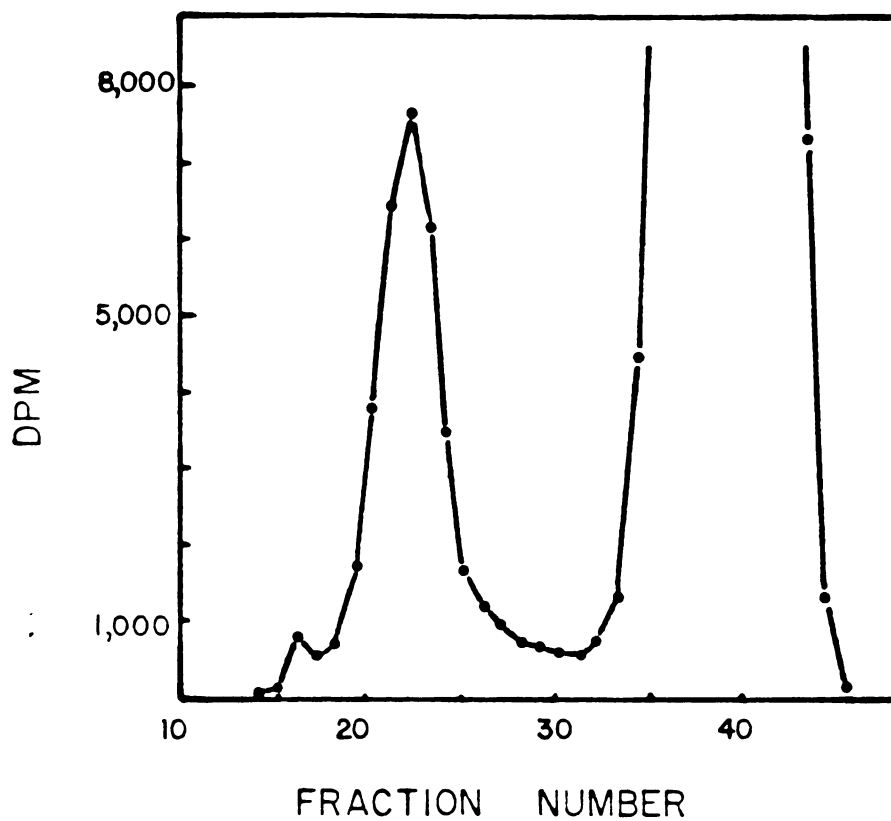


Figure II.4. A typical elution profile of tritiated radioactivity present in the liver cytosol chromatographed on Biogel A 0.5m. Fractions #15-18 represent the void volume. The enzyme complex FdUMP-TS elutes with fractions #19-24. Radioactivity associated with the low molecular weight species elutes with fractions #36-44 (salt volume).

presence of catabolic products (see metabolic scheme Figure I.2.).

From the area under the curve (AUC) of the FdUMP-TS chromatographic peak (fractions #19-24) the amounts of TS forming a stable covalent enzyme complex with FdUMP was calculated.

Under the experimental conditions 5930 FdUMP-TS complexes/liver cell were analyzed (Table II.1.). Assuming an average liver weight of 9 g, re-calculation of the above figure yielded 22 pmol thymidylate synthetase in the whole organ (Table II.2.).

Table II.3. shows the results of a series of experiments in which liver homogenates were incubated with increasing amounts of FdUMP in order to evaluate the optimum incubation conditions. This led to an increase in FdUMP-TS complex formation in vitro. However, FdUMP levels above 1 nmol did not significantly increase the enzyme complex formation, apparently due to saturation of all available thymidylate synthetase. Because of the rapid metabolic degradation of FdUMP in the incubation mixture (tissue homogenate), it was necessary to add a  $>10^4$ -fold excess of FdUMP to obtain maximum complex formation.

In two selected cases, the liver was divided into two equal portions which were incubated under identical conditions in order to evaluate the assay variability. The range of values obtained was within  $\pm 10\%$  of the mean (Table

Table II.1. In vitro quantitation of available thymidylate synthetase (TS) in liver and spleen, and in isolated liver cells. Data are expressed as number of complexes formed per cell.

		FdUMP-TS / Cell <sup>1)</sup>		
Organ <sup>2)</sup>	Liver	5930	(±2933)	(n=16)
	Spleen	1862	(± 425)	(n=5)
Isolated Cells	Hepatocytes	8906	(±5451)	(n=8)
	NPC	391	(± 221)	(n=3)

1) Values are expressed as mean (±SD),  
n signifies the number of experiments.

2) Cell count:  $2.5 \times 10^8$  cells/g liver  
 $2.3 \times 10^9$  cells/g spleen



Table II.2. Amount of FdUMP-TS complexes expressed on a molar basis as recalculated from Table II.1.

Organ	FdUMP-TS mole / g	FdUMP-TS mole / organ
Liver	$2.4 \times 10^{-12}$	$2.2 \times 10^{-11}$ 1)
Spleen	$7.3 \times 10^{-12}$	$5.5 \times 10^{-12}$ 2)

1) Average liver weight of 9.1 g ( $\pm 1.8$ )(n=26)

2) Average spleen weight of 0.75 g ( $\pm 0.1$ )(n=27)

Table II.3. In vitro measurements of FdUMP-TS complex formation in liver homogenates in the presence of increasing amounts of FdUMP in the incubation mixture. Data are expressed as number of complexes formed per liver cell.

FdUMP pmole	FdUMP-TS <sup>1)</sup>
6	369
31	893
83	1799
162	3987 <sup>2)</sup>
185	6239 <sup>2)</sup>
568	6396

Incubation time: 2 hours on ice

- 1) Enzyme complexes / liver cell
- 2) Mean values from two identical incubations; all other values are from single experiments.

II.3.).

In one experiment a comparison was made between incubation of total liver homogenate or cell cytosol with FdUMP, both obtained from the same rat in order to avoid inter-individual variation. The result showed little difference in the amount of FdUMP-TS complex formed, indicating no interference by noncytosolic constituents in the tissue homogenate.

#### Evaluation of TS Level in Isolated Liver Cells

After assessing the TS level in the whole organ it was desirable to measure its distribution between the two major cell populations in the liver: hepatocytes and non-parenchymal cells. The liver cells were separated as outlined in Chapter IV. Complex formation was then initiated in the same way as for the whole organ homogenates.

The number of cells present in the incubation mixture was estimated in two ways: (i) Cells in an aliquot of the cell suspension were counted under the microscope using a hemocytometer. At the same time, cell viability was estimated by Trypan Blue exclusion and found to be generally >80%. (ii) Protein was measured in an aliquot of the cell homogenate (for assay conditions see Chapter IV). The results were correlated with literature values for hepatocyte and non-parenchymal cell protein content (Weibel, 1969; Blouin, 1977). In general, good agreement between both

measurements was found.

In the isolated hepatocytes 8909 FdUMP-TS complexes/cell were measured. The amount of complex formed in non-parenchymal cells was lower: 391 FdUMP-TS complexes/cell (Table II.1.). The ratio of enzyme complex formed in hepatocytes and NPC correlates with both their cell volume and protein content. However, as in the whole organ, a large inter-individual variation was seen in both cell types.

#### Evaluation of Thymidylate Synthetase in the Spleen

In rat spleen homogenate 1862 FdUMP-TS complexes/cell were measured (Table II.1.). Spleen cells are generally smaller than liver cells; there are  $2.35 \times 10^9$  cells/g spleen in contrast to  $2.5 \times 10^8$  cells/g liver (Jandle, 1965; v.Moellendorf, 1969). The presence of higher enzyme level per g of tissue in the spleen relative to liver may reflect the reproductive activity in this organ. However, total amount of TS in the spleen did not exceed that in the liver (Table II.2.).

#### Molecular Weight Determination of FdUMP-TS Complex

In early experiments Sephadex G-25 was employed to separate the enzyme complex from non-bound FdUMP and its radiolabeled metabolic degradation products present in the cell cytosol (Washtien, 1979). Sephadex G-25 is a gel fil-

tration medium with an upper exclusion limit of 5,000 D, thus all molecular weight species above 5,000 D eluted with the void volume. Since the FdUMP-TS complex was reported to be about 60,000-70,000 D, a gel filtration material was sought which was capable of separating proteins in the molecular weight range of 10,000 and 150,000 D. Biogel A 0.5m is an agarose gel with good separation properties for molecular species between 10,000 - 500,000 D. A 1.5x50 cm column gave a good resolution of the four calibration marker substances: ferritin, rabbit antimouse IgG, albumin and potassium dichromate. The plot of the elution volume versus the log of the molecular weight showed the expected linear relationship (Figure II.5.). Chromatographing the total cell cytosol, or the void-volume fraction obtained from chromatographing the cell cytosol on the Sephadex G-25, the molecular weight of the enzyme complex (UNKOWN) was read from the the calibration curve. In both cases, the fractions containing the radiolabeled macromolecular species eluted at a position corresponding to 60,000-70,000 D. <sup>1)</sup> This suggested that the macromolecular-bound radioactivity represented the enzyme complex FdUMP-TS.

---

<sup>1)</sup> As an alternative method for determining the molecular weight of the enzyme complex, gel electrophoresis was carried out following the procedure described by Fairbanks (1971). However, due to the low amount of enzyme complex present in the cell cytosol and the presence of a variety of other proteins, the attempt did not yield meaningful results.

## CALIBRATION CURVE OF BIOGEL A 0.5m

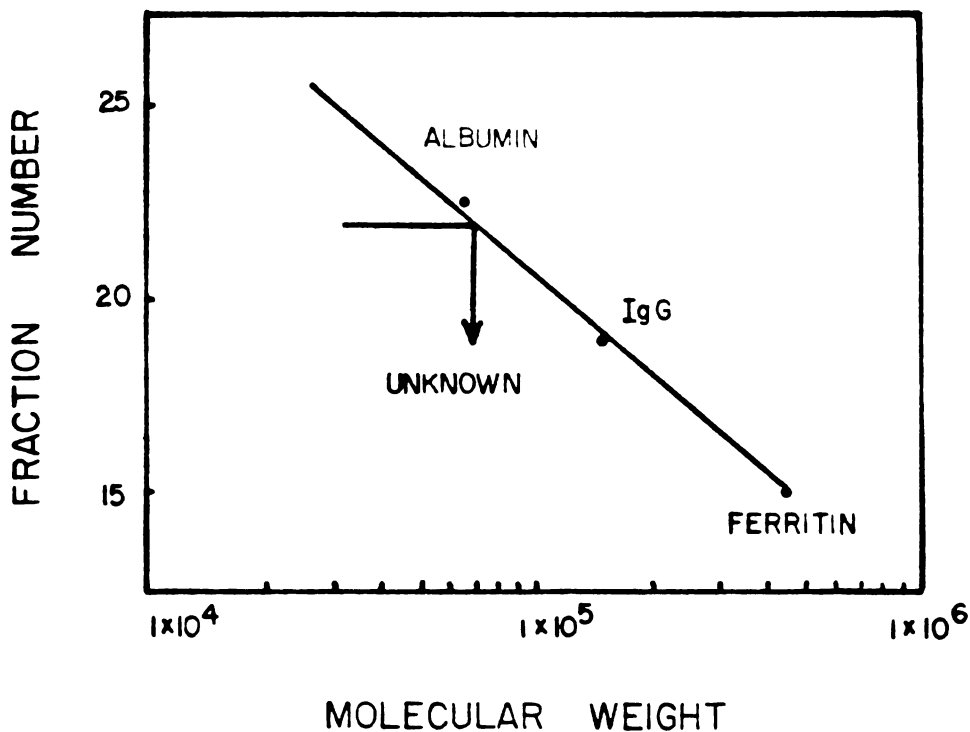


Figure II.5. A typical calibration curve for the molecular weight determination of the enzyme complex FdUMP-TS (UNKNOWN) on Biogel A 0.5m using albumin, IgG and ferritin as molecular weight standards. The macromolecular bound radioactivity (UNKNOWN) present in liver and spleen cytosol eluted corresponding to a molecular weight of 60,000 - 70,000 D, the reported molecular weight of the FdUMP-TS complex.

### Dissociation Kinetics

The FdUMP-TS complex formed in vitro and in vivo was exposed to four different temperatures (0, 23, 37, 65° C). Measuring the loss of <sup>3</sup>H-radioactivity from the complex with time yielded pseudo first-order kinetics data. Table II.4. and Table II.5. list the dissociation rate constants,  $k$ , and the half-times  $t_{1/2}$  at various temperatures and in the different tissues of FdUMP-TS origin, after formation in vitro and in vivo, respectively.

From these data an Arrhenius Plot was constructed (Figure II.6.), which showed linearity over the examined temperature range. The energy of activation ( $E_a$ ) was calculated to be 25 kcal/mol.

These results are consistent with the presence of a single molecular species. The  $E_a$  was comparable to that reported in the literature, even though the enzyme complex studied here originated from a different cell system (Santi, 1974).

### Comparison of the Amount of Enzyme Complex Formed In Vitro and In Vivo

The FdUMP-TS enzyme complex formation was studied after administration of FdUrd, the precursor of FdUMP, in vivo. The possibility was considered that during the homogenization and in vitro incubation available TS might be damaged,

Table II.4. Dissociation rate constants,  $k$ , and corresponding half-times,  $t_{1/2}$ , for the temperature dependent loss of  $^2$  FDUMP-TS complex formed in vitro in liver, spleen and hepatocyte homogenates.

Organ	Temp. °C	$t_{1/2}$	$k$ sec <sup>-1</sup>
Liver	0	9.5 d	$8.41 \times 10^{-7}$
	0	9.7 d	$8.20 \times 10^{-7}$
	0	11.9 d	$6.83 \times 10^{-7}$
Spleen	0	7.9 d	$10.13 \times 10^{-7}$
Hepatocytes	0	8.4 d	$9.56 \times 10^{-7}$
Liver	23	499 min	$2.31 \times 10^{-5}$
	23	388 min	$2.96 \times 10^{-5}$
Spleen	23	449 min	$2.56 \times 10^{-5}$
Liver	37	60 min	$1.91 \times 10^{-4}$
Hepatocytes	37	89 min	$1.28 \times 10^{-4}$
Liver	65	2.0 min	$5.76 \times 10^{-3}$
Spleen	65	2.3 min	$4.96 \times 10^{-3}$
Hepatocytes	65	3.2 min	$3.61 \times 10^{-3}$



Table II.5. Dissociation rate constants,  $k$ , and corresponding half-times,  $t_{1/2}$ , for the temperature dependent loss of FdUMP-TS complex formed in vivo in liver and spleen after administration of FdUMP containing liposomes.

Organ	Temp. °C	$t_{1/2}$	$k$ sec <sup>-1</sup>
Liver	0	5.5 d	$14.60 \times 10^{-7}$
Spleen	0	10.3 d	$7.75 \times 10^{-7}$
Liver	23	659 min	$1.75 \times 10^{-5}$
	23	595 min	$1.93 \times 10^{-5}$
Liver	37	94 min	$1.22 \times 10^{-4}$
	37	83 min	$1.38 \times 10^{-4}$
Spleen	37	75 min	$1.54 \times 10^{-4}$
Liver	65	4.9 min	$2.33 \times 10^{-3}$
	65	4.7 min	$2.45 \times 10^{-3}$
Spleen	65	3.5 min	$3.30 \times 10^{-3}$

## ARRHENIUS PLOT

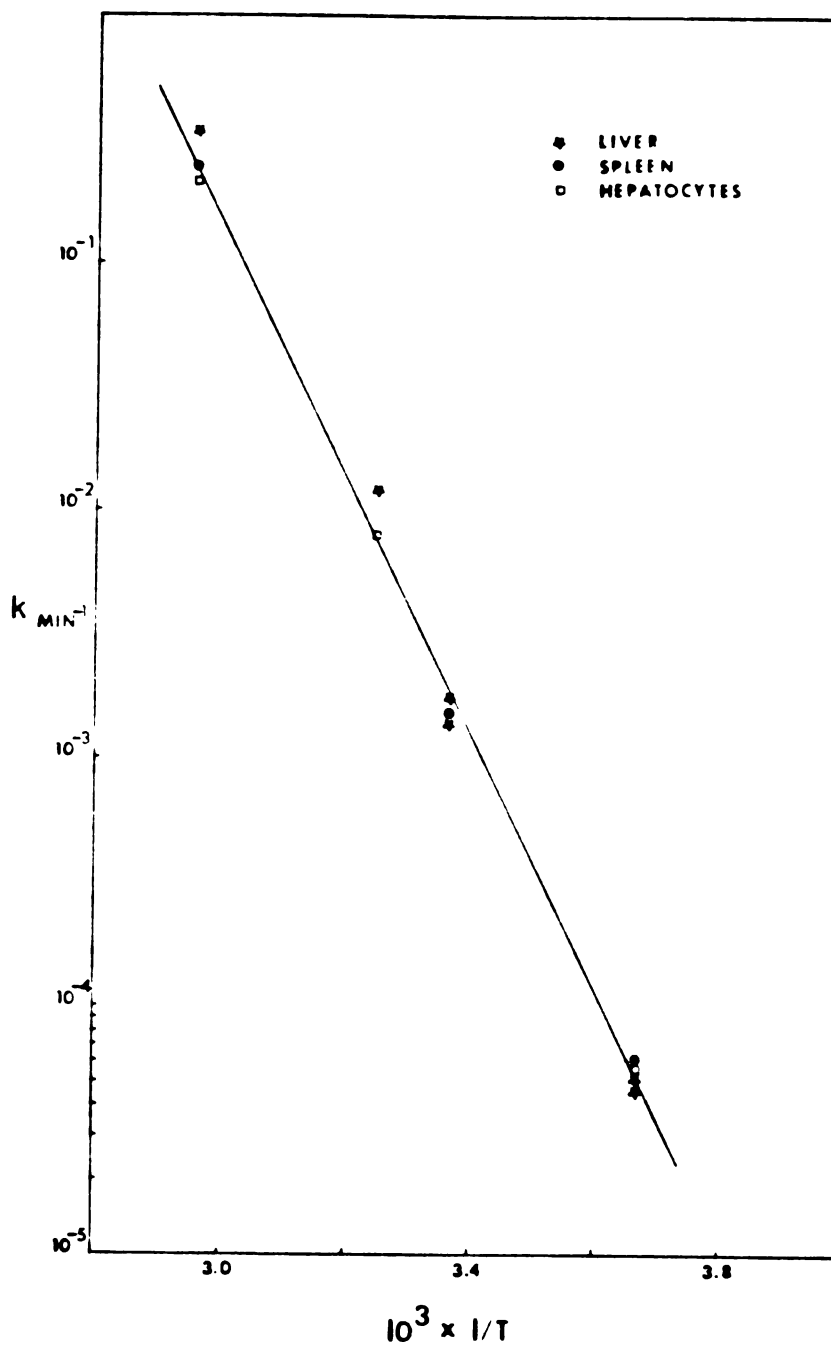


Figure II.6. The Arrhenius plot shows the linear relationship between the dissociation rate constant  $k$  of the enzyme complex and the reciprocal temperature ( $T$ ).

thereby artificially lowering the enzyme-substrate complex formation. However, the amount of FdUMP-TS complex isolated after in vivo complex formation was consistent with levels measured in vitro for both liver and spleen (Table II.6. and II.7.).

#### Radiopurity of $^3\text{H}$ -FdUMP

The  $R_F$  value of FdUMP and its hydrolytic degradation product, fluorodeoxyuridine, obtained by cellulose TLC in solvent A, were reported to be 0.19 and 0.75, respectively (Ciardi, 1968). Viewing the TLC plates under UV light revealed a single spot at  $R_F$  0.17. When the radioactivity profile was measured, a single peak having the expected  $R_F$  value of 0.17, indicating a co-migration of the radiolabeled FdUMP with the unlabeled cold carrier (Figure II.7.). In all cases the radiopurity obtained by this method was found to be >97%.

Table II.6. Number of FdUMP-TS complexes formed in the liver after administration of 15 nmol of 5-fluorodeoxyuridine in vivo.

Time (hrs)	FdUMP-TS / Cell <sup>1)</sup>		
2	5300	(±107)	(n=3)
5	5807	(±2265)	(n=3)
24	3840	(±323)	(n=2)

1) Values are expressed as mean (±SD), n signifies the number of animals.

Table II.7. Number of FdUMP-TS complexes formed in the spleen after i.v. administration of 15 nmol 5-fluorodeoxyuridine.

---

Time (hrs)	FdUMP-TS / Cell <sup>1)</sup>
2	1579 ( $\pm$ 730) (n=3)
5	936 ( $\pm$ 421) (n=3)
24	676 ( $\pm$ 90) (n=2)

---

1) Values are expressed as mean ( $\pm$ SD), n signifies the number of animals.

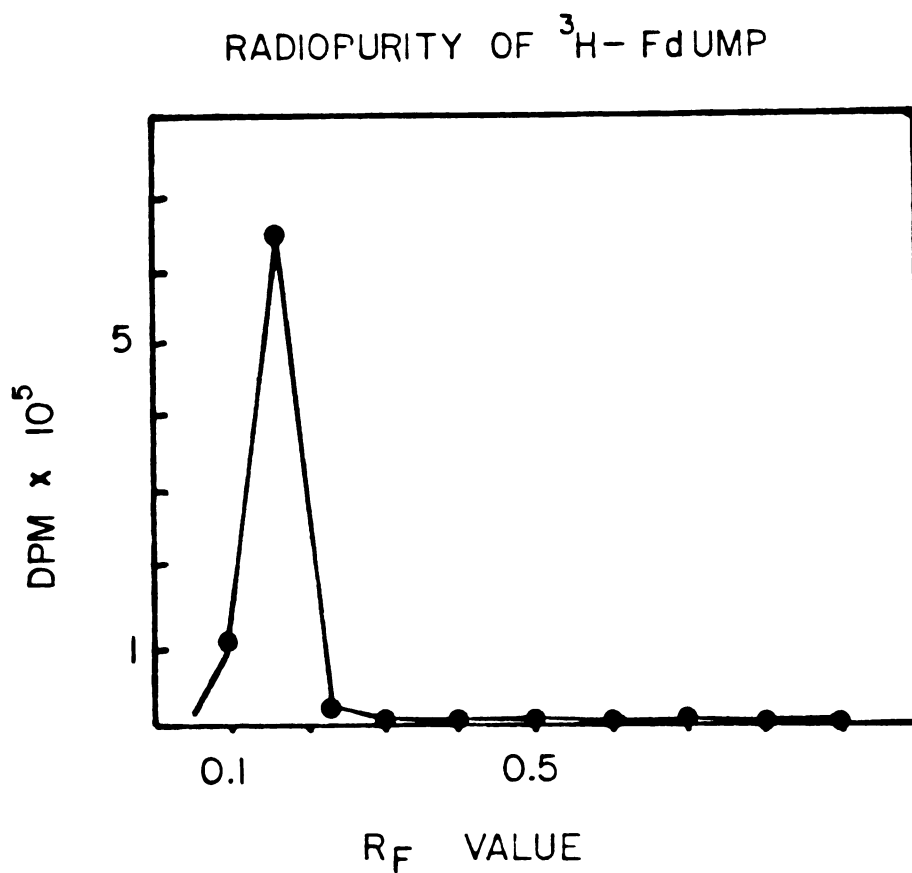


Figure II.7. Radioactivity profile of  $^3\text{H}$ -FdUMP on TLC (solvent A). The single peak at R<sub>F</sub> of 0.17 indicates the presence of FdUMP.

## Discussion

Thymidylate synthetase was known to exist and has been extensively studied in proliferating tissues. However, no quantitative evaluation of thymidylate synthetase in nonproliferating mammalian tissues has been reported prior to this study. Based on existing knowledge, low amounts of thymidylate synthetase were expected and confirmed in rat liver and spleen. Furthermore, FdUMP was expected to bind exclusively to TS yielding a single radiolabeled macromolecular species with a molecular weight of 60,000-70,000 D which was confirmed in our study.

The results indicated the availability of functioning enzyme TS in only pmol quantities/ g tissue. Thymidylate synthetase levels were higher in the spleen relative to liver (approximately by a factor of 3) which might be a reflection of the spleen's activity to produce new cells: lymphocytes and reticulocytes (Spencer, 1975).

Since in vitro and in vivo complex formation resulted in comparable quantities of thymidylate synthetase, it was concluded that the level of enzyme analyzed in the rat liver and spleen reflected the true available and functioning thymidylate synthetase.

Evaluation of the enzyme TS in isolated liver cells showed that hepatocytes contained approximately ten-fold higher levels of TS than non-parenchymal cells. Considering

the different sizes of both cell types - parenchymal cells have about 7 times the volume and about 10 times the protein content of NPC as reported in the literature (Weibel, 1968; Blouin, 1977) - both cells contained about the same relative amount of enzyme.

The results of the kinetic studies and molecular weight determination were consistent with a single radiolabeled macromolecular protein with a molecular weight of 60,000-70,000 D.

Finally, considering the overall objective of this investigation, the evaluation of the enzyme thymidylate synthetase has shown that sufficient amounts of this enzyme are present and in an active form in the rat liver and spleen to utilize the enzyme as an intracellular target for the evaluation of the therapeutic availability of liposome encapsulated fluorodeoxyuridine monophosphate (FdUMP).



Chapter III: Therapeutic Availability of a Liposome Encapsulated Drug to Rat Liver and Spleen

Introduction

In this chapter, studies were designed and performed to test the hypothesis that the therapeutic availability of a drug can be changed, e.g., increased, by use of a liposomal drug carrier. For this purpose, a unique model drug was entrapped within liposomes. The critical characteristics of the model drug were discussed in Chapter I and are briefly recalled here: (i) inability to permeate cell membranes, (ii) a short circulatory half-life and, (iii) once introduced into the cell, expression of bioactivity by covalently binding to an intracellular macromolecule. Of all the drugs we considered, only FdUMP was identified to reasonably satisfy all of these criteria. Through drug-enzyme complex formation, a direct measurement of therapeutic availability, as defined in Chapter I, was possible.

The co-encapsulation of an inert marker, inulin, in conjunction with the model drug, FdUMP, made it possible to study the mechanistic events leading to the therapeutic availability of the experimental drug. Of particular interest was the differentiation of extracellular release of liposomal content from liposome-mediated drug delivery to liver and spleen, as well as the intracellular processing of liposome-entrapped material after direct delivery. This

chapter discusses the experimental methods and the corresponding results addressing the above issues. The results indicated that by encapsulation of the model drug into liposomes the therapeutic availability of FdUMP was improved for liver and spleen.

## Materials and Methods

HEPES Buffered Saline. For the encapsulation of the aqueous space marker into liposomes a phosphate-free buffer composed of 140 mM NaCl, 10 mM HEPES (pH7.4 with 2.5 N NaOH) was used. Buffers were routinely filtered through a 0.22  $\mu$ m membrane filter before use.

### Preparation of Liposomes

The liposomes used throughout this study were mechanically dispersed multilamellar vesicles composed of phosphatidylcholine : phosphatidic acid : cholesterol :  $\alpha$ -tocopherol (PC:PA:Chol: $\alpha$ -T) in a molar ratio of 4:1:5:0.1. Prior to use, PA was extracted with chloroform from an acidic methanol solution of sodium phosphatidate. The lipid mixture in chloroform was evaporated to dryness under reduced pressure at 30°C. HEPES buffered saline containing FdUMP ( $^3$ H-FdUMP, 18 mCi/mmol) was added, the flask was purged with nitrogen and then stoppered. In double-label experiments an additional marker, inulin ( $^{14}$ C-inulin, 5 mCi/mmol) was also encapsulated. The suspension was mechanically dispersed at room temperature until all lipid was removed from the flask wall, usually 1-2 hrs. The resulting multilamellar liposomes ranged from about 0.2 to 5  $\mu$ m (Olson, 1979). To narrow the size distribution, the suspension was extruded through a 1  $\mu$ m polycarbonate membrane

(Nucleopore) under positive pressure.

### Dialysis

The removal of nonentrapped material was carried out at room temperature in a 1 ml dialysis cell equipped with a 0.4 um polycarbonate membrane (Nucleopore). Liposomes were dialyzed against an equal volume of HEPES buffered saline. The dialysate was changed 10-12 times over the 12 hour dialysis period. Removal of nonentrapped FdUMP was confirmed by measuring aliquots of the dialysate for radioactivity. Although loss of lipid material was not measured, using the 0.4 um membrane may have narrowed the vesicle size distribution by allowing the smallest vesicles to pass through the membrane pores into the dialysate (Bosworth, 1982).

### Column Chromatography

To ensure complete removal of the nonentrapped marker, a sample of the final liposome preparation was analyzed using Sephadex G-200 gel exclusion chromatography. This chromatographic system was prepared by swelling the dry powder in degassed buffered saline overnight, pouring the slurry into a column and equilibrating with 3 bed volumes of buffered saline. Packed columns were routinely stored under 0.02% sodium azide. Prior to use, the gel was equilibrated with the fresh buffer and calibrated with Dextran Blue (MW

2,000,000) as void-volume marker and potassium dichromate (MW 294) as salt marker. Void volume and salt volume were defined as minimum and maximum retention volume, respectively. UV absorbance was measured by an in-line, flow-through UV cell (LKB, Model 2138 Unicord S). After application of a sample (10 ul) of liposome preparation, the eluent was fractionated and counted for radioactivity. Liposomes eluted with the void volume, whereas residual nontrapped solutes eluted with the salt volume. Columns containing preswollen Biogel A 0.5m were prepared in the same way.

#### Quantitation of Lipid

Stock solutions of lipid and liposomal lipid were quantified by measuring the inorganic phosphate colorimetrically according to the method of Bartlett (1959), which employed the following stock solutions:

- (1) ANSA Reagent: 250 mg of 1-amino-2-naphthol-4-sulfonic acid (ANSA) were dissolved in 100 ml of 15% sodium bisulfite solution by heating. Then 500 mg of sodium sulfite were added. The solution was cooled, filtered if cloudy, and stored in an amber bottle at room temperature.
- (2) Molybdate Reagent: 2.2 g ammonium molybdate were dissolved in 25 ml of 10 N sulfuric acid. Distilled water was added to make 1000 ml of reagent which was stored in an amber bottle at room temperature.

(3) Hydrogen Peroxide Solution: 30% hydrogen peroxide was diluted to 10% with distilled water.

Assay Procedure: The sample, 10 ul, was hydrolyzed by adding 0.4 ml of 10 N sulfuric acid followed by heating at 170°C for 30 minutes. Samples found to contain more than 200 nmol of phosphorus were diluted and re-analyzed. After cooling to room temperature, 0.1 ml hydrogen peroxide solution was added and the mixture was digested for an additional 30 minutes at 170°C. After cooling again to room temperature, 4.6 ml molybdate reagent and 0.2 ml ANSA reagent were added and the mixture vortexed immediately. The mixture was heated for 10 minutes in a boiling water bath and after cooling, the absorbance was read at 800 nm.

A standard curve was prepared using a sodium phosphate solution (0-200 nmol) (Figure III.1.).

#### Liposome Stability During Storage

The long term stability of a liposome preparation, stored at 4°C, was evaluated by column chromatography. After 3, 13 and 24 days an aliquot (20 ul) was chromatographed on Sephadex G-200, and fractions were assayed as described above.

## PHOSPHATE ASSAY STANDARD CURVE

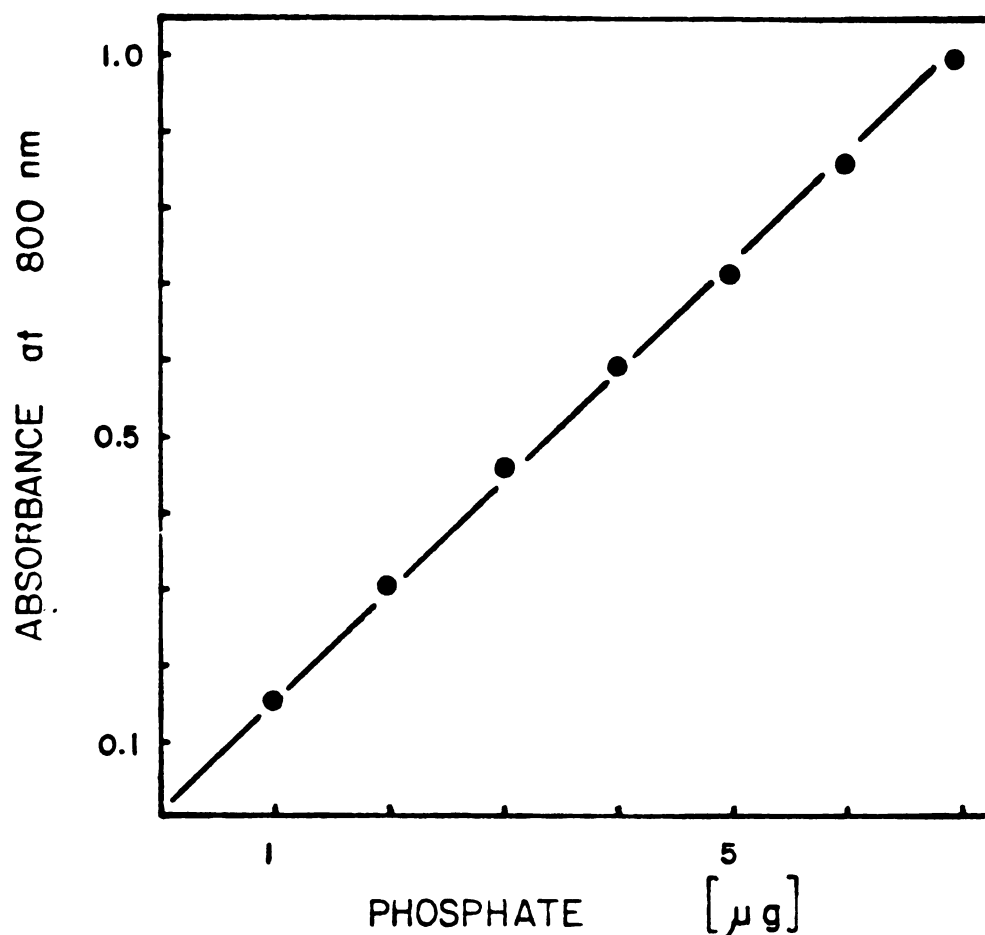


Figure III.1. Typical standard curve for the inorganic phosphate assay used for the phospholipid quantitation. Each point represented the average of duplicate determinations; in each case the range of values was covered by the height of the symbol. The range was independent of concentration.

### Stability of Liposomes in Rat Plasma

Liposomes encapsulating  $^3\text{H}$ -FdUMP and  $^{14}\text{C}$ -inulin were incubated in rat plasma at  $37^\circ\text{C}$ . Leakage of both markers (FdUMP 340 MW, inulin ~5000 MW) was measured after incubation for 2, 5 and 7 hours. Samples (10 ul) were quantified following chromatography as described above.

### FdUMP Stability After Encapsulation and During Storage

The entrapped FdUMP was tested for chemical stability by TLC after extraction of the lipids with chloroform. A sample of the extract, 20 ul, was spotted on plastic cellulose TLC plates, and developed in solvent A (95% EtOH 70 ml, 1 M ammonium acetate 35 ml). The plates were viewed under UV light at 254 nm, then cut into 0.5 cm strips and placed into scintillation vials. After addition of 1 ml water, the vials were sonicated for 5 minutes to dissolve the radioactive material, scintillation fluid (18 ml PCS) was added and the samples were then counted as described in Chapter II.

### FdUMP Stability in Physiologic Fluids

The stability of FdUMP in vitro was studied at  $37^\circ\text{C}$  in electrolyte solution (Krebs, 1932), rat plasma, and a lysosomal enzyme solution. Rat plasma was obtained by heart puncture of an anesthetized rat. The blood was immediately centrifuged to obtain a clear yellow plasma.



Lysosomal enzymes were obtained from mouse liver homogenate following differential centrifugation. The minced mouse liver was homogenized in 0.25 M sucrose, 10 mM Tris-HCl (pH 7.5), 0.1 mM Tosyl fluoride (3 ml/g liver) at 4°C using a Potter Elvehjem Teflon homogenizer (6 strokes, 700 RPM). The homogenate was centrifuged (1475 g) at 4°C for 10 minutes, and the pellet containing the cellular debris was discarded. The supernatant was recentrifuged (20,000 g) at 4°C for 30 minutes, and the pellet containing the lysosomes was resuspended in 0.5 ml of 0.15 M sodium acetate (pH 4.5). The lysosomes were stored frozen until used. Prior to use, the lysosomal suspension was freeze-thawed 3 times in order to break the lysosomal membranes and release enzymes into solution.

The incubation mixture contained 400 nmol FdUMP (1 uCi <sup>3</sup>H-FdUMP) in 0.2 ml of electrolyte solution, rat plasma or lysosomal enzyme solution, respectively. Duplicate incubation mixtures were kept at 37°C in an incubator for 1 and 2 hours for the rat plasma and the lysosomal enzymes, and for 3 hours for the electrolyte solution. At the end of the incubation, FdUMP was separated from its metabolites by TLC as previously described.

#### In Vivo Experimental Set-up

Female Sprague Dawley rats weighing 230-260 g were used. The animals were housed in the Animal Care Facility

at UCSF and received water and Purina Rat Chow ad libitum. The rats were restrained for tail vein injection which was done with a disposable Tuberculin syringe (1 cc). Liposomes were kept at 4°C until they were injected. The experimental group received a 0.5-0.6 ml liposome dose, whereas control animals were injected with free <sup>3</sup>H-FdUMP and/or <sup>14</sup>C-inulin in 0.5-0.6 ml HEPES buffered saline. Rats receiving an imperfect injection were not included in the study.

At 2, 5 and 24 hours after dose administration, the animals were anesthetized with ether, and the liver and spleen were removed. Tissue homogenization and isolation of the enzyme complex, FdUMP-TS, then commenced as described in Chapter II.

#### Identification of Radioactivity Eluting with the Void and the Salt Volume

Aliquots of the cytosol eluting with the void volume (fractions #15-18) and the salt volume (fractions 36-43)(Biogel A 0.5m) were analyzed for FdUMP and its metabolites using the TLC procedure. Aliquots of the void volume fractions were also precipitated with trichloroacetic acid (TCA) (10% final concentration) to detect the presence of radiolabeled macromolecular species other than FdUMP-TS.

## Results

### Stability of Liposomes

The leakage of encapsulated FdUMP from single-labeled liposomes upon cold storage was evaluated over 24 days. Vesicles chromatographed on Sephadex G-200 eluted with the column void volume, whereas free marker material eluted with the salt volume, well resolved from the vesicles. Figure III.2. shows the result of a typical column run. From the area under the void volume peak, which contained the liposomes, and the total radioactivity eluted from the column, the percent of entrapped FdUMP was calculated. Generally more than 90% of the radioactivity present in the liposome preparation was entrapped in liposomes. The encapsulation volume was 3.6  $\mu\text{l}/\mu\text{mol}$ .

Studying the stability of single-labeled liposomes during cold storage, it was observed that after 24 days 95% of the originally encapsulated FdUMP was still liposome-associated, indicating that the preparation was stable under these conditions.

### Leakage of Encapsulated Markers from Liposomes

Evaluating the leakage of encapsulated FdUMP and inulin from liposomes incubated in rat plasma at 37°C for 7 hours showed that 80% of the initially encapsulated FdUMP and 85%

## SEPHADEX G-200 ELUTION PROFILE

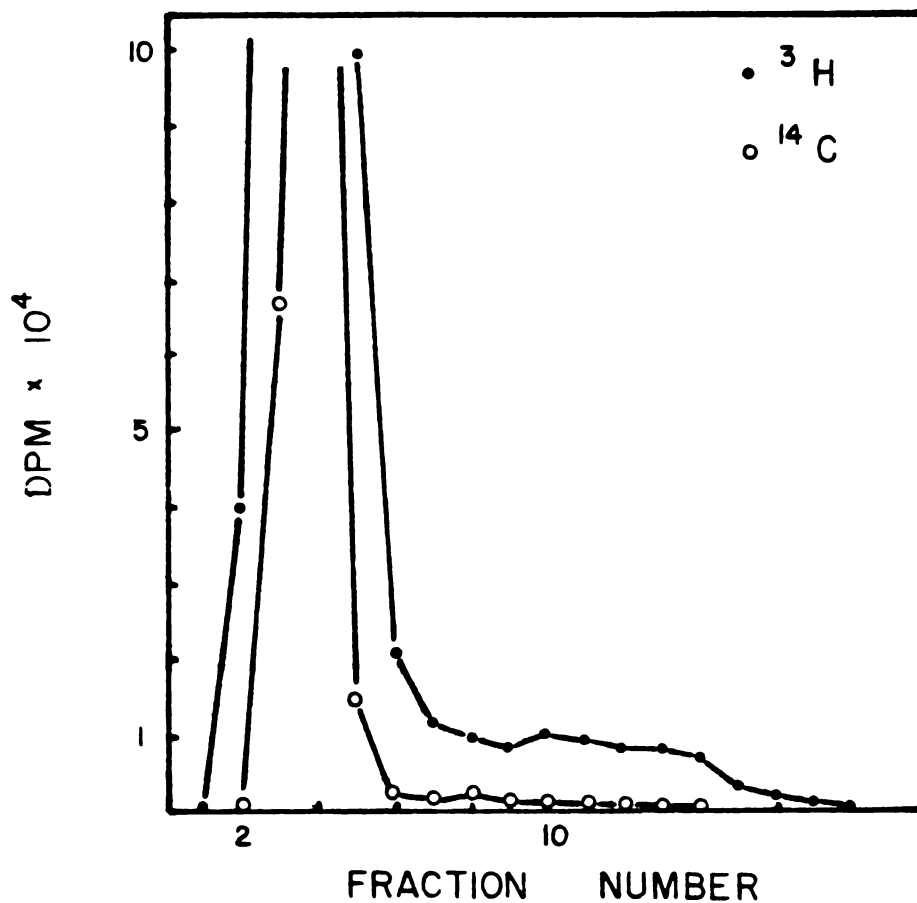


Figure III.2. Typical elution profile of double-labeled liposomes on Sephadex G-200. Fraction #2 represented the void volume. More than 95% of both markers (<sup>3</sup>H-FdUMP, <sup>14</sup>C-inulin) eluted with the void volume and were therefore entrapped in liposomes.

of the initially encapsulated inulin remained liposomally entrapped under those conditions, indicating no differential leakage from the vesicles in vitro.

#### STABILITY OF DOUBLE-LABELED LIPOSOMES IN PLASMA

Time hrs	Percent Entrapped	
	FdUMP	Inulin
0	100	100
2	85	88
5	80	86
7	80	85

#### FdUMP Stability After Encapsulation and Storage

The chemical stability of the aqueous space marker FdUMP when encapsulated and stored under the same conditions was examined by TLC following extraction of lipid material with chloroform. Tritiated radioactivity was found at a  $R_F$  value of 0.17 (Ciardi, 1968) which clearly indicated that FdUMP remained stable within the vesicles and that no hydrolytic degradation of FdUMP occurred.

#### Stability of FdUMP in Physiologic Fluids

The stability of FdUMP in physiologic fluids was assessed by incubating the nucleotide in electrolyte solution (Krebs, 1932), rat plasma and a lysosomal enzyme solution.

In both electrolyte solution and rat plasma, FdUMP was stable. A single radiolabeled spot co-migrated to the same  $R_F$  value of 0.17 as a stock solution of FdUMP. No degradation products were detected. However, incubation of FdUMP with lysosomal enzymes revealed, that after 1 hour the majority of the radioactivity (>80%, and after 2 hours >90%) migrated to an  $R_F$  value of 0.75 corresponding to FdUrd, indicating rapid hydrolysis of FdUMP. The remainder was located at  $R_F$  of 0.17, corresponding to nonhydrolyzed FdUMP. The following table summarizes the results:

STABILITY OF FdUMP IN PHYSIOLOGIC FLUIDS

	Electrolyte Solution	Rat Plasma	Lysosomal Enzymes
	%	%	%
FdUMP ( $R_F=0.17$ )	100	100	10
FdUrd ( $R_F=0.75$ )	0	0	90

Disposition of Single-Labeled Liposomes

After the administration of a liposome dose of 20-35  $\mu\text{mol}$  lipid/animal containing FdUMP (1-4 nMol,  $^3\text{H}$ -FdUMP 20 mCi/mol) or free FdUMP (1-6 nMol,  $^3\text{H}$ -FdUMP, 20 mCi/mol) to the control group, the disposition of the tritiated radioactivity was followed in liver and spleen 2, 5 and 24 hours after dosing.

Table III.1. shows the results in the liver. A 10-fold increase in drug/organ association was found at 2 and 5 hours when FdUMP was delivered encapsulated in liposomes (35% and 25% of the dose, respectively). When nonencapsulated FdUMP was administered, a much lower organ association was found (4% and 2% of the dose at 2 and 5 hours, respectively). When free FdUMP and empty liposomes were injected the results were similar to the first control group, indicating no interaction or interference in the presence of liposomal material with respect to either drug uptake or enzyme binding. Due to metabolic processes, total organ radioactivity declined in both experimental and control groups with time (data not shown).

In the spleen a trend similar to that in the liver was found. The increase of total organ radioactivity after encapsulation of FdUMP into liposomes was more pronounced, amounting to ~20-fold (Table III.2.). Although the metabolic pattern differed in liver and spleen, the decline in organ radioactivity reflected both catabolism of FdUMP and clearance from the organ.

In summary, entrapment of FdUMP in liposomes increased the association of radiolabel in both organs dramatically to values of 35% in the liver and 7% in the spleen. The total amount of <sup>3</sup>H-radioactivity after injection of free FdUMP was less than 5% of the dose in the liver and less than 0.5% in

Table III.1. Percent of  $^3\text{H}$ -radioactivity in the liver after i.v. administration of encapsulated (Liposome) or free (Control) FdUMP

% of Dose / Liver <sup>1)</sup>		
Time (hrs)	Liposome	Control
2	35.6 ( $\pm 7.2$ ) (n=9)	4.3 ( $\pm 1.9$ ) (n=9)
5	25.7 ( $\pm 7.9$ ) (n=10)	2.3 ( $\pm 0.3$ ) (n=9)
24	4.6 ( $\pm 1.9$ ) (n=4)	nd <sup>2)</sup>

1) Values are expressed as mean ( $\pm$  SD), n signifies the number of animals.

2) Not determined.



Table III.2. Percent of  $^3\text{H}$ -radioactivity in the spleen after i.v. administration of encapsulated (Liposome) or free (Control) FdUMP

Time (hrs)	% of Dose / Spleen <sup>1)</sup>	
	Liposomes	Control
2	7.4 ( $\pm 2.1$ ) (n=10)	0.3 ( $\pm 0.1$ ) (n=5)
5	3.0 ( $\pm 1.1$ ) (n=10)	0.2 ( $\pm 0.02$ ) (n=5)
24	0.6 ( $\pm 0.3$ ) (n=5)	nd <sup>2)</sup>

1) Values are expressed as mean ( $\pm$  SD),  
n signifies the number of animals.

2) Not determined.

the spleen at all times (Table III.1 and III.2.).

#### Disposition of Double-labeled Liposomes

A series of experiments using double-labeled liposomes containing  $^3\text{H}$ -FdUMP and  $^{14}\text{C}$ -inulin was carried out in order to investigate the mechanistic events involved in liposomal drug delivery in the liver and spleen.

Disposition in the Liver: In the liver the initial ratio of  $^3\text{H}/^{14}\text{C}$  was unchanged within the time period of 2 hours (Table III.3.). Subsequently, the greater part of the  $^3\text{H}$ -label was eliminated from the organ similar to results observed after dosing with single-labeled FdUMP-liposomes. Twenty-four hours after dosing, only 5% of the  $^3\text{H}$ -label remained in the liver. A different pattern was observed for the  $^{14}\text{C}$ -inulin: 2 and 5 hours after dosing, a relatively constant amount (40% of the dose) was associated with the liver, thereafter declining to about 30% of the dose within 24 hours. Since free inulin is rapidly cleared from the body via urinary excretion (see also control values), the latter inulin levels suggested either intracellular delivery and trapping or accumulation of inulin within the cell, or a mechanism by which extracellular inulin is protected from clearance, i.e. in extracellularly adsorbed liposomes.

Disposition in the Spleen: In the spleen the administration of double-labeled liposomes led to a distribution pattern similar to that seen in the liver. The initial

Table III.3. Association of radiolabel with the liver after administration of double-labeled liposomes (Liposomes) or free marker material (Control).

Time (hrs)	% of Dose / Liver <sup>1)</sup>			
	Liposomes		Control	
	FdUMP	Inulin	FdUMP	Inulin
2	40.5 ( $\pm$ 6.4) (n=3)	40.6 ( $\pm$ 9.5)	4.3 ( $\pm$ 1.9) (n=9)	0.2 (n=2)
5	22.2 ( $\pm$ 4.1) (n=3)	40.4 ( $\pm$ 6.9)	2.3 ( $\pm$ 0.3) (n=9)	nd <sup>2)</sup>
24	5.5 ( $\pm$ 1.9) (n=2)	31.6 ( $\pm$ 5.9)	nd	nd

1) Values are expressed as mean ( $\pm$ SD),  
n signifies the number of animals.

2) Not determined.

$^3\text{H}/^{14}\text{C}$ -ratio was approximately maintained over a period of 2 hours (Table III.4.). Thereafter,  $^3\text{H}$ -radiolabel declined faster than the  $^{14}\text{C}$ -label, with less than 1% of the tritium remaining in the organ 24 hours after dosing, in contrast to a remainder of 7% of  $^{14}\text{C}$ .

#### Therapeutic Availability of FdUMP

Whether or not the observed increase of  $^3\text{H}$  radioactivity in liver and spleen after FdUMP encapsulation concomitantly improved the therapeutic availability of the drug, in this case the model substance FdUMP, at the enzyme target site was tested. Table III.5. and Table III.6. present the results expressed as the number of FdUMP-TS complexes formed per liver and spleen cell, respectively.

Comparing the results of the experimental with the control group, a 2-3 fold increase in therapeutic availability of encapsulated drug can be seen at 2 and 5 hours. The covalent enzyme complex levels in the liver were 1882 FdUMP-TS complexes/cell at 2 hours and 2453 FdUMP-TS complexes/cell at 5 hours after dosing of encapsulated FdUMP (Table III.5.). The administration of free FdUMP also led to intracellular complex formation. The amounts isolated were significantly lower (971 FdUMP-TS complexes/cell at 2 hours, 819 FdUMP-TS/cell at 5 hours). At the given dose neither entrapped nor free drug was delivered in quantities sufficient to complex all available hepatic thymidylate

Table III.4. Association of radiolabel with the spleen after administration of double-labeled liposomes (Liposomes) or free marker material (Control).

Time (hrs)	% of Dose / Spleen <sup>1)</sup>			
	Liposomes		Control	
	FdUMP	Inulin	FdUMP	Inulin
2	5.3 ( $\pm 0.6$ ) (n=4)	9.6 ( $\pm 3.3$ )	0.3 ( $\pm 0.1$ ) (n=5)	0.02 (n=2)
5	2.5 ( $\pm 1.2$ ) (n=3)	8.9 ( $\pm 3.3$ )	0.2 ( $\pm 0.02$ ) (n=5)	nd <sup>2)</sup>
24	0.7 ( $\pm 0.3$ ) (n=3)	6.9 ( $\pm 1.5$ )	nd	nd

1) Values are expressed as mean ( $\pm$ SD), n signifies the number of animals.

2) Not determined.

Table III.5. Number of FdUMP-TS complexes formed per liver cell after administration of encapsulated (Liposome) and free (Control) FdUMP

Time (hrs)	FdUMP-TS / Liver Cell <sup>1)</sup>	
	Liposome	Control
2	1882 (±1086) (n=6)	971 (±371) (n=5)
5	2453 (± 620) (n=9)	819 (±567) (n=5)
24	574 (± 329) (n=4)	nd <sup>2)</sup>

1) Values are expressed as mean (± SD),  
n signifies the number of animals.

2) Not determined.

Table III.6. Number of FdUMP-TS complexes formed per spleen cell after administration of encapsulated (Liposomes) or free (Control) FdUMP

Time (hrs)	FdUMP-TS / Spleen Cell <sup>1</sup>	
	Liposome	Control
2	2833 (±1941) (n=9)	620 (±211) (n=5)
5	1498 (± 738) (n=9)	708 (±311) (n=5)
24	472 (± 213) (n=5)	nd <sup>2)</sup>

1) Values are expressed as mean (± SD),  
n signifies the number of animals.

2) Not determined.

synthetase (compare in vitro evaluation of the TS in Chapter II. Table II.1: 5930 FdUMP-TS complexes per liver cell).

In the spleen, FdUMP was delivered more effectively when encapsulated. A 2-4 fold increase in enzyme complex formation 2 and 5 hours after dosing was found (Table III.6.). As in the liver, a plateau situation was reached at 2 hours in both the experimental as well as the control group. It is noteworthy that in the spleen all available enzyme could be complexed with encapsulated FdUMP (compare in vitro data, Chapter II. Table II.1: 1862 FdUMP-TS complexes per spleen cell) which is in contrast to the results observed in the liver.

In summary, the following statement can be made: Although the therapeutic availability can be increased in both organs by using encapsulated drug, only a small percentage (<2%) of the drug was complexed with the enzyme thymidylate synthetase at any particular time. Furthermore, in the liver neither the liposomes encapsulated nor the free drug bound all available TS, whereas in the spleen maximum therapeutic availability could be achieved after entrapment of the drug into liposomes.

#### Identity of Non-Enzyme Bound Radioactivity in the Cell Cytosol

Figure III.3. shows a typical Biogel A0.5m chromatogram of a liver cytosol. The radioactive material in the eluent



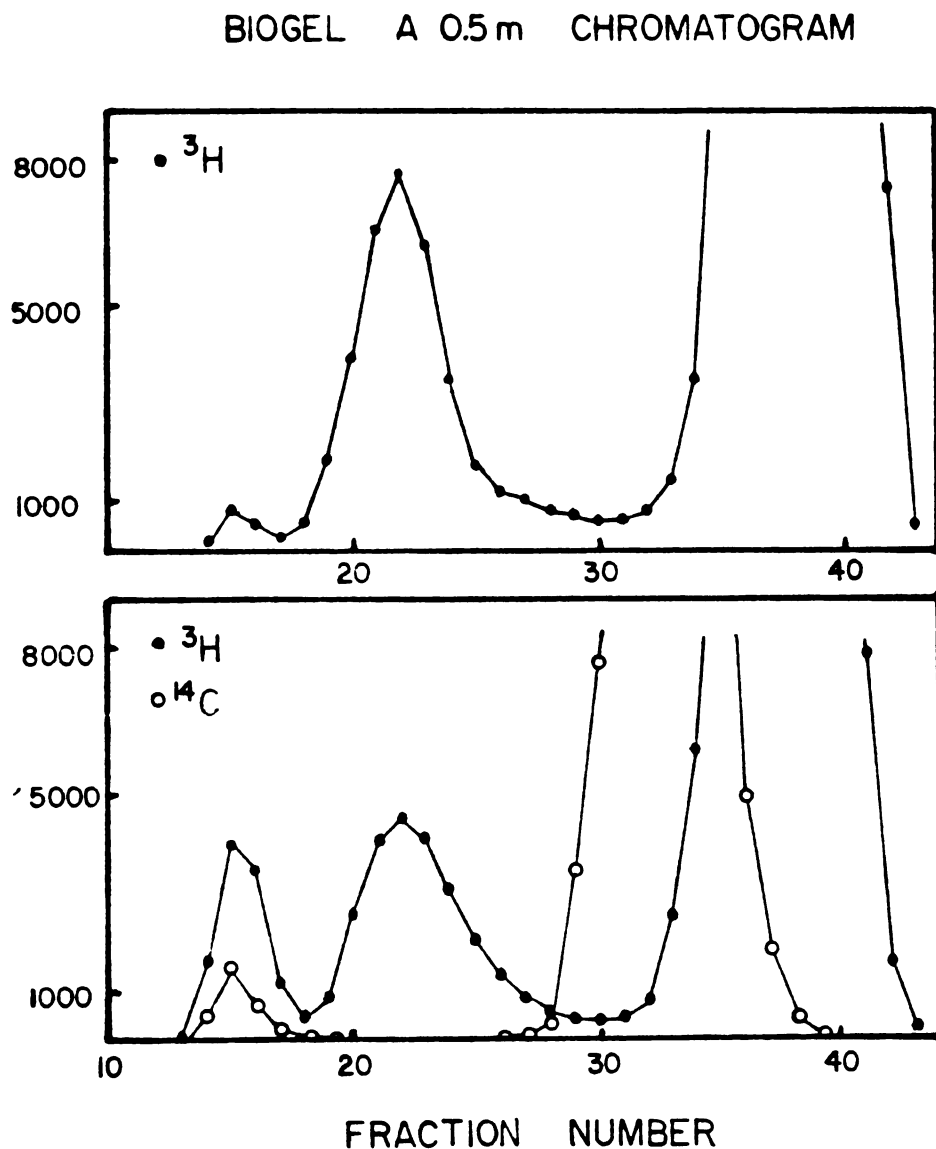


Figure III.3. A typical elution profile of radioactivity present in liver cytosol chromatographed on Biogel A 0.5m. The upper profile was obtained two hours after dosing of free  $^3\text{H}$ -FdUMP; the lower profile after dosing of double-labeled liposomes encapsulating  $^3\text{H}$ -FdUMP and  $^{14}\text{C}$ -inulin. Fractions #15-18 represent the column void volume, fractions #19-25 the enzyme complex FdUMP-TS, and fractions #35-44 the salt volume.

was fractionated according to molecular size. The lower panel depicts the radioactivity profile versus elution volume of encapsulated FdUMP, the upper panel that of free FdUMP. Fractions #15-18 (<10% of the cytosolic radioactivity) corresponded to the void volume of the column. Fractions #19-24 contained the enzyme complex FdUMP-TS (see Chapter II.) and fractions #36-43 represented the salt volume of the column. In all cases these fractions contained the major portion of radioactivity present in the cytosol.

When aliquots of the pooled void volume were chromatographed on TLC, the majority of the radioactivity in both liver and spleen cytosol represented FdUMP ( $R_F=0.17$ ). When aliquots of the same column fractions were precipitated with TCA, all radioactivity could be accounted for in the TCA soluble supernatant indicating the absence of radiolabeled macromolecular species.

When samples of the pooled salt volume were chromatographed on TLC, a different pattern was observed for each organ: The majority of the liver cytosolic low molecular weight species migrated to give an  $R_F$  value corresponding to fluoroalanine ( $R_F = 0.45$ ), the catabolic endproduct of FdUMP. In the spleen, the radioactivity associated with the low molecular weight species migrated to an  $R_F$  value of 0.75, indicating the presence of FdUrd (Figure III.4.). A summary of the results is given in the following table:

## TLC - LOW MOLECULAR WEIGHT SPECIES

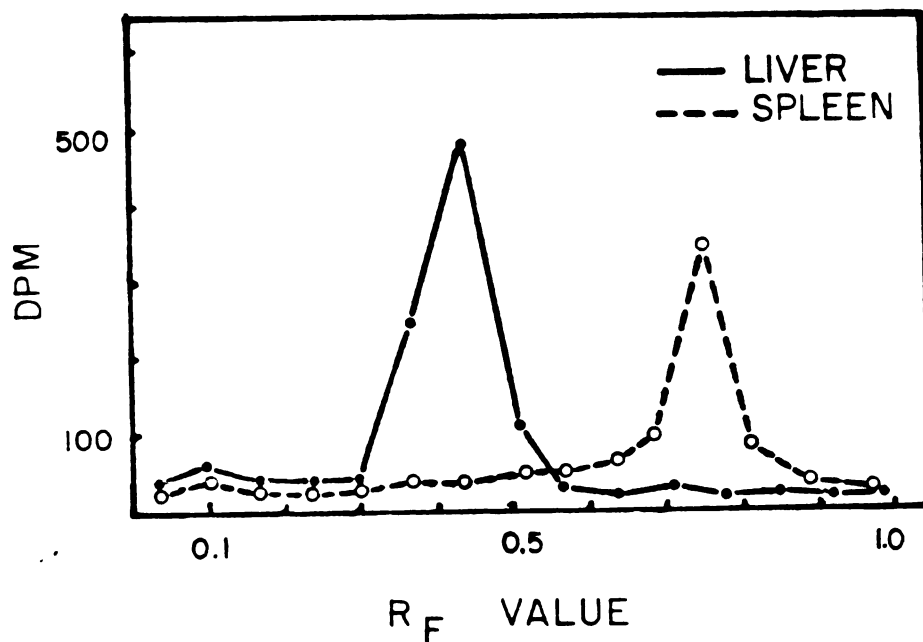


Figure III.4. A typical radioactivity profile obtained by thin layer chromatography of an aliquot of the salt volume (Biogel A 0.5m; fractions #36-44) of liver and spleen cytosol. The  $R_F$  values indicate the presence of fluoroalanine ( $R_F$  of 0.45) in the liver cytosol and FdUrd ( $R_F$  of 0.75) in the spleen cytosol.

## TLC - LOW MOLECULAR WEIGHT SPECIES

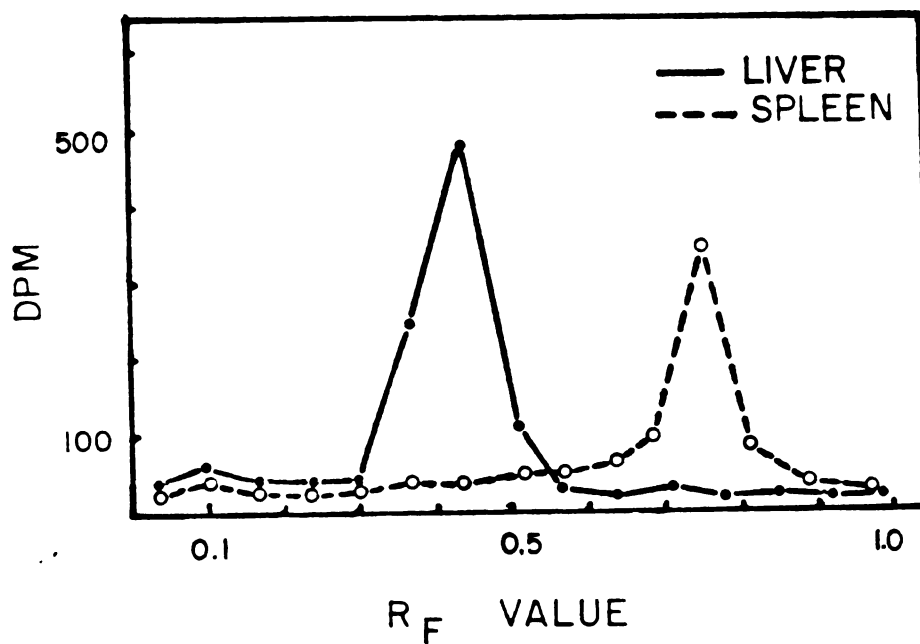


Figure III.4. A typical radioactivity profile obtained by thin layer chromatography of an aliquot of the salt volume (Biogel A 0.5m; fractions #36-44) of liver and spleen cytosol. The  $R_F$  values indicate the presence of fluoroalanine ( $R_F$  of 0.45) in the liver cytosol and FdUrd ( $R_F$  of 0.75) in the spleen cytosol.

## IDENTITY OF RADIOLABELED MATERIAL IN THE CYTOSOL

$R_F$	Species	Found in:
0.17	FdUMP	Void Volume: Liver and Spleen
0.45	Fluoroalanine	Salt Volume: Liver
0.75	FdUrd	Salt Volume: Spleen

Thus, the low molecular weight species in both liver and spleen cytosol represented catabolic low molecular weight species only: fluoroalanine in the liver and FdUrd in the spleen.

Presence of Intact Liposomes in the Void Volume

When the liver cytosol was chromatographed after administration of double-labeled liposomes the  $^{14}\text{C}$ -radioactivity profile showed two peaks: a small void volume peak and a major peak close to the salt peak. The major peak represents free inulin in the cell cytosol since inulin is metabolically inert. The  $^3\text{H}$  radioactivity profile was discussed above.

The ratio of  $^3\text{H}/^{14}\text{C}$  radioactivity in the void volume approximately corresponded to the ratio of  $^3\text{H}/^{14}\text{C}$  in the original liposome dose. Since it was confirmed by TLC that tritiated radiolabel in the void volume represented FdUMP, it was suggested that the void volume contained intact liposomes.

To confirm the presence of liposomes in the cell cytosol, liver homogenates were incubated with free and encapsulated FdUMP. After incubation with free FdUMP the void volume radioactivity was missing, the salt volume contained only catabolic products of FdUMP, mainly fluoroalanine. However, after incubation of encapsulated FdUMP with a liver homogenate ~10% of the total radioactivity eluted with the void volume. When examined by TLC, more than 80% represented FdUMP. Again, FdUMP metabolites eluted with the salt peak only.

Incubating a liver homogenate with inulin, the gel chromatogram of the cytosol contained only a single peak, close to the salt volume.

Summarizing the above discussion, the following statements can be made:

- Exposure of FdUMP to liver homogenates resulted in complete catabolic degradation of FdUMP.
- The presence of approximately 10% of the radioactivity as nucleotide FdUMP after incubation of FdUMP-liposomes with liver homogenates suggested liposomal protection against metabolic degradation.
- Elution of FdUMP with the void volume further supported the presence of intact liposomes.
- Exposure of inulin to liver homogenates and chromatography of the cytosol resulted in a single peak close to

the salt volume only.

- The presence of FdUMP and inulin in the void volume ( $^3\text{H}/^{14}\text{C}$  ratio similar as in the original liposome preparation) after in vivo administration of double-labeled liposomes strongly supported the presence of intact liposomes.

Therefore, the presence of some residual intact liposomes in the cell cytosol seemed likely. However, since most of the liposomes did not survive homogenization and chromatography after in vitro incubation, the fraction might be underestimated.

#### Incorporation of Tritiated Radioactivity into RNA

The intracellular presence of radiolabeled 5-fluorouracil might lead to incorporation of radiolabel into RNA. In our chromatographic system (Biogel), radiolabeled RNA is expected to elute with the void volume and to precipitate after exposure to trichloroacetic acid (TCA). However, it was shown that no TCA precipitable radiolabel was present in the void volume. This indicated that no FdUMP-originating radioactivity was incorporated into RNA, although the possibility of degradation of RNA during the homogenization cannot be totally excluded.

## Discussion

Based on existing literature, the following events were expected with regard to the disposition of liposomally encapsulated drug after i.v. application: retention of a major fraction of the dose in the organs of the RES, liver and spleen through initial adsorption of the vesicles to the surfaces of cells lining the vasculature. There, liposomes can (i) extracellularly leak their content which in turn might be taken up by the tissue or lost from the organ, or (ii) be taken up as intact vesicles by Kupffer cell phagocytosis. The intracellular processing would presumably proceed via the phagosomal route. This could lead to release of FdUrd from the lysosome into the cell cytosol and formation of FdUMP-TS complex. In liver, an intracellular excess of entrapped drug, relative to TS levels, might lead to extrusion of FdUrd from Kupffer cells followed by uptake of FdUrd by hepatocytes and endothelial cells, or clearance from the organ. FdUrd taken up by hepatocytes could undergo anabolic and catabolic conversion as described previously.

Clearly, when measuring drug-radioactivity associated with the whole organ, this does not provide information about the actual location of the drug or its metabolic status at any given time. Radioactivity in the total organ reflects:

- drug encapsulated within intact vesicles that are bound extracellularly to cell surfaces or located



intracellularly, whereby the drug can still be either liposome-associated, free in the cytosol or bound to the target enzyme, or

- extracellularly released drug that has been taken up by the tissue.

Thus, increased total organ radioactivity after administration of FdUMP entrapped in liposomes need not reflect an increased therapeutic availability of the drug.

Extracellular release of FdUMP from absorbed (and slowly degrading) liposomes and reabsorption of the metabolite FdUrd confounds our measures of the actual intracellular delivery by liposomes. In fact, a testable hypothesis is that this process may be the major route for FdUMP-TS formation. That this hypothesis did not hold true in this study has been shown by employing a nonmetabolizable, nonpermeable marker, inulin, in addition to FdUMP. When experiments using these two markers were performed the results did not support extracellular stable adsorption of liposomes followed by extracellular release and absorption of the drug as a predominant mechanism for the following reasons: At early times after dosing, approximately equal dose fractions of both metabolizable (FdUMP) and nonmetabolizable (inulin) markers were associated with the liver. A plateau level of approximately 30% was maintained by the nonmetabolizable marker after 24 hours, whereas the liver concentrations of metabolizable marker declined to 5%. Assuming that the

identical in vitro leakage rate for both markers applied also to the in vivo situation, a hypothetical extracellular adsorption of marker within intact liposomes would have shown both markers at a comparable plateau level. Since this was not the case and since free inulin is cleared rapidly (Jackson, 1980), it may be concluded that the inulin plateau resembled intracellularly deposited inulin. With the same reasoning it may be concluded that a comparable amount of metabolizable marker was delivered intracellularly, hence metabolized and eliminated.

However, it should be noted that the initial inulin disposition in the liver (40% of the dose in the liver homogenate) levelled off at approximately 75% of the initial value (30% of the dose) indicating some loss of inulin from the tissue. This suggested degradation of extracellularly adsorbed liposomes followed by renal elimination of the marker. Again assuming similar leakage rates of FdUMP and inulin from extracellularly adsorbed liposomes, only a small fraction of the total organ associated dose was released extracellularly, and only a fraction thereof would be absorbed following extracellular hydrolysis of FdUMP to FdUrd. The latter can also be renally eliminated (Myers, 1976). Based on the inulin data a hypothetical indirect delivery of FdUMP via extracellular release and uptake of the metabolite FdUrd would constitute only a minor delivery route.

There was further supporting evidence obtained in our laboratory, that only a small fraction of vesicles released their content into the vasculature, followed by excretion of the released material. When urinary excretion of inulin, which was entrapped in liposomes with the same lipid composition, was measured in rats two hours after dosing, only about 10% of the dose was recovered in the urine (Dr. Kiwada, personal communication). This indicated that the vesicles remained stable while circulating in the vasculature or after adsorption to the cell surfaces. It followed then that the results were consistent with our initial expectations: the majority of the drug and the inert marker were delivered intracellularly via a liposome-mediated process.

#### Therapeutic Availability of FdUMP

The evaluation of the therapeutic availability of FdUMP at the target enzyme showed that more drug was delivered intracellularly after encapsulation.

Liver: A more than 2-fold increase in enzyme complex was observed in the liver. However, the delivery of the drug via liposomes did not lead to complex formation of all hepatic enzyme thymidylate synthetase. This is consistent with the expectation that the majority of the vesicles presumably interacted with the Kupffer cells. Intracellular processing of the liposomes was followed by FdUMP-TS complex

formation in these cells. Extrusion of an excess of the drug's metabolite FdUrd from Kupffer cells relative to the enzyme TS levels might have led to uptake of FdUrd by hepatocytes and endothelial cells, but also to catabolic degradation to fluoroalanine, which was analyzed in the cell cytosol.

However, if the rate of catabolic conversion exceeded the rate of enzyme complex formation, FdUMP would be eliminated before it had a chance to bind to the target. Since these intracellular rate constants are unknown, this possibility cannot be excluded.

Taking the results from double-labeled liposome experiments into account, an attractive explanation for the results seen in the liver was that most of the FdUMP entrapped in liposomes was phagocytically delivered to non-parenchymal cells (NPC). After release from the vesicles and hydrolysis of the drug, FdUrd was

- rephosphorylated to FdUMP either binding to the enzyme TS saturating all TS in NPC, or
- excess of drug was extruded from the NPC with the possibility of uptake of FdUrd into hepatocytes, where it either underwent conversion to FdUMP with subsequent binding to TS, or was metabolically degraded to fluoroalanine.

Saturation of all NPC-TS without any complex formation in hepatocytes would theoretically result in 140 FdUMP-TS complexes/liver cell. If all liver TS is complexed we would expect to recover about 5900 FdUMP-TS per liver cell. The values measured exceeded the theoretical value for NPC binding only, but did not reach levels which would indicate saturation in both cell populations (Table III.5.). Since excess of FdUMP was delivered to NPC, FdUrd presumably was transported out of these cells and subsequently taken up into hepatocytes, forming some FdUMP-TS complex. Due to the heterogeneity of the liposome preparation the possibility cannot be excluded that some small vesicles gained access to the hepatocyte surface, where they might be endocytically taken-up. This possibility will be further discussed in Chapter IV.

If inulin uptake resulted mainly from phagocytosis of liposomes into NPC, then one must postulate that FdUMP uptake into NPC was followed by a partial transfer of FdUrd to hepatocytes to account for the therapeutic availability measured in the liver.

Spleen: In the spleen, the evaluation of therapeutic availability of the drug also showed a 2-4 fold increase in drug enzyme complex formation after entrapment of the drug into liposomes. In contrast to the liver, the amount of FdUMP-TS formed indicated that all available TS was complexed after FdUMP-liposome administration.

Unlike the liver, the morphology of the spleen has not been studied quantitatively. However, being part of the reticuloendothelial system, a certain fraction of the spleen cells are phagocytic active macrophages. Based on per gram of spleen tissue, the ability to take-up liposomes appeared to exceed that of the liver. This observation has been reported previously by Bosworth (1980).

Due to differences in metabolic capacity the low molecular weight species in the spleen cytosol were found to be FdUrd, whereas in the liver the terminal metabolic species was fluoroalanine. It is conceivable then that FdUrd was extruded from the spleen macrophages and subsequently taken up by the cells of the white and red pulp, followed by FdUMP-TS formation, thereby giving rise to the levels of enzyme complex observed.

#### Identity of Low Molecular Weight Radioactivity in the Cytosol

Since the liver - specifically hepatocytes - is highly metabolically active, it was not surprising that the small molecular weight species present in the cytosol mainly represented fluoroalanine, the metabolic endproduct of FdUMP (Figure III.4.). In contrast, in the less metabolic active spleen tissue most of the cytosolic radioactivity represented FdUrd (Figure III.4.). The competing metabolic degradation may have prevented all available hepatic TS from

complexing with the drug. This is in contrast to the results obtained in the spleen.

#### Stability of Liposomes

The stability of liposomes and leakage of encapsulated marker during cold storage was found to be minimal over the evaluated time period studied. This result was not unexpected since these multilamellar liposomes contained 50 mol percent cholesterol. Including cholesterol in the bilayer has been reported to reduce the permeability of liposomes to small molecules and to have a protective effect against induction of leakage due to liposome serum protein interaction (Black, 1976; Abra, 1980; Kirby, 1980; Hunt, 1981,1982; Senoir, 1982). This was confirmed after incubation of liposomes with rat plasma. Although two very different markers, FdUMP and inulin, were encapsulated both leakage rates were almost the same (about 3%/hour), indicating no differential leakage.

#### Stability of FdUMP in Physiologic Fluids

The nucleotide FdUMP was found to be stable in Krebs Henseleit solution as well as in rat plasma. However, once in contact with lysosomal enzymes, hydrolysis of FdUMP to the corresponding nucleoside FdUrd occurred at a rapid rate.

This did not represent an unexpected finding since the acidic pH of the lysosomal enzymes as well as the presence of lysosomal acid phosphatases promoted the hydrolytic degradation of the nucleotide. This finding was important with regard to phagocytic uptake of liposomes and intracellular processing which included exposure of the drug to lysosomal enzymes. Assuming transfer of FdUrd across the lysosomal membrane, the nucleoside FdUrd will reach the cytosol for further anabolic and catabolic utilization.

In summary, it has been shown in this chapter that the therapeutic availability of the drug in the liver and spleen was improved after encapsulation of FdUMP into liposomes. The use of double-labeled liposomes allowed us to conclude that the majority of the liposome encapsulated material was delivered via a liposome-mediated process. In the next chapter the question will be addressed which cells of the liver are involved in this liposome-mediated delivery. The distribution of FdUMP and inulin will be investigated in hepatocytes and non-parenchymal cells and the mechanistic events leading to therapeutic availability of the drug will be discussed.



Chapter IV: Interaction of Liposomes with Hepatocytes and Non-Parenchymal Cells

Introduction

Liposome clearance in the liver has been mostly ascribed to Kupffer cell activity and, likewise, to macrophage uptake in the spleen. Yet, the reports from researchers who have actually studied the intrahepatic disposition of liposomes following i.v. injection do not always conform. The involvement of hepatocytes, either directly or indirectly, has been reported by several investigators (De Barsey, 1976; Gregoriadis, 1972; Segal, 1974; Wisse, 1976; Roerdink, 1981; Rahman, 1980,1983; Scherphof, 1983). It is important to know if the parenchymal cells of the liver are capable of internalizing liposomes. Hepatocytes make up approximately 90% of the liver mass and they contain the enzyme systems which constitute the typical liver functions such as metabolic degradation, protein synthesis and glycogen storage. Due to the endothelial lining, larger liposomes should be precluded from direct access to hepatocytes. Although the endothelial fenestrae have been reported to be approximately 0.1  $\mu\text{m}$  in diameter (Wisse, 1970), the critical size for liposomes to pass through the fenestration is unknown, but may be in the range of 0.1-0.5  $\mu\text{m}$ .

The experiments described in this chapter concern the distribution of FdUMP and inulin to hepatocytes and non-

parenchymal cells in the liver. Drug and marker material were detected in both cell populations to varying degrees. The experimental drug was also available to the target enzyme thymidylate synthetase in hepatocytes and non-parenchymal cells, saturating all available thymidylate synthetase in the NPC. However, in hepatocytes less than 7% of the available TS was found covalently bound to the drug, indicating restricted access of liposomal contents to these cells.

#### Background Information

The phagocytic capability of Kupffer cells is well recognized (Dijkstra, 1983), but the ability of liver parenchymal cells to take-up particulate matter is being actively debated.

Any substance in the sinusoidal space must pass the endothelial lining to reach hepatocytes. Small molecules such as most drugs as well as endogeneous macromolecules like lipoproteins apparently have direct access to hepatocytes. For these substances the endothelial cells do not function as a barrier. The existence of fenestrae in the endothelial cell lining conceivably aids in this exchange; their size has been reported to be approximately 0.1  $\mu\text{m}$  (Wisse, 1970). It is difficult to conceive how large vesicles could be capable of squeezing through fenestrae approximately 1/5 of the vesicle size to reach the vicinity of the

hepatocyte surface. On the other hand, the plasticity of the vesicles and the dynamics of the fenestration may allow the passage of liposomes larger than the size of the fenestrae.

A number of reports have indicated a possible participation of both parenchymal and non-parenchymal cells in hepatic uptake of liposomes. However, some early studies with membrane-permeating or metabolizable marker substances (i.e., drugs) which emphasized hepatocyte delivery of liposomes have recently been revised. The employment of non-permeating and nonmetabolizable model substances, such as poly(vinylpyrrolidone) or inulin, liposome compositions which are stable in vivo (high cholesterol content), in conjunction with advances in cell separation and electron microscopic techniques have improved our understanding of liposome-cell interactions in vitro and in vivo. It should be pointed out that the fate of liposomal lipid (which in turn has often been confused with the fate of liposomes) does not necessarily allow conclusions regarding the fate of encapsulated substances and vice versa. In a series of elegant studies, the group of Scherphof and co-workers (1982,1983) have provided evidence for the presence of liposomal lipid and liposomally encapsulated inulin in hepatocytes. These studies indicated that there was a considerable shift of the lipid initially in Kupffer cells to hepatocytes with time. This type of cell-to-cell transfer has also been proposed for liposomally delivered material, such

as inulin, although the mechanisms remain unknown (Scherphof, 1982, 1983; Freise, 1980). In an effort to shift uptake of multilamellar liposomes from non-parenchymal cells to hepatocytes, the inhibition of phagocytosis in Kupffer cells with rare earth metals, lanthanum and gadolinium, did not prove successful. Roerdink et al (1981) concluded that the concomitant decrease of lipid radioactivity in hepatocytes was an argument in favor of an intermediary role of Kupffer cells in this uptake process. However, the effect of the blocking agents on hepatocytes is not fully understood (Lazar, 1973). Haley (1965) reports that a major fraction of a lanthanum dose is deposited in and eliminated from the liver via bile secretion. The impact of these substances on the animals as a whole and on hepatocytes in particular might further complicate the interpretation of the results reported by Roerdink (1981).

The dominant role of liposome size with regard to distribution of liposomes within the respective liver cell populations has been demonstrated by Rahman and co-workers (1982,1983). The hepatocyte recovery from an iron overload was more effective with small liposomes which were believed to pass through the endothelial fenestration. It was concluded that liposomes gained access to the target hepatocytes. There are alternative explanations for the removal of the iron overload which do not rely on a direct liposome-hepatocyte interaction. However, they have not

been tested rigorously.

The endocytic uptake of liposomes in cell cultures has been visualized by means of electron microscopy. Straubinger (1983) employed encapsulated gold colloid to demonstrate that liposomes can be internalized by cells via coated pits, a finding which may have importance with respect to liposomal uptake mechanisms in hepatocytes.

Based on current knowledge, one would conclude that the cellular distribution of liposomes in the liver is still controversial. At this point, it can be concluded that liposome uptake by Kupffer cells is rapid (specifically with regard to large liposomes), that uptake into endothelial cells is questionable, and that uptake by hepatocytes may be limited to small liposomes only.

This chapter describes the experimental procedure for the liver cell separation and an evaluation of liposomal drug delivery to the two major liver cell populations. The therapeutic availability of the experimental drug is assessed in non-parenchymal cells and hepatocytes. Based on the disposition of the inert marker in the isolated cells, the mechanisms of liposomal delivery, as described in the previous chapter, are discussed in light of the new results.

## Materials and Methods

The following buffer solutions were used for liver perfusions and cell separations. All buffers were routinely filtered through a 0.22  $\mu\text{m}$  millipore membrane (Nucleopore).

Calcium-free Pre-perfusion Buffer. The calcium-free buffer (pH 7.4) consisted of the following solutes: NaCl 142.0 mM, KCl 6.7 mM, HEPES 10.1 mM, 1 M NaOH 4.5 ml/L in distilled water (Seglen, 1975).

Collagenase Digestion Buffer. The following substances were dissolved in distilled water and the pH was adjusted to 7.6: NaCl 66.7 mM, KCl 6.7 mM,  $\text{CaCl}_2 \cdot 2\text{H}_2\text{O}$  4.8 mM, HEPES 100.7 mM, 1 M NaOH 66 ml/L. Prior to use, 0.05 g collagenase was dissolved in 80 ml of the collagenase buffer and filtered through a 0.2  $\mu\text{m}$  millipore membrane (Seglen, 1975).

Hanks Balanced Salt Solution (HBS). NaCl 137 mM, KCl 5.4 mM,  $\text{MgSO}_4 \cdot 7\text{H}_2\text{O}$  0.8 mM,  $\text{CaCl}_2$  1.3 mM,  $\text{Na}_2\text{HPO}_4 \cdot 2\text{H}_2\text{O}$  0.4 mM,  $\text{KH}_2\text{PO}_4$  0.4 mM were dissolved in distilled water (Hanks, 1949).

### Liver Preparation for Perfusion

Surgery. Liver cell separation was initiated two hours after dosing with double-labeled liposomes as described in Chapter III. The animals were anesthetized with ether and when deep anesthesia was reached the abdomen was opened by

cutting from the pubis to the xiphisternum and well into the flanks. After exposing the posterior abdominal wall, the vena cava was ligated above the renal vein and two loose ligatures were placed around the portal vein about 1 cm apart. Before inserting the portal vein cannula which was connected to a reservoir containing heparinized, oxygenated saline, the flow rate was adjusted to 20 drops/min. To avoid liver embolli formation, air was expelled from the cannula. After ligation of the abdominal vena cava and portal vein a small incision was made into the portal vein and the cannula, which was held in place by the third ligature, was inserted. The liver was continuously flushed with heparinized saline by gravity flow. The rib cage was then widely excised exposing the thoracic cavity. After placing a loose ligature around the inferior vena cava above the diaphragm a small incision in the right atrium of the heart facilitated the insertion of the vena cava cannula.

While the saline flush continued, the liver was removed from the donor. After dissecting the spleen, the gastrohepatic ligaments were cut without perforating the gastrointestinal tract. After dissecting the diaphragm from the posterior rib cage wall, the inferior vena cava was dissected above the right kidney just below the ligature. The liver, free from all attachments, was now transferred to a warmed humidified tray of the perfusion apparatus. The portal vein cannula was then connected to the perfusate

already slowly circulating through the perfusion circuit. The flow rate was increased to the desired flow of 30-35ml/min. The whole procedure of setting the liver up for perfusion did not take longer than 10 minutes in order to assure maximum organ viability (Ross, 1972; Ritchie, 1973).

#### Liver Cell Separation

The cells were separated according to the technique described previously (Seglen, 1975; Munthe-Kaas, 1975; Berry, 1969).

Enzymatic Digestion. Once the organ was set up for perfusion a 10-minute single-pass perfusion was initiated with calcium-free buffer to extract extracellular calcium. The appearance of radiolabel in the calcium-free buffer after passage through the liver was measured. During this period the color of the tissue became pale (blanched). The digestion of the connected tissue proceeded by perfusing the liver with a collagenase buffer for 15-25 minutes in a recirculating mode. The perfusate was oxygenated in an artificial lung to ensure maximum cell viability. Tissue swelling and "sweating" indicated a successful tissue dispersion. The liver was transferred to a petri dish and the cannulas and all nonhepatic tissue were removed. After mincing, the tissue was dispersed in 50 ml fresh collagenase buffer and gently shaken in a 37°C water bath for 10 minutes after addition of 50 ug Deoxyribonuclease (DNase) to prevent



clumping of cells due to the release of DNA from damaged cells. Cells still loosely attached to one another or to the vasculature were separated during this process. The cell suspension was filtered through 2 layers of gauze to eliminate tissue debris.

Separation of Hepatocytes and NPC. Purification of hepatocytes was achieved by sedimenting them by gravity for 10 min. The supernatant containing NPC was saved. The hepatocyte pellet was washed twice with HBS, sedimented by gravity and the final hepatocyte pellet resuspended in 1-3 ml HBS.

Non-parenchymal cells were separated from remaining hepatocytes in the supernatant by centrifugation. During a 1 minute spin (Beckman centrifuge, Model TJ-6, TH-4 rotor, 700 RPM=100 g) residual hepatocytes were pelleted. The supernatant was centrifuged again (8 min, 1600 RPM=500 g), pelleting non-parenchymal cells which were washed and resuspended in HBS.

#### Quantitation of Isolated Cells

The isolated cells were quantified by two different methods: by measuring the protein content in the cell homogenate and by counting the cells in suspension on a hemocytometer.

Protein Assay. The modified Lowry protein assay (1951) as described by Markwell (1978) was employed. This assay measured the protein content spectrophotometrically. The following reagents were used:

Reagent A: 2.0% sodium carbonate, 0.4% NaOH, 0.16% sodium tartrate and 1% sodium dodecyl sulfate in water.

Reagent B: 4.0%  $\text{CuSO}_4 \cdot \text{H}_2\text{O}$  in water.

Assay Procedure: Prior to analysis, 100 ml reagent A were mixed with 1 ml reagent B to give reagent C. To 100 ul protein sample 2 ml reagent C was added. The mixture was vortexed and allowed to set for 10 minutes. While vortexing, 100 ul Folin-Phenol Reagent was added and the mixture allowed to stand 45 minutes at room temperature for color development. Absorbance was measured at 660 nm. Samples were diluted 1:1, 1:2 and 1:4 and duplicates were assayed. Bovine serum albumin (range 0-100 ug/ml) was used as a standard and a typical standard curve is reproduced in Figure IV.1.

Microscopic Quantitation of Cell Yield: To quantitate the cells under the light microscope, the cell suspensions were generally diluted twice and aliquots were counted on a hemocytometer. Cell viability was estimated after addition of Trypan Blue (0.6% in Hanks Balanced Salt Solution).

## STANDARD CURVE FOR PROTEIN ASSAY

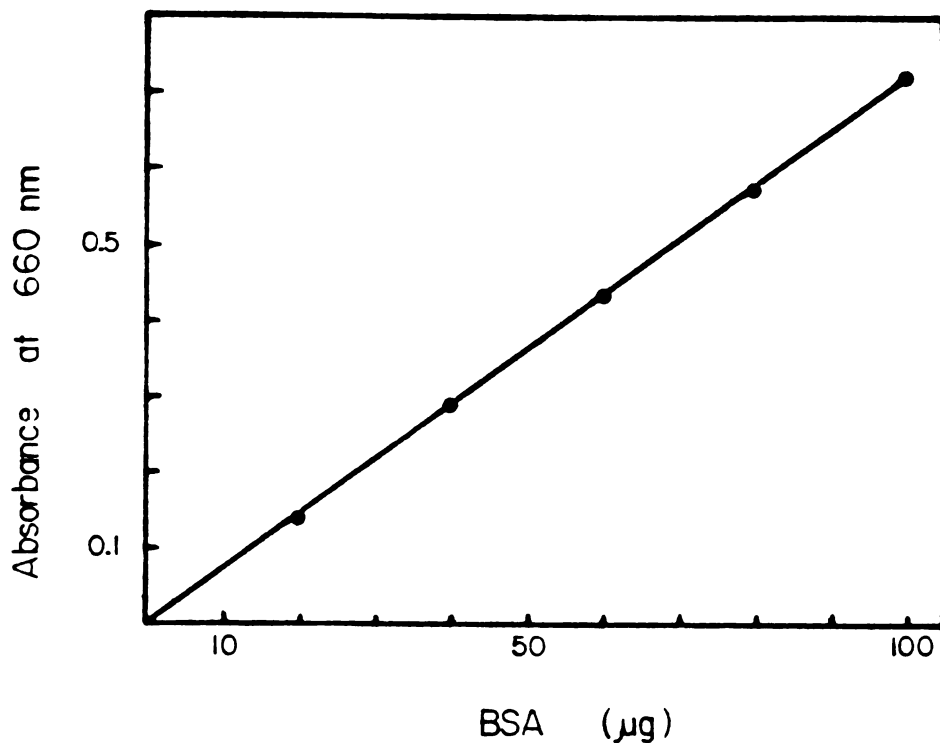


Figure IV.1. Typical standard curve for the protein assay using bovine serum albumin (BSA) as a standard. Each point represents the average of duplicate determinations, in each case the range of values is covered by the height of the symbol. The range was concentration independent.

## Results

### Cell Yield

Since not all liver cells were successfully suspended during enzymatic cell separation, the cell yield was measured by direct counting of intact, separated cells, or by protein assay. Generally, more than 55% of the liver tissue was suspended in the collagenase solution after removal of nondigested tissue debris. Calculations were based on reported liver protein measurements indicating 192 (+19 mg) protein/g liver (Knox, 1972) and assuming  $2.5 \times 10^8$  cells/g liver. The original distribution of hepatocytes and non-parenchymal cells is shown in Figure IV.2. Hepatocyte and non-parenchymal cell yield was between 15-45% and 15-30%, respectively. Hepatocytes in the parenchymal cell fraction were confirmed by light microscopy. The NPC fraction contained a mixture of Kupffer cells and endothelial cells. Viability for both cell types was generally >80% based on Trypan Blue exclusion.

### Loss of Radiolabel During Cell Separation

A considerable volume of calcium-free buffer has to be passed through the liver tissue in a single-pass perfusion during the cell separation procedure. Measuring an aliquot of the eluate revealed that the loss of liver associated radioactivity amounted to 5-10% of the tritium radioactivity

DISTRIBUTION OF HEPATOCYTES  
AND NPC IN RAT LIVER

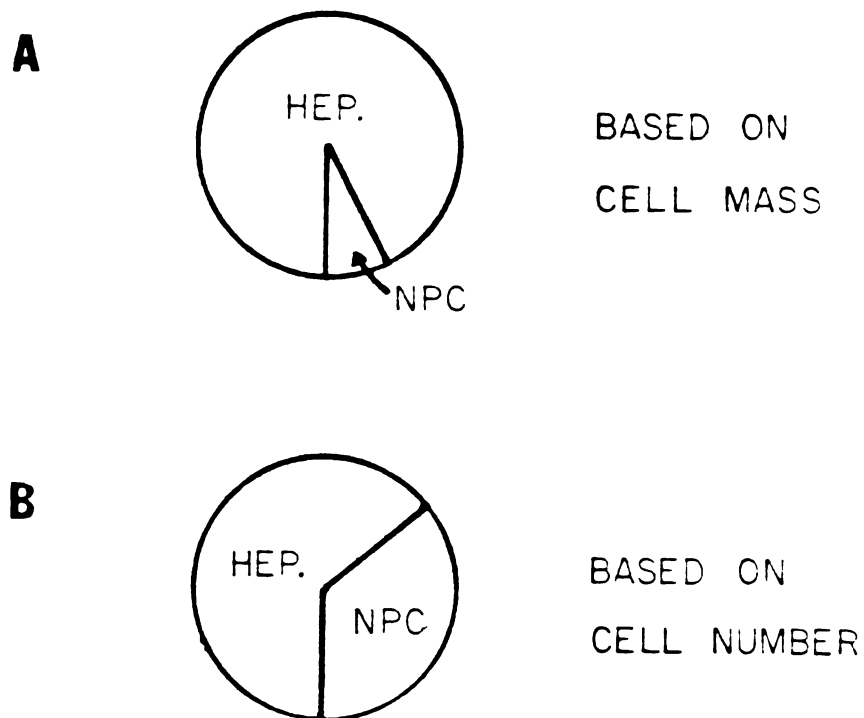


**Figure IV.2.** The distribution of hepatocytes (HEP) and non-parenchymal cells (NPC) in the liver based on cell mass (A) or cell number (B).

in contrast to less than 0.5% of the  $^{14}\text{C}$  label.

Association of Liposome Markers with Hepatocytes and Non-Parenchymal Cells

After administration of double-labeled liposomes the metabolizable FdUMP and nonmetabolizable inulin marker were measured in both cell populations: hepatocytes and non-parenchymal cells. In hepatocytes, tritiated radioactivity accounts for 18% of the dose; 19% of the inulin marker was present in the same cells. In non-parenchymal cells, 7% of the tritium label and 10% of the  $^{14}\text{C}$ -inulin label were found (Table IV.1.). When these results were normalized based on equal cell mass - hepatocytes amount to 90% of the liver tissue (dividing % of dose/hepatocytes by a factor of 9) - 2% of both  $^3\text{H}$  and  $^{14}\text{C}$  label were associated with hepatocytes and 7%  $^3\text{H}$  label and 10%  $^{14}\text{C}$  label were associated with the total mass of NPC (Table IV.2.). Although the endothelial lining was thought to be a barrier for the multilamellar liposomes, 66% of the inulin in the liver was recovered from hepatocytes (Figure IV.3.)

Therapeutic Availability of FdUMP in Hepatocytes and Non-Parenchymal Cells

Isolation and quantitation of FdUMP-TS complexes formed in both cell types 2 hours after administration of double-labeled liposomes resulted in 586 FdUMP-TS complexes/

Table IV.1. Association of  $^3\text{H}$  and  $^{14}\text{C}$  radiolabel with hepatocytes and non-parenchymal cells two hours after dosing of double-labeled liposomes. Data are expressed as % of dose per total liver hepatocytes or NPC.

	% of Dose <sup>1)</sup>		
	$^3\text{H}$ -label	$^{14}\text{C}$ -inulin	
Hepatocytes	18.8 ( $\pm 3.8$ )	19.9 ( $\pm 11.3$ )	(n=4)
NPC	7.1 ( $\pm 3.7$ )	10.1 ( $\pm 7.6$ )	(n=4)

1) Values are expressed as mean ( $\pm$ SD),  
n signifies the number of experiments.

Table IV.2. Association of  $^3\text{H}$  and  $^{14}\text{C}$  radiolabel with hepatocytes and non-parenchymal cells two hours after dosing of double-labeled liposomes. Data are expressed as % of dose per equal cell mass.

	% of Dose / Equal Cell Mass <sup>1)</sup>		
	$^3\text{H}$ -label	$^{14}\text{C}$ -inulin	
Hepatocytes	2.1 ( $\pm 0.4$ )	2.2 ( $\pm 1.2$ )	(n=4)
NPC	7.1 ( $\pm 3.7$ )	10.1 ( $\pm 7.6$ )	(n=4)

1) Values are expressed as mean ( $\pm$ SD)  
n signifies the number of experiments.



DISTRIBUTION OF RADIOLABEL  
IN HEPATOCYTES AND NPC

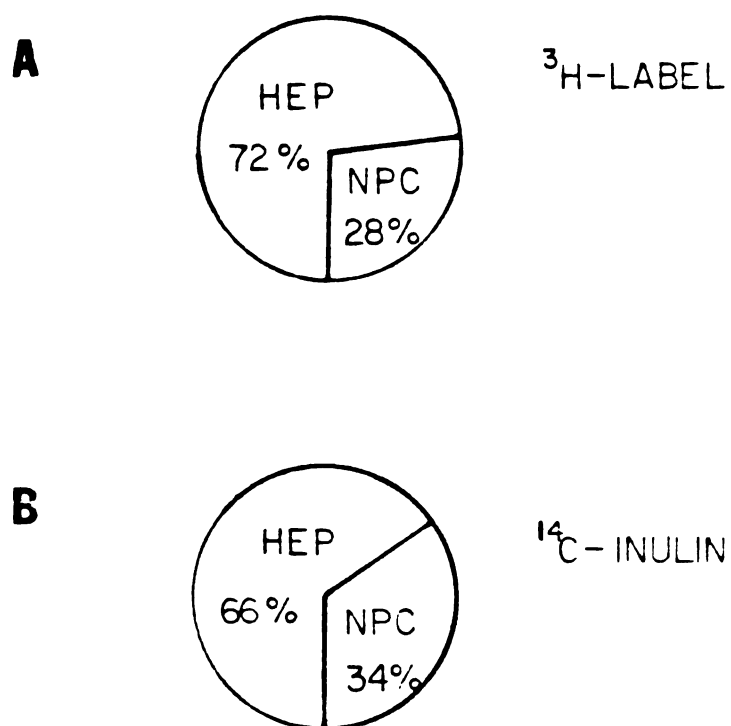


Figure IV.3. The association of both radiolabels , <sup>3</sup>H-FdUMP (A) and <sup>14</sup>C-inulin (B), with hepatocytes (HEP) and non-parenchymal cells (NPC) indicates a similar distribution of both liposome markers in both cell populations.

hepatocyte and 487 FdUMP-TS complexes/NPC (Table IV.3.). The results indicated that all available NPC-TS was complexed with the drug. In contrast, in hepatocytes less than 7% of the available thymidylate synthetase was found covalently bound with the experimental drug (Figure IV.4.).

Table IV.3. In vivo formation of FdUMP-TS complexes in hepatocytes and non-parenchymal cells separated from the same liver two hours after dosing of double-labeled liposomes.

Cell Type	FdUMP-TS / cell	1)
Hepatocytes	586 ( $\pm 207$ )	(n=4)
NPC	487 ( $\pm 456$ )	(n=4)

1) Values are expressed as mean ( $\pm$ SD),  
n signifies the number of experiments.

DISTRIBUTION OF TS AND FdUMP-TS  
IN HEPATOCYTES AND NPC

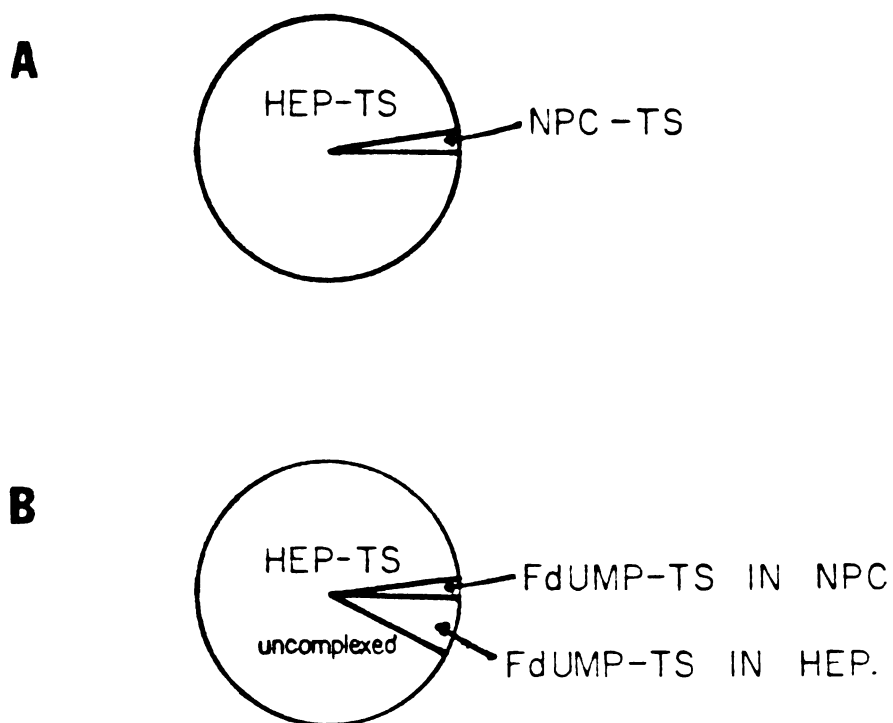


Figure IV.4. The distribution of the enzyme TS in the untreated liver as measured in vitro (Chapter II.) is shown in the upper part of the graph (A). After dosing of FdUMP encapsulated in liposomes in vivo all available enzyme in NPC is complexed whereas only 7% of the hepatocyte TS was measured as FdUMP-TS complex (B).

## Discussion

The uptake of two liposome encapsulated markers,  $^3\text{H}$ -FdUMP and  $^{14}\text{C}$ -inulin was determined in isolated liver hepatocytes and NPC. In each experiment these two major liver cell populations were separated from the same liver by collagenase digestion and centrifugation.

### Dissociation of Radiolabel During the Cell Separation

During the enzymatic cell separation, more of the tritium label (5-10% of the dose) was lost ( $^{14}\text{C}$  label: <0.5% of the dose). In a report by Gotfredsen (1982) such loss of liposomal marker material during cell separation was attributed to detachment of extracellularly bound liposomes. Our experimental data did not support such an explanation because comparable amounts of both radiolabels should have been lost from the tissue, and they were not. Thus, there may have been an efflux of tritiated FdUMP metabolites during the single-pass perfusion. We could not say if there were differences in loss from either hepatocytes or non-parenchymal cells. The lack of significant loss of inulin was consistent with this marker being intracellularly trapped. This was consistent with the argument presented in Chapter III, where inulin levels associated with the liver at later times were taken as an indication of prior intra-

cellular delivery of liposomal marker material.

Uptake of Liposomes in Non-Parenchymal Cells and Therapeutic Availability of the Drug

Both  $^3\text{H}$ -FdUMP and  $^{14}\text{C}$ -inulin were successfully delivered to NPC. Such delivery would be expected if, in fact, these vesicles behave like colloidal particles, such as carbon or gold, and are phagocytized. The phagocytic activity of NPC, mainly Kupffer cells, has been well documented (see RES, Chapter I). When the amount of radioactivity delivered to liver non-parenchymal cells was calculated as percent of dose per total NPC and compared with the radiolabel associated with total hepatocytes, only a relatively small dose fraction was associated with NPC (Table IV.1.). However, normalization for equal cell mass - NPC account for only 10% of the liver mass - revealed that 5 times more  $^{14}\text{C}$ -inulin and 3 times more  $^3\text{H}$  radiolabel was delivered to NPC than to hepatocytes (Figure IV.2.). Since FdUMP metabolites, in contrast to inulin, can efflux from the cell, the assumption that equal amounts of both markers were initially delivered to non-parenchymal cells seemed reasonable.

One goal of this investigation was to assess whether or not therapeutic availability of a drug is changed when delivered to the liver by a liposomal carrier. The therapeutically availability of FdUMP was improved. (Table

IV.3.). Kupffer cells are believed to phagocytose a major fraction of a given liposome dose. Because phagocytic active Kupffer cells constitute only about one-third of the non-parenchymal cells (the remainder being endothelial and fat storing cells) it was expected that not all NPC-TS would be found complexed with the experimental drug. However, maximum therapeutic availability was measured based on FdUMP-TS complex analyzed. Considering the fraction of the drug delivered to non-parenchymal cells (7% of the dose equals approximately  $10^{-10}$  Mol FdUMP) and the fraction thereof bound to the enzyme TS ( $6 \times 10^{-13}$  Mol FdUMP), maximum therapeutic availability could be explained by noting that there was a thousand-fold excess of the drug relative to TS enzyme levels. It is assumed that FdUrd may be transported out of Kupffer cells followed by uptake and complex formation in endothelial cells.

Measurements of therapeutic availability in separated cells after dosing of free FdUMP was omitted since less than 5% of the dose was associated with the whole organ (see Table III.1.) at any time. Because loss of tritiated radioactivity occurred during the cell separation procedure and the low liver association of tritiated radioactivity after doses of free FdUMP, quantitation of therapeutic availability was not possible, the amount present would be below

detection limits.

Liposome Interaction with Hepatocytes and Therapeutic Availability

Recovery of both radiolabels in comparable amounts from the hepatocyte compartment (72%  $^3\text{H}$ , 66%  $^{14}\text{C}$ ) was unexpected since the multilamellar vesicles (approximate diameter of 0.5  $\mu\text{m}$ ) were specifically chosen to avoid direct access to hepatocytes (Table IV.1.). Yet, about two-thirds of both radiolabels associated with the liver were recovered from parenchymal cells. However, when the data were adjusted based on the radioactivity present in a cell mass equal to the NPC cell mass, hepatocytes were apparently significantly less capable than NPC of taking-up liposomal material. A similar finding has been reported by Rahman (1982) for the distribution of another nonpermeable liposome marker - an iron chelating agent - in the mouse liver. The route by which liposomal contents were delivered to hepatocytes is still not clear. Some liposomes - specifically small vesicles - may actually gain direct access to hepatocytes. Further, material that was initially taken-up by non-parenchymal cells may be delivered via some unknown transfer processes from phagocytic cells to hepatocytes. This issue has also been addressed by Scherphof (1983).

Evaluation of the therapeutic availability of the experimental drug to hepatocytes revealed that less than 7%



of the available TS was complexed with the experimental drug whereas essentially all thymidylate synthetase in non-parenchymal cells was complexed. There was only a ten-fold excess of  $^3\text{H}$  label relative to the total amount of hepatocyte-TS ( $4 \times 10^{-10}$  Mol FdUMP associated with hepatocytes,  $10^{-12}$  Mol FdUMP bound to hepatocyte-TS complexing about 7% of the hepatocyte TS) - two orders of magnitude less than observed for NPC. This limited excess and the rapid and competitive catabolic degradation of the drug in hepatocytes might thus have precluded the achievement of higher therapeutic availability.

Proposed Mechanisms for the Uptake of Liposome Encapsulated Material into Hepatocytes

The following possibilities for the delivery of liposomal material to hepatocytes were considered:

- (1) Extracellular release of marker material from the liposomes followed by uptake of free marker.
- (2) Phagocytosis of intact liposomes into NPC as the dominant liposome uptake mechanism.
- (3) Passage of liposomes through the endothelial fenestrae.
- (4) Transport of liposomes across endothelial cells.
- (5) A mechanism whereby liposomes mimic chylomicrons or their remnants, possibly as a result of attachment of

apolipoprotein E.

Regarding (1): The same reasoning which was used against substantial extracellular leakage of both markers followed by subsequent uptake of liposomal content - in case of FdUMP, its metabolite FdUrd - also applies here. This has been discussed in Chapter III and is briefly recalled here: Comparable levels of both liposome markers FdUMP and inulin (about 40% of the dose) at early times and an inulin plateau level (about 30% of the dose at 24 hours) strongly suggested intracellular delivery of both markers as opposed to uptake of FdUrd after extracellular release from the vesicles. Therefore, extracellular release of marker material with subsequent uptake of free material has to be rejected as the dominant mechanism governing the delivery of liposome encapsulated material to hepatocytes.

Regarding (2): There is no doubt that an important fraction of the dose was taken-up phagocytically by non-parenchymal cells. However, this delivery mechanism alone could not fully account for the results observed, since about two-thirds of both labels were distributed to hepatocytes.

As for the tritium label it is conceivable that after phagocytosis the intracellular excess of FdUrd (relative to TS) was extruded from Kupffer cells and subsequently gained access to hepatocytes leading to the observed tritium levels. A shift of liposomal lipid from the primary site of

uptake, Kupffer cells, to hepatocytes has been observed by Scherphof (1982).

Evidence supporting such a transfer was reported by Thomas (1977,1978) in a different model system. Exclusive Kupffer cell uptake of the glycoprotein carcinoembryonic antigen (CEA) was initially observed by autoradiography and light microscopy. Subsequently, CEA was transferred to hepatocytes and excreted in the unchanged form via the biliary route. The actual mechanism was not understood. An indirect transfer of hydrophilic substances from Kupffer cells to hepatocytes would explain (i) the levels of tritiated radiolabel associated with the hepatocyte compartment and the therapeutic availability observed in these cells, and (ii) the observation that therapeutic availability to non-parenchymal cells was maximum.

However, such a mechanism would not explain the results obtained for inulin. If most of the liposomes were taken-up phagocytically by NPC, the inulin should remain trapped within these cells due to its physico-chemical properties. Yet, this was not observed. About two-thirds of the inulin associated with the liver were recovered from the hepatocyte compartment (Table IV.1.). Even if inulin followed the same path as FdUrd out of Kupffer cells, it would not be taken-up by hepatocytes - it would simply be eliminated. This study was not the first to observe liposome encapsulated inulin being delivered to hepatocytes. Tanaka (1975) reported a

30% and 70% distribution of liposomally entrapped inulin in hepatocytes and NPC, respectively, 15 minutes after dosing. More recently, Scherphof (1983) reported a distribution of inulin within non-parenchymal cells and hepatocytes similar to the findings in this study. According to Scherphofs results, there was not only a recovery of inulin from hepatocytes, but there was a shift of inulin radiolabel from NPC to hepatocytes with time (1 - 6 hours), which had previously been observed only for liposomal lipid. No mechanistic explanation was offered for this apparent translocation by the respective authors.

Concluding from the discussion above, phagocytosis of liposomes into NPC clearly cannot be regarded as the only mechanism governing the hepatic clearance of liposomes.

Regarding (3): For liposomes to gain direct access to hepatocytes it is necessary that the vesicles cross the endothelial lining. Microscopic studies have revealed that this lining is discontinuous and contains fenestrae with an average diameter of 0.1  $\mu\text{m}$  (Wisse, 1970). The multilamellar liposomes used in this study were specifically chosen to preclude a direct access to hepatocytes. However, due to the heterogeneity of the liposome preparation, a fraction of the liposome preparation may pass through the fenestration. Yet, this fraction was believed to be negligible. Even if liposomes can reach the hepatocyte surface, how would these vesicles deliver their content to these cells, which are

reported not to be phagocytic active? A discussion of this question follows.

Regarding (4): When liposomes pass through the liver, vesicles will adsorb to cell surfaces of all sinusoidal cells, Kupffer and endothelial cells. The adsorption to the Kupffer cell surface probably resulted in the phagocytic uptake of liposomes. In contrast to Kupffer cells, endothelial cells have little, if any, phagocytic activity (Roerdink, 1981). However, endothelial cells have been reported to actively participate in vesicular transport. In an electron microscopy study it was observed that low density lipoproteins were transported across arterial endothelial cells (Stein, 1973). A similar transport mechanism was also proposed to account for the uptake of chylomicrons by mamillary glands (Scow, 1976). Characteristically, the material was translocated in a plasma membrane surrounded vesicle and traversed the cytoplasm of the endothelial cells without being exposed to it. It is conceivable that by such an endothelial transport mechanism liposomes might be shuttled into close proximity with hepatocyte surfaces. We know that holes - fenestrations - are always present on hepatic endothelial cells, and that they are numerous. A possibility is that after binding to endothelial cells, the liposome is 'rolled' or 'moved' along the cell surface and through a nearby fenestrae. The liposome may or may not arrive on the other side intact. The

possibility of intact liposomes to be then taken-up by hepatocytes, however, must be rejected in absence of any evidence for phagocytic activity in these cells. If during the endothelial transport process liposomal contents - specifically inulin - were released from the vesicles there is no reason that a large fraction should be taken-up. It should equilibrate with hepatic plasma and subsequently, be excreted in urine. Fluid-phase pinocytosis, which is continuously occurring at hepatocyte surfaces might offer a partial explanation. However, if significant amounts of inulin were taken-up by fluid-phase endocytosis into hepatocytes, liver levels of inulin after administration in its free form should be much higher than those observed in our experiments and those by others (Abra 1981; Scherphof, 1983; Jackson, 1980). The prolonged, constant, direct exposure of free inulin to hepatocyte surfaces may be a necessary and important factor for significant fluid-phase pinocytosis-mediated uptake to occur. Although it seems unlikely that such a mechanism would account for the uptake seen, this hypothesis could be tested by dosing inulin as a slow infusion.

Regarding (5): The liver has the ability to remove chylomicron remnants from the circulation (Cooper, 1978). Recent evidence indicated that chylomicron remnants contain apolipoprotein B and E (Windler, 1980) and that apolipoprotein E receptors on the hepatic surface recognize and initiate chylomicron remnant uptake (Sherrill, 1980). Because

liposomes interact with plasma proteins it is conceivable that apolipoprotein E might attach to the vesicle surface. Thereby liposomes might be mistaken for chylomicron remnants and be taken-up or 'processed' by the receptor-mediated process. This may be an explanation for the observed inulin levels although it would seem that the vesicles would have to become smaller or be subdivided in order to reach the hepatocyte surface. To test this hypothesis one could coat liposomes with apolipoprotein E and follow their distribution and the fate of their contents in the liver.

## Chapter V: Conclusions

The objective of this research was (i) to investigate if a change in therapeutic availability of a drug can be brought about by the liposomal drug delivery system and (ii) to evaluate the mechanisms of the liposome-mediated drug delivery. A unique model drug, FdUMP, which - by itself - cannot cross cell membranes was encapsulated. Once delivered intracellularly, FdUMP exerts bioactivity by acting as a suicide substrate for the intracellular enzyme thymidylate synthetase, forming a covalent drug-enzyme complex, FdUMP-TS.

Experiments were designed to measure the therapeutic availability of the drug in the rat liver and spleen by administering tritiated FdUMP-liposomes and free FdUMP. The therapeutic availability was defined in this study as the fraction of a dose being complexed with the intracellular target enzyme or alternatively, the number of FdUMP-TS complexes formed per cell. The therapeutic availability of the free drug served as a reference. Furthermore, the mechanistic events leading to therapeutic availability of the model drug were investigated by co-encapsulation of an inert marker,  $^{14}\text{C}$ -inulin. Specific emphasis was placed on the differentiation of liposome-mediated drug delivery processes from uptake of the drug in the form of its metabolite after vascular release from the vesicles.



The liposomes used in this study (PC:PA:Chol:a-T, 4:1:5:0.1 molar ratio) did not significantly release their contents after exposure to physiologic fluids. This stability has been observed for liposomes with a high cholesterol content in vitro (Black, 1976; Kirby, 1980; Senior, 1982), and has been confirmed in this study in vivo as well as in vitro.

By measuring the association of a radiolabel in the whole organ, the assumption is often made that the therapeutic availability can be predicted. However, therapeutic availability within the liver and spleen was not a constant fraction of total organ radioactivity, for either free or encapsulated drug, no matter when therapeutic availability was measured after dosing. The decline of tritiated radioactivity in the liver with time did not reflect the actual changing hepatic therapeutic availability of the drug. In liver the trends were opposite: total organ radioactivity declined while the therapeutic availability increased slightly with time (Table V.1.). Therefore, measurement of the drug associated with a tissue cannot be used as an estimate nor a prediction of therapeutic availability.

Administration of entrapped drug increased the therapeutic availability in the liver as well as in the spleen (Table III.5 and 6). However, with the dose given, maximum therapeutic availability could not be reached in the liver. This was not surprising since only Kupffer cells which con-

Table V.1. Association of  $^3\text{H}$  radioactivity with the whole organ and therapeutic availability of the drug after administration of FdUMP encapsulated in liposomes.

FdUMP-Liposomes <sup>1)</sup>		
Time (hrs)	% of Dose	FdUMP-TS / Liver Cell
2	35.6 ( $\pm 7.2$ ) (n=9)	1882 ( $\pm 1086$ ) (n=6)
5	25.7 ( $\pm 7.9$ ) (n=10)	2453 ( $\pm 620$ ) (n=9)
24	4.6 ( $\pm 1.9$ ) (n=4)	574 ( $\pm 329$ ) (n=4)

1) Values are expressed as mean ( $\pm$ SD)  
n signifies the number of experiments.

stitute a small fraction of all liver cells (Figure IV.2.) are phagocytically active. The Kupffer cells were expected to account for the majority of liposomal removal from the blood passing through the liver.

Yet, after cell separation, a varying extent of therapeutic availability of the experimental drug was observed in both cell types. In non-parenchymal cells, maximum therapeutic availability was achieved, a fact that clearly supported the argument that NPC are involved in the liposome-mediated drug delivery. But the experimental drug was also therapeutically available to hepatocytes, although less than 7% of the thymidylate synthetase present in these cells was complexed. Rapid catabolic degradation of the drug in hepatocytes might have prevented a higher therapeutic availability.

In the spleen the situation was different. Maximum therapeutic availability was achieved. This presumably resulted from phagocytic uptake of liposome encapsulated drug by macrophages. Any excess of drug (relative to TS levels) may have been extruded from these cells in the form of FdUrd which, in turn, could have been taken-up by other spleen cells. Maximum therapeutic availability was reached in the spleen because, unlike in hepatocytes, there was no significant, parallel metabolic competition for the drug.

The mechanistic events leading to liposome-mediated drug delivery of each label were studied in the two major

liver cell populations. The extent of inulin association with hepatocytes was unexpected. About two-thirds of the inulin in the liver was recovered from the hepatocyte compartment, the remainder was in non-parenchymal cells (Figure IV.3.). The mechanism for the inulin delivery to non-parenchymal cells was readily explained by phagocytosis of liposomes. The mechanism(s) for inulin uptake and delivery to hepatocytes, however, has been difficult to identify. Various possibilities have been considered, and several mechanisms have been eliminated based on evidence presented in this study. The remaining proposed mechanisms for the delivery of an inert marker to hepatocytes do not involve Kupffer cell phagocytosis. It would be very important to analyze what exactly these mechanisms are and whether or not these uptake mechanisms necessitate that all liposomal material passes through the lysosomes, which is the case after Kupffer cell phagocytosis. Given that there are quite distinct mechanisms for the removal of liposomes from the blood, future studies should address the question how changes in liposome characteristics (i.e., cholesterol content, surface properties, size) may effect the fraction processed by nonphagocytic uptake routes.

We were not able to identify the route by which the inulin was delivered to hepatocytes. However, the idea that phagocytic removal of liposomes by Kupffer cells is the dominant mechanism governing liposome clearance from the circu-

lation - an idea that appears to be widely accepted - must be seriously re-evaluated in light of the data presented here and that being recently collected in other laboratories (Scherphof, 1983; Rahman, 1983)

Appendix: Synthesis of 5-Fluoro-2'-deoxyuridine-5'-<sup>32</sup>P  
-monophosphate (<sup>32</sup>P-FdUMP)

Introduction

The synthesis of the nucleotide <sup>32</sup>P-FdUMP from the nucleoside flourodeoxyuridine (FdUrd) (Figure A.1.) was initiated because there was the potential that important questions concerning liposome-cell interactions and liposome mediated delivery of entrapped material could be answered. Technical problems, however, precluded us from reaching our goal.

Although the radiolabeled material was not commercially available, an enzymatic synthesis of tritiated FdUMP from tritiated FdUrd has been published utilizing thymidine kinase (TK) as catalytic enzyme and adenosine triphosphate (ATP) as phosphate donor (Wataya, 1977). Since the enzyme thymidine kinase required for the conversion of FdUrd to FdUMP was also not commercially available, it was necessary to isolate thymidine kinase prior to FdUMP synthesis following a procedure described by Okasaki (1964) with modifications according to Burgess (1975).

Rationale for Entrapping <sup>32</sup>P-FdUMP into Liposomes

Various possible modes of liposome-cell interactions were outlined in Chapter I. By using liposome encapsulated <sup>32</sup>P-FdUMP, the following questions could be addressed:

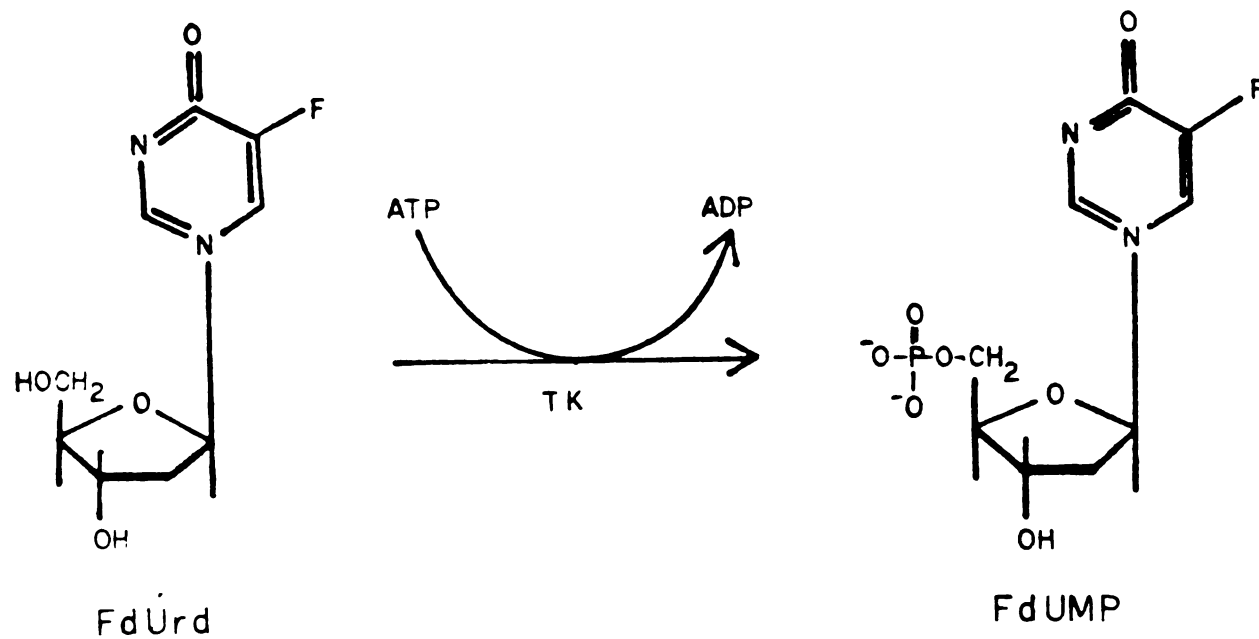


Figure A.1. Reaction scheme for the enzymatic conversion of 5-fluoro-2'-deoxyuridine (FdUrd) to 5-fluoro-2'-deoxyuridine-5'-monophosphate (FdUMP) by thymidine kinase (TK) utilizing adenosinetriphosphate (ATP) as phosphate donor.

- Does phagocytic uptake of intact liposomes represent the major mode of liposome drug delivery?
- Does extracellular release of drug from liposomes and subsequent uptake of free drug account for a sizable fraction of liposomally delivered drug?
- Are liposomes capable of delivering entrapped material directly into the cell cytosol in vivo?

The phagocytic uptake of liposomes exposes entrapped FdUMP to lysosomal enzymes, which presumably would result in release of FdUrd into the cytosol as discussed in Chapter I. It has been shown that FdUrd can be rephosphorylated intracellularly prior to binding to thymidylate synthetase (TS). Due to loss of the radiolabeled  $^{32}\text{P}$ -phosphate group, this mode of delivery would yield unlabeled FdUMP-TS. The inorganic  $^{32}\text{P}$ -phosphate ( $^{32}\text{P}_i$ ) is expected to enter the endogeneous phosphate pool. The probability of intracellular rephosphorylation of FdUrd to FdUMP with  $^{32}\text{P}$ -phosphate was considered negligible. The released  $^{32}\text{P}_i$  should be readily diluted throughout the total body water at least throughout total cellular phosphate pool.

After leakage of drug from the vesicles in the vasculature, FdUMP can be either rapidly excreted in urine or hydrolyzed to FdUrd by cell surface phosphorylases (Jung, 1982). FdUrd, in turn, can enter the cell via the transport protein and undergo the anabolic and catabolic conversions discussed in Chapter I. However, neither FdUrd nor the



resulting FdUMP-TS would then be radiolabeled.

The only route which would result in a  $^{32}\text{P}$ -FdUMP-TS complex, would be the direct cytosolic liposomal drug delivery. FdUMP delivered directly into the cytosol could bind to the enzyme TS without further conversion. Since the direct cytosolic delivery route presumably represents the least likely delivery mode, it was necessary to obtain a  $^{32}\text{P}$ -labeled FdUMP with relative high specific activity. Furthermore, the encapsulation of a relative large amount of drug was necessary in order to be able to measure the fraction of the enzyme complex which might be labeled.

#### Theoretical Considerations

Before starting the synthetic work, calculations were carried out to estimate the amount of  $^{32}\text{P}$ -FdUMP necessary for successfully conducting the experiments proposed to answer the objectives stated above. The following assumptions were made: The conversion of FdUrd to FdUMP would proceed with a 70% yield. During the liposome preparation 10% of the dispersion fluid containing the radiolabeled drug would be entrapped. After in vivo administration of  $^{32}\text{P}$ -FdUMP liposomes, 10% of the drug delivered to the liver would enter the cell via the cytosolic route. The amount of drug finally binding to the enzyme would be at least 0.5% of the total dose. Finally, the maximum amount of cytosol which could be applied on the gel exclusion column, would be

approximately 5% of the liver cytosol.

From these assumptions 0.0025% of the dose must be labeled in order for the FdUMP-TS complex to be above detection limits. It follows that  $10^8$  dpm  $^{32}\text{P}$ -FdUMP must be administered per animal. Taking 10% entrapment during liposome preparation into account and the requirement for 6 animals (3 time points, duplicates) 3 mCi  $^{32}\text{P}$ -FdUMP would need to be synthesized. Since the optimum reaction conditions operate with a 7:1 surplus of ATP over FdUrd, the reaction should be carried out starting with 30 mCi  $^{32}\text{P}$ -ATP.

Materials and MethodsBuffers and Solutions

The following two buffers were used for the thymidine kinase extraction from Escherichia coli:

Grinding Buffer:

		final concentration
2 M Tris-HCl	25 ml	0.05 M
Glycerol	50 ml	5% (v/v)
0.2 M EDTA (pH 7.9)	10 ml	2 mM
Dithiothreitol	15.4 mg	1 mM
1 M Mercaptoethanol	1 ml	1 mM
4 M NaCl	58.25 ml	233 mM
Lysozyme	130 mg	130 ug/ml
phenylmethylsulfonyl fluoride	23 mg	23 ug/ml
Water	ad 1000 ml	

TGED Buffer:

		final concentration
2 M Tris-HCl (pH 7.9)	5 ml	0.01 M
Glycerol	50 ml	5% (v/v)
0.2 M EDTA (pH 7.9)	0.5ml	0.1 mM
Dithiothreitol	15.4ml	0.1 mM
4 M NaCl	50 ml	0.2 M
Water	ad 1000 ml	

The following stock mixture was used in the enzymatic conversion of FdUrd to FdUMP.

Stock mixture:

		final concentration
2 M Tris-HCl (pH 7.8)	75 ul	150 mM
0.1 M Magnesium chloride	300 ul	30 mM
BSA	1 mg	1 g/ml
Water	ad 1 ml	

### Preparation of Thymidine Kinase from E. Coli

Since thymidine kinase was not commercially available the enzyme was purified from *Escherichia coli* strain B (Okasaki, 1964; Burgess, 1975).

Purification procedure: All steps were carried out at 4°C unless otherwise noted. Lyophilized *Escherichia coli* B lyophilized cells (50 g) were blended in a 1 L Waring Blender in 300 ml grinding buffer at low speed for 2.5 min. After 20 min, 5 ml 4% (w/v) sodium deoxycholate was added with stirring until its final concentration reached 0.05%. The mixture was blended at low speed for 30 sec. After 20 min. at 8-10°C the mixture was blended for 30 sec. at high speed to shear the DNA. Next, 250 ml TGED was added, and the mixture was sheared again at high speed for 30 sec. The cell extract was centrifuged at 4°C for 1 hr at 12,000 RPM (23,300 g) in 250 ml bottles in a GSA rotor of a Sorvall RC-2B centrifuge. The clear, amber, somewhat viscous supernatant was collected (fraction I), frozen, and stored overnight.

Heat Treatment: Fraction I was thawed in a waterbath at 15-20°C, divided into 10-12 ml portions in glass test tubes, and heated for 5 min in a water bath at 70-72°C with occasional stirring with a glass rod. The tubes were chilled quickly in ice water and then the contents were centrifuged at 4°C for 40 min at 10,000 RPM (16,300 g) in 250 ml bottles in a GSA rotor of a Sorvall RC-2B centrifuge. The

supernatant fluids were collected (Fraction II).

Streptomycin Treatment: 95 ml of 5% streptomycin sulfate were added over a 20-minute period to fraction II, while stirring. After 1 hr of additional stirring, the supernatant was centrifuged at 12,000 RPM (23,300 g, GSA rotor) for 1 hr. The supernatant was clarified by filtration through a fluted Whatman No 1 paper (fraction III). Fraction III was frozen at  $-10^{\circ}\text{C}$  and stored overnight.

Ammonium Sulfate Treatment: Over 50 min, 117 g ammonium sulfate (special enzyme grade) was added to fraction III under constant stirring. After an additional hour, the suspension was centrifuged in 250 ml bottles at  $4^{\circ}\text{C}$  at 8,500 RPM (15,000 g). The precipitate was dissolved in 6 ml 50 mM Tris-HCl buffer (pH 7.8) and then centrifuged at 15,000 RPM for 30 min (Sorvall, SS 34 rotor, 27,000 g). After this last centrifugation step the supernatant contained the enzyme; 1 ml portions of the enzyme preparation were stored in Eppendorf centrifuge tubes at  $-20^{\circ}\text{C}$  until further use.

#### Synthesis of Fluorodeoxyuridine- $^{32}\text{P}$ -Monophosphate

Enzymatic reaction: Radiolabeled  $^{32}\text{P}$ -FdUMP was enzymatically synthesized from 5-fluoro-2'-deoxyuridine using thymidine kinase, isolated from Escherichia coli (Wataya, 1977). The reaction mixture (10  $\mu\text{l}$ ) contained 10 nmol FdUrd, 75 nmol ATP (containing 5 or 10 mCi, specific activity 3000 Ci/mmol), 0.3  $\mu\text{mol}$  KF, 1.2  $\mu\text{l}$  thymidine kinase

preparation (9 ug protein) and 2.5 ul stock mixture. Since the  $^{32}\text{P}$ -ATP is available only as 1 mCi/0.1 ml, it was lyophilized in the presence of the correct amount of cold ATP overnight, prior to adding all the other above noted reaction constituents into the same reaction vessel. The reaction mixture was incubated for 2 hours at  $37^{\circ}\text{C}$ . The reaction was stopped by heating in a boiling waterbath for 2 min.

Separation of the nucleotides from the nucleosides:

FdUMP was separated from unreacted FdUrd, ATP and ADP by anion exchange chromatography (Rustum, 1973). Preswollen DEAE cellulose (20 g) was suspended in 400 ml 300 mM ammonium formate (pH 4.4). After readjusting the pH to 4.4 with formic acid, the fines were decanted from the slurry and the process was repeated 3 times. The resin was resuspended in 3 mM ammonium formate which, in turn, was replaced 3 times by decanting. The DEAE slurry was poured into a 1x10 cm column until the resin reached a height of 5 cm. The column was equilibrated with 5 bed volumes of 3 mM ammonium formate.

At the end of the incubation the reaction mixture was diluted with 10 volumes of water, applied on the DEAE cellulose column and eluted with a linear salt gradient, which was produced by 150 ml 3 mM ammonium formate in the mixing chamber and 150 ml 300 mM ammonium formate in the reservoir. UV absorbance was monitored in the eluate fractions. A sam-

ple of each fraction was measured for radioactivity. The synthesized FdUMP was well resolved from the unreacted FdUrd, ATP and ADP. To calibrate the column, 100 nmol of FdUMP, FdUrd, ATP and ADP were applied, and the elution order was: FdUrd (3-4.5 ml), FdUMP (40.5-60 ml), ADP (87.5-106.6 ml) and ATP (129.5-167 ml)(Figure A.2.). Figure A.3. shows the radioactivity profile measuring  $^{32}\text{P}$ -radioactivity in the reaction mixture. The pooled fractions containing  $^{32}\text{P}$ -FdUMP and  $^{32}\text{P}_i$  were lyophilized and reconstituted in 50% aqueous ethanol (Fraction P1).

#### Removal of Inorganic Phosphate from $^{32}\text{P}$ -FdUMP

Because anion exchange chromatography did not resolve  $^{32}\text{P}$ -FdUMP from inorganic  $^{32}\text{P}$ -phosphate, an additional chromatographic step was introduced (Uematsu, 1976). Inorganic phosphate can be removed from the nucleoside monophosphate using Biobead SM4 beads (BioRad Lab). The column material was prepared by extensive washing with methanol. After drying, the resin was ground with a mortar and pestle, and the resin beads of 100-200 mesh were collected on Nitex screening fabric (Nitex, HC 3-60, 280 mesh; HC 3-150, 120 mesh). After resuspending in methanol, the slurry was poured into a 1x10 cm column up to a height of 5 cm. The methanol was then displaced by washing with 10 bed volumes of water. The column was then equilibrated with 50 mM triethylammonium bicarbonate (TEA) (pH 7.6) which was

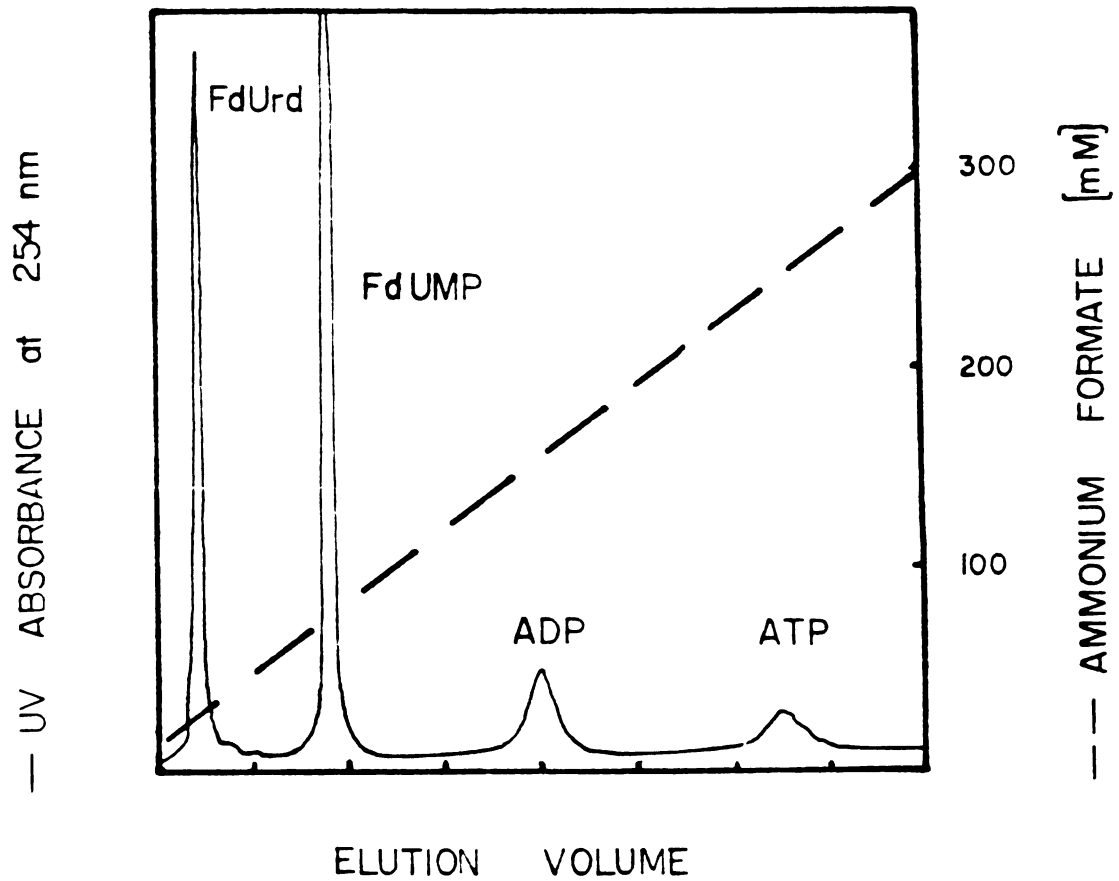
CALIBRATION OF ANION EXCHANGE  
COLUMN

Figure A.2. UV profile of nucleotides and nucleosides chromatographed on DEAE anion exchange column after application of a spiked sample. The resolution of the nucleoside FdUrd from the nucleotides FdUMP, ATP and ADP is shown.



## ANION EXCHANGE CHROMATOGRAPHY

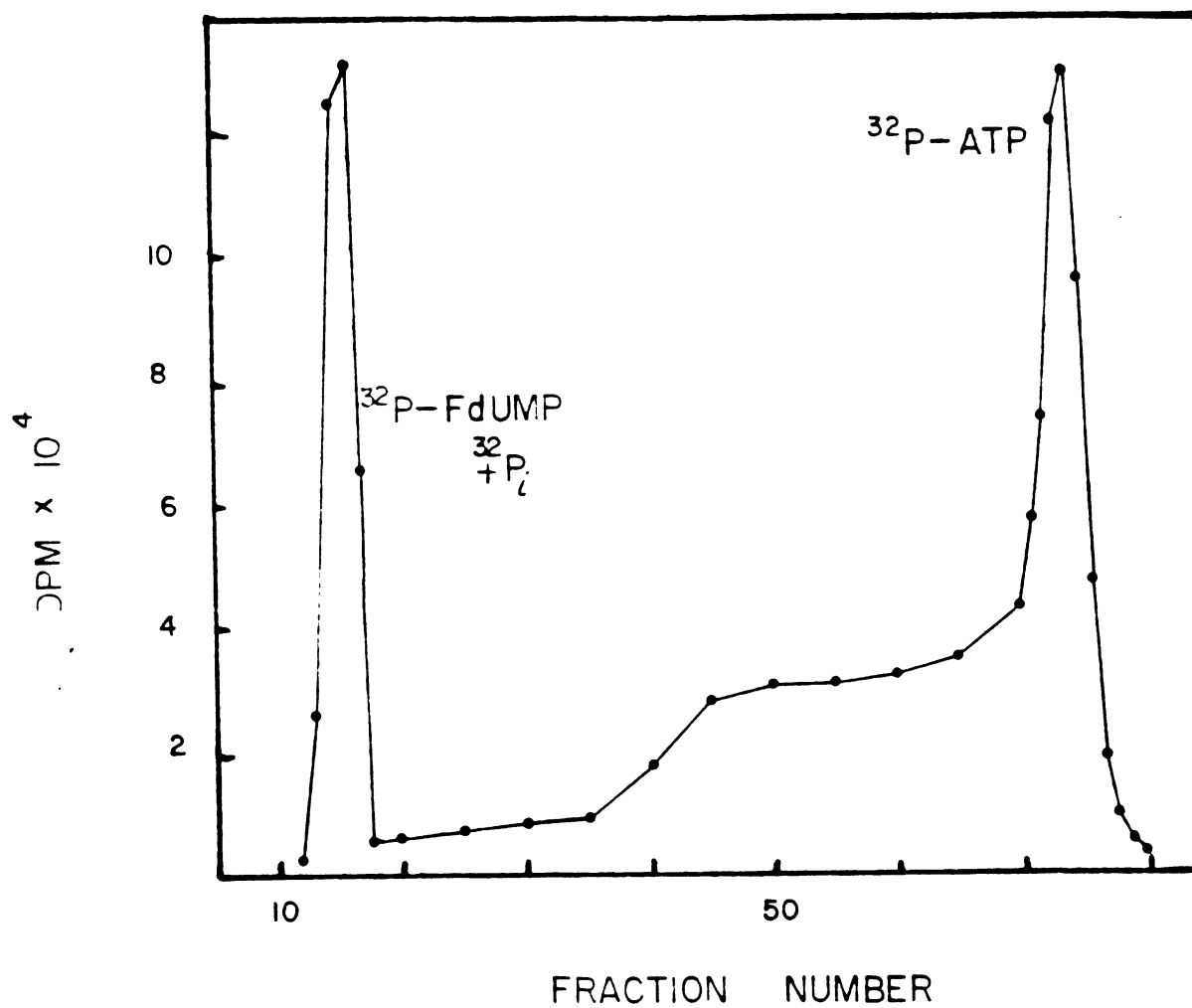


Figure A.3. Elution of  $^{32}\text{P}$ -radioactivity from a DEAE anion exchange column. The separation of both  $^{32}\text{P}$ -FdUMP and  $^{32}\text{P}_i$  (fractions #12-16) from  $^{32}\text{P}$ -ATP (fractions #70-86) is shown.

prepared from triethylamine and carbon dioxide.

Fraction P1 was applied on the SM4 column and eluted with a linear gradient of TEA (150 ml 100 mM TEA, 150 ml 400 mM TEA). The inorganic phosphate is well-resolved from the FdUMP (6.2-12.5 ml and 35-45 ml, respectively)(Figure A.4.). The fractions containing the  $^{32}\text{P}$ -FdUMP were lyophilized, reconstituted in 50% aqueous ethanol and stored at  $-20^{\circ}\text{C}$ .

#### Purity and Quantitation of $^{32}\text{P}$ -FdUMP

The purity of  $^{32}\text{P}$ -FdUMP was analyzed by thin layer chromatography (TLC) as described in Chapter II. The specific activity of the synthesized FdUMP was estimated by counting  $^{32}\text{P}$  radioactivity of an aliquot. Total FdUMP concentration ( $^{32}\text{P}$ -FdUMP and nonlabeled FdUMP) was measured spectrophotometrically by UV absorption ( $\lambda_{\text{max}}=268\text{ nm}$ ,  $\epsilon=8200\text{ M}^{-1}$ ). A standard curve was prepared with varying amounts of FdUMP (Figure A.5.) and the amount of FdUMP synthesized read from the graph.

#### Radiopurity of Adenosine-gamma- $^{32}\text{P}$ -Triphosphate ( $^{32}\text{P}$ -ATP)

The radiopurity of  $^{32}\text{P}$ -ATP was determined by thin layer chromatography following the procedure described by Rowley (1974). An aqueous solution of  $^{32}\text{P}$ -ATP plus cold carrier was spotted on PEI-cellulose plastic TLC sheets (Baker) and the

## BIOBEAD SM 4 CHROMATOGRAPHY

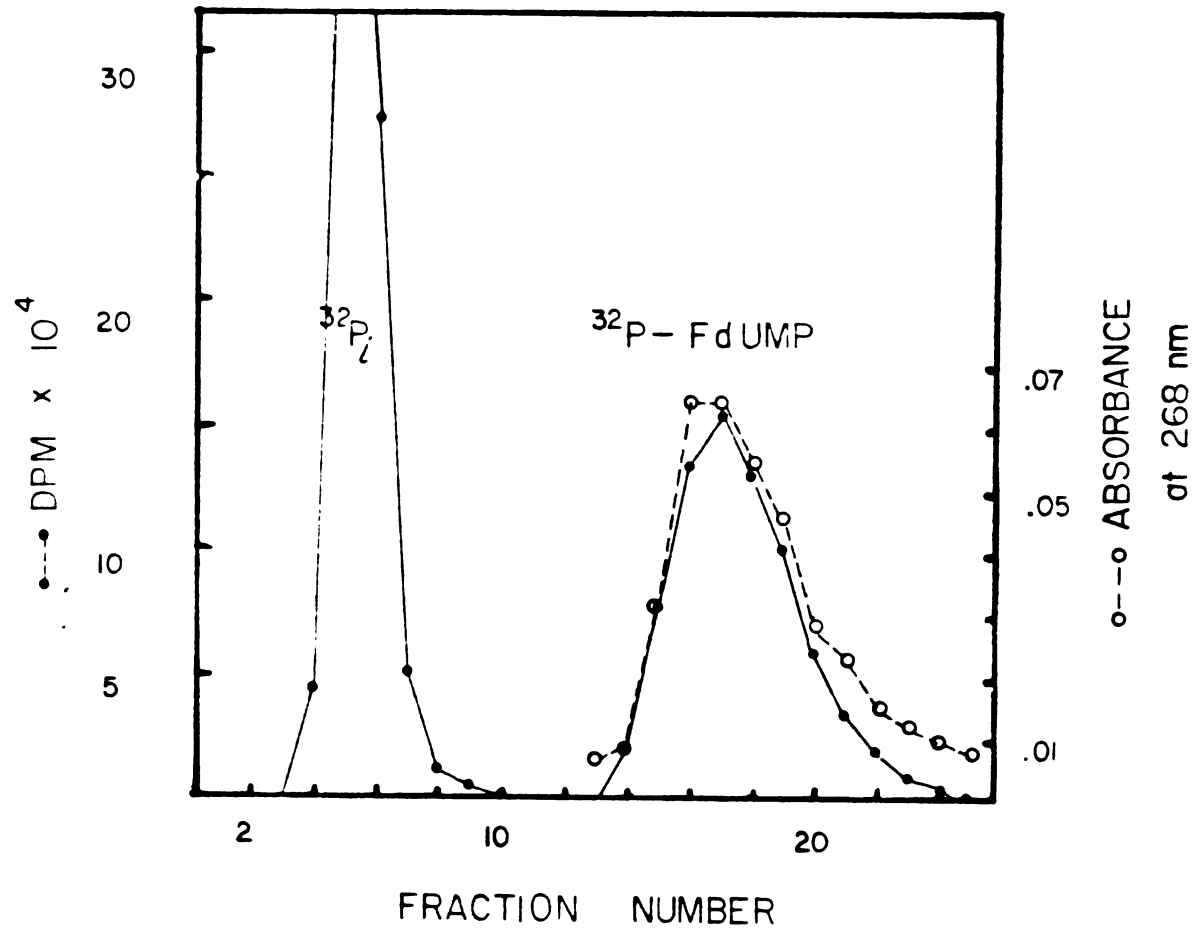


Figure A.4. Elution of  $^{32}\text{P}$ -radioactivity from the Biobead SM 4 column, showing the separation of inorganic  $^{32}\text{P}$ -phosphate ( $^{32}\text{P}_i$ ) (fractions #4-9) from  $^{32}\text{P}$ -FdUMP (fractions #14-21). UV absorbance at 268 nm was monitored confirming the presence of  $^{32}\text{P}$ -FdUMP in fractions #14-21.

STANDARD CURVE FOR  
FdUMP QUANTIFICATION

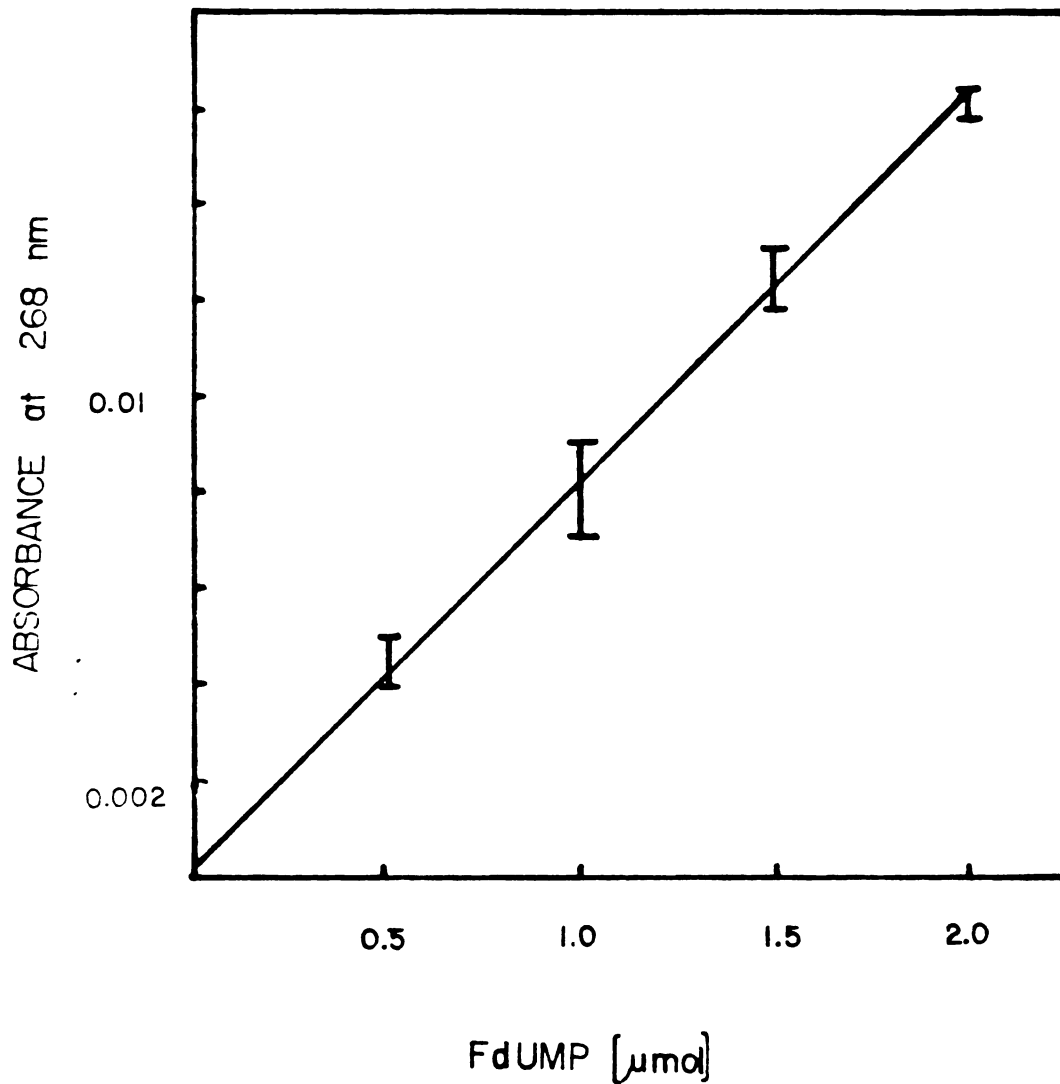


Figure A.5. Standard curve for the quantification of FdUMP. The UV absorbance at 268 nm was measured in triplicate samples containing four different known amounts of FdUMP. The range is shown by the heights of the bars.

chromatogram was developed with 2 M NaCl. After drying the plates, the phosphates were visualized with a molybdate spray reagent (Bandurski, 1951). The plates were dried in an oven at 90°C for 20 minutes. After steaming the plates, they were placed under UV light for 8 minutes. This process was repeated once. At this stage the plates were usually blue-green. After steaming and brief exposure to ammonia vapor, the background color faded leaving blue spots on a pale yellow background indicating the position of any phosphorus containing compounds. The position of the  $^{32}\text{P}$ -ATP was confirmed and the amount quantified after cutting the plates in 5 mm strips, suspending them in 1 ml of water, vortexing, and adding 18 ml scintillant PCS (Amersham).

#### Laboratory Safety

$^{32}\text{P}$ -phosphate is a highly energetic beta emitter. For the safety of all persons involved in the synthesis, the entire work was carried out behind a 1 inch plastic shield and the work area was periodically checked for radioactivity using a portable Geiger-Mueller counter. For the direct handling of the radioactive material care was taken to avoid direct contact under all circumstances. Disposable labware was utilized whenever possible.

## Results and Discussion

### Radiopurity of Adenosine-<sup>32</sup>P-Triphosphate

The radiopurity of <sup>32</sup>P-ATP was confirmed by TLC on PEI-cellulose plates (Rowley, 1975). In this chromatographic system ATP, ADP and P<sub>i</sub> were well resolved. Therefore, the hydrolytic degradation of ATP to ADP as well as the position of the <sup>32</sup>P-radiolabel with respect to the alpha, beta or gamma position was verified. The results showed that >97% of the radiolabel co-migrates with the cold ATP carrier to an R<sub>F</sub> value of 0.27 and less than 3% of the radioactivity corresponded to inorganic phosphate (<sup>32</sup>P<sub>i</sub>) (R<sub>F</sub> = 0.78). Moreover, no radioactivity was detected at an R<sub>F</sub> value corresponding to ADP (cold carrier, R<sub>F</sub> = 0.41) indicating labeling of <sup>32</sup>P-ATP.

### Testing the Enzyme Activity of Thymidine Kinase

The activity of the purified enzyme thymidine kinase was tested under the same reaction conditions described by Wataya (1977). The FdUrd/ATP ratio was 1:7 (umol) in a volume of 1 ml with tracer amounts of <sup>3</sup>H-FdUrd added for detection purposes. The amount of thymidine kinase and the incubation time were varied to establish optimum conditions. The yield of FdUMP was monitored by analyzing <sup>3</sup>H-FdUMP either by TLC as in Chapter II, or by anion exchange chromatography. The addition of 120 ul of the thymidine kinase

preparation followed by an incubation for 2 hours at 37°C resulted in a greater than 70% conversion of FdUrd to FdUMP (Table A.1.).

Scaling-down of the Reaction Conditions and  $^{32}\text{P}$ -FdUMP Synthesis

Since the specific activity of  $^{32}\text{P}$ -FdUMP should be as high as possible, the reaction conditions had to be scaled-down to a nmol range. It was important to keep all constituents of the reaction constant since incubating 1 nmol FdUrd and 7 nmol ATP in a 1 ml volume decreased the yield of FdUMP to less than 15% (Table A.2.). No conversion of FdUrd to FdUMP was observed when employing a FdUrd/ATP ratio of 1:1 or 7:1 in a reaction volume of 1 ml. Therefore, the reaction volume was decreased to 10  $\mu\text{l}$ . Again the FdUrd/ATP ratio of 1:7 was found to be optimum (Table A.2.). Although the yield dropped to about 40%. Table A.3. shows the results of varying TK concentrations, reaction time and volume. Again, optimum conditions were observed with a 1:7 FdUrd/ATP ratio.

Reaction of 5-10 mCi  $^{32}\text{P}$ -ATP in 10  $\mu\text{l}$  volume under optimum conditions surprisingly yielded less than 5%  $^{32}\text{P}$ -FdUMP (Table A.4.). It was noted that the  $^{32}\text{P}_i$  content in the reaction mixture increased to 40% of the starting  $^{32}\text{P}$ -ATP. To find a reason yield other than the volume for the decreased yield, the hydrolytic loss of  $^{32}\text{P}$ -ATP during the

Table A.1. Optimum reaction conditions for the conversion of FdUrd to FdUMP were established by varying the amount of enzyme thymidine kinase (TK) and the incubation time. The yield was measured by adding tracer amounts of tritiated FdUrd.

<sup>3</sup> H-FdUrd umol	ATP umol	TK ul	Time hrs	<sup>3</sup> H-FdUMP % Yield 1)	
				TLC	DEAE
1.5	7.5	15	1.5	--	27
1.5	7.5	60	1.5	37	30
1.0	7.5	60	2	54	63
1.0	7.5	60	2	--	62
1.0	7.5	120	2	--	73

1) Reaction volume: 1 ml



Table A.2. The reaction conditions are scaled-down to nmol quantities and the yield<sub>3</sub> of FdUMP is monitored by tracer amounts of <sup>3</sup>H-FdUrd.

<sup>3</sup> H-FdUrd nmol	ATP nmol	Time hrs	<sup>3</sup> H-FdUMP % Yield <sup>1)</sup>	
			TLC	DEAE
10	70	2	46	30
10	70	2	67	77
10	30	2	5	--
10	10	2	13	--
1	7	2	41	--
2	14	2	32	21
2	14	3	5	10
1 <sup>2)</sup>	7	2	--	<15

1) Reaction volume: 10 ul, TK: 1.2 ul

2) Reaction volume 1ml, TK: 60 and 120 ul

Table A.3. Effect of diluting the reaction mixture and varying the incubation time on the yield of FdUMP measured by addition of tracer amounts of  $^3\text{H-FdUrd}$  to the reaction mixture.

$^3\text{H-FdUrd}$	ATP	Reaction Volume	TK	Time	$^3\text{H-FdUMP}$ <sup>1)</sup>
nmol	nmol	ul	ul	Hours	% Yield
10	75	50	0.6	2	0
10	75	50	0.6	3	3
10	75	50	0.6	17	3
10	75	50	6	3	4
10	75	50	6	4	7
10	75	50	6	17	3
10	75	100	1.2	2	0
10	75	100	1.2	3	2
10	75	100	1.2	17	2
10	75	100	12	3	4
10	75	100	12	4	4
10	75	100	12	17	1
50	350	50	6	2	50 <sup>2)</sup>
50	350	50	6	3	55 <sup>2)</sup>

1) FdUMP yield measured by TLC

2) Optimum reaction conditions

Table A.4. Optimum reaction conditions for reaction volumes of 100  $\mu$ l and 10  $\mu$ l,  $^{32}$ P-FdUMP was synthesized using  $^{32}$ P-ATP.

FdUrd	$^{32}$ P-ATP	Reaction Volume	$^{32}$ P-FdUMP 1)
nmol	nmol	$\mu$ l	% Yield
100	750	100	1
100	750	100	5
100	750	100	4
10	75	10	0.3
10	75	10	0.3

1) Incubation time: 2 hours

37°C incubation was studied by omitting FdUrd from the reaction mixture. The formation of inorganic  $^{32}\text{P}_i$  was analyzed by PEI-TLC. The results show that less than 10% ATP was spontaneously hydrolyzed during the incubation. However, since the reaction mixture contained a 7:1 excess of ATP, minor nonspecific degradation should not effect the FdUMP yield significantly. Varying the KF concentrations to inhibit nonspecific enzyme activity (i.e., proteases) present in the TK preparation did not obviate the problem.

Since it was necessary to lyophilize the commercially available  $^{32}\text{P}$ -ATP, the influence of lyophilization on the stability of ATP was analyzed and a minimal degradation (<2%) was found. FdUMP was equally stable to lyophilization. Co-lyophilization of  $^{32}\text{P}$ -ATP with cold ATP did not appreciably increase the  $^{32}\text{P}$ -FdUMP yield.

Since the synthesis was carried out in a nmol/ul scale, it was important to verify that no appreciable loss of radioactive material occurred due to adhesion to the reaction vessel wall (Eppendorf centrifuge tube). Less than 2% of the radioactivity could be detected on the vessel wall after the reaction mixture was further processed.

### Conclusion

An attempt was made to synthesize  $^{32}\text{P}$ -FdUMP, which is not commercially available. The enzymatic conversion of FdUrd to FdUMP requires the enzyme thymidine kinase which was successfully isolated from *Escherichia coli* utilizing an ammonium sulfate precipitation technique. The enzyme preparation was not homogeneous, but contained sufficient TK for the purpose of this work. The suggested optimum condition (Wataya, 1977) of FdUrd/ATP ratio of 1:7 was confirmed when working on a  $\mu\text{mol}$  scale utilizing  $^3\text{H}$ -FdUrd in tracer amounts. Up to 70% of the nucleoside was successfully converted to the corresponding nucleotide FdUMP.

Scaling the reaction down resulted in more than 40% conversion to  $^3\text{H}$ -FdUMP. However, adding 5-10 mCi  $^{32}\text{P}$ -ATP under the latter conditions failed to produce a satisfactory yield of 5-fluoro-2'-deoxyuridine-5'- $^{32}\text{P}$ -monophosphate. Although several attempts were made to explain the observed discrepancy between the yield of  $^{32}\text{P}$ -radiolabeled FdUMP and either unlabeled or  $^3\text{H}$ -FdUMP, the cause of this unpredictable result remained unclear.

With less than 1% utilization of the starting radiolabeled  $^{32}\text{P}$ -ATP the synthesis of  $^{32}\text{P}$ -FdUMP was not economically feasible.

## References

- Abra, R.M., Bosworth, M.E., Hunt, C.A., Liposome Disposition In Vivo: Effects of Pre-dosing with Liposomes, Res. Commun. Chem. Pathol. Pharmacol. 29:349-360 (1980)
- Abra, R.M., Hunt, C.A., Liposome Disposition In Vivo III. Dose and Vesicle-Size Effects, Bioch. Bioph. Acta 666:493-503 (1981)
- Aldridge, W.N., Reiner, R., Enzymatic Inhibitors as Substrates. Interactions of Esterases with Esters of Organophosphorus and Carbamic Acid, Front. Biol. 26:91-100 (1972)
- Alving, C.R., Steck, E.A., Chapman, W.L., Waits, V.B., Hendriks, L.D., Swartz, G.M., Hanson, W.L., Therapy of Leishmaniasis: Superior Efficacies of Liposome-Encapsulated Drugs, Proc. Acad. Nat. Sci. USA 75:2959-2963 (1978)
- Alving, C.R., Immune Reaction of Lipids and Lipid Model Membranes, in Antigen, ed. Sela, M., Acad. Press, NY, pp 1-72 (1977)
- Armstrong, D.R., Diasio, R.B., Metabolism and Biological Activity of 5'-Deoxy-5-Fluorouridine, a Novel Fluoropyrimidine, Cancer Res. 40:3333-3338 (1980)
- Armstrong, D.R., Diasio, R.B., Selective Activation of 5'-Deoxy-5-Fluoropyrimidine by Tumor Cells as a Basis for an Improved Therapeutic Index, Cancer Res. 41:4891-4894 (1981)
- Bandurski, R.S., Axelrod, B., The Chromatographic Identification of Some Biologically Important Phosphate Esters, J. Biol. Chem., 193:405-410 (1951)
- Bangham, A.D., Lipid Bilayers and Biomembranes, Ann. Rev. Biochem. 41:753-776 (1972)
- Bangham, A.D., Standish, M.M., Watkins, J.C., The Action of Steroids and Streptolysin S on the Permeability of Phospholipid Structures to Cations, J. Mol. Biol. 13:238-252 (1965)
- Bangham, A.D., Standish, M.M., Watkins, J.C., Diffusion of Univalent Ions across the Lamellae of Swollen Phospholipids, J. Mol. Biol. 13:138 (1965)
- Bartlett G.R., Phosphorus Assay in Column Chromatography, J. Biol. Chem. 234:466-468 (1959)
- Benacerraf, B., Quantitative Aspects of Phagocytosis, in: Liver Function, ed. Bauer, R.N., Waverly Press, Baltimore, pp 205-234 (1958)

- Berg T. and Boman D., Distribution of Lysosomal Enzymes Between Parenchymal and Kupffer Cells of Rat Liver, *Bioch. Bioph. Acta* 324:585-596 (1973)
- Berlin, R.D., Oliver, J.M., Membrane Transport of Purine and Pyrimidine Bases and Nucleosides in Animal Cells, *Int. Rev. Cytolog.* 42:287-336 (1975)
- Berry, M.N., and D.S.Friend, High Yield Preparation of Isolated Rat Liver Parenchymal Cells, *J. Cell Biol.* 43(3):506-520 (1969)
- Biozzi, G., Stiffel, C., The Physiology of the Reticuloendothelial Cells in Liver and Spleen, in: *Progress in Liver Disease*, ed. Popper, H., Schaffner, F., Grune and Stratton Inc, New York (1965)
- Black, C.D.V., Gregoriadis, G., Interaction of Liposomes with Plasma Proteins, *Biochem. Soc. Trans.* 4:253 (1976)
- Blouin, A, Morphometry of Liver Sinusoidal Cells, in *Kupffer Cells and Other Sinusoidal Cells*, ed. Wisse, E, and Knook, D.L., Elsevier Biomedical Press, (1977)
- Bosworth, M.E., Evaluation of Liposomes as a Drug Delivery System, Thesis, University of California, San Francisco, 1980
- Bosworth, E.M., Hunt, C.A., Pratt, D., Liposome Dialysis for Improved Size Distribution, *J. Pharm. Sci.* 71(7):806-812 (1982)
- Boyden, F., Cellular Recognition of Foreign Matter, *Int. Rev. Exp. Pathol.* 2:311-356 (1963)
- Bundgaard, M., Transport Pathways in Capillaries - in Search of Pores, *Ann. Rev. Physiol.* 42:325-336 (1980)
- Burgess, R.R., Jendrisak, J.J., A Procedure for the Rapid, large-scale Purification of Escherichia coli DNA-Dependent RNA Polymerase Involving Polymin P Precipitation and DNA-Cellulose Chromatography, *Biochemistry*, 14:4634-4638 (1975)
- Cass, C., Dahlig, E., Lau, E.Y., Lynch, T.P., Paterson, A.R.P., Fluctuation in Nucleoside Uptake and Binding of the Inhibitor of Nucleoside Transport, Nitrobenzylthioinosine, during the Replication Cycle of HeLa Cells, *Cancer Research*, 39:1245-1252 (1979)
- Ciardi, J.E., Anderson, E.P., Separation of Purine and Pyrimidine Derivatives by Thin Layer Chromatography, *Anal. Biochem.* 22:398-408 (1968)
- Cohen, S.S., Flakes, J.G., Barner, H.D., Loeb, M.R., Lichtenstein, J., Mode of Action of 5-Fluorouracil and Its Derivatives, *Proc. Nat. Acad. Sci. USA* 44:1004-1012 (1958)

- Cooper, A.D., Yu, P.Y.S., Rates of Removal and Degradation of Chylomicron Remnants by Isolated Perfused Rat Liver, *J. Lipid Res.* 19:635-43 (1978)
- Damen, J., Regts, J., Scherphof, G., Transfer and Exchange of Phospholipids between Small Unilamellar Liposomes and Rat Plasma High Density Proteins. Dependence on Cholesterol Content and Phospholipid Composition, *Bioch. Bioph. Acta* 665:538-545 (1981)
- Danenberg, P.V., Thymidylate Synthetase - A Target Enzyme in Cancer Chemotherapy, *Bioch. Bioph. Acta* 473:73-92 (1977)
- Danenberg, P., Montag, B.J., Heidelberger, C., Studies of Fluorinated Pyrimidines IV: Effects of Nucleic Acid Metabolism In Vivo, *Cancer Res.* 18:329-332 (1958)
- Danenberg, P.V., Heidelberger, C., The Effect of Raney on the Covalent Thymidylate Synthetase-5-fluoro-2'-deoxyuridilate-5,10-methylenetetrahydrofolate Complex, *Biochemistry* 15:1331-1337 (1976)
- Danenberg, P.V., Langenbach R.J., Heidelberger, C., Structures of Reversible and Irreversible Complexes of Thymidylate Synthetase and Fluorinated Pyrimidine Nucleotides, *Biochemistry* 13: 926-933 (1974)
- De Barys, Th., De Vos, P., Van Hoff, F., A Morphologic and Biochemical Study of the Fate of Antibody-Bearing Liposomes, *Lab. Invest.* 34:273-282 (1976)
- DeDuve, C., The Separation and Characterization of Subcellular Particles, *Harvey Lecture*, 59:49-87 (1965)
- Dijkstra, J., van Galen, W.J.M., Roerdink, F.H., Regts, D., Scherphof, G.L., Uptake of Liposomes by Kupffer Cells in Vitro, in Sinusoidal Liver Cells, eds. Knook, D.L., Wisse, E., Elsevier Biomedical Press, North-Holland, pp 297-303 (1982)
- Dijkstra, J., Uptake and Processing of Liposomes by Rat Liver Macrophages In Vitro, Thesis, University of Groningen, 1983
- Docherty, K., Maguire, G.A., Hales, C.N., Permeability Properties of Lysosomal Membranes, *Biosc. Rep.*, 3:207-216 (1983)
- Dunlap, R.B., Hardin, N.G.L., Huenekens, F.M., Thymidylate Synthetase from Amethopterin-resistant *Lactobacillus Casei*, *Biochemistry* 10:88-97 (1971)
- Fairbanks, G., Steck, T.L., Wallach, D.F.H., Electrophoretic Analysis of the major Polypeptides of the Human Erythrocyte Membrane, *Biochem.* 10:2606-2617 (1971)



- Fraley, R., Straubinger, R., Rule, G., Springer, L., Papahadjopoulos, D., Liposome-Mediated Delivery of DNA to Cells: Enhanced Efficiency of Delivery by Changes in Lipid Composition and Incubation Conditions, *Biochemistry* 20:6978-6987 (1981)
- Freise, J., Muller, W.H., Brotsch, C., Schmidt, F.W., In Vivo Distribution of Liposomes Between Parenchymal and Non-parenchymal Cells in Rat Liver, *Biomedicine*, 32:118-123 (1980)
- Godfredsen, C.F., Cellular and Tissue Uptake, Distribution and Metabolism of Liposomes, Thesis, University Catholique de Louvain, pp 182, (1982)
- Gordon, S., Cohn, Z.A., The Macrophage, *Internat. Rev. Cytolog.* 36:171-214 (1973)
- Goz, B., Prusoff, W.H., Pharmacology of Viruses, *Ann. Rev. Pharmacol.* 10:143-170 (1970)
- Gregoriadis, G., Ryman, B.E., Fate of Protein-Containing Liposomes in Rats, *Eur. J. Biochem.* 24:485-491 (1972)
- Gregoriadis, G., Neerunjun, D.E., Control of the Rate of Hepatic Uptake and Catabolism of Liposome-Entrapped Proteins Injected into Rats, *Eur. J. Biochem.* 47:179-185 (1974)
- Haley, T.J., Pharmacology and Toxicology of Rare Earth Elements, *J. Pharm. Sci.* 54:663-670 (1965)
- Hanks, J.H., Wallace, R.E., Relation of Oxygen and Temperature in Preservation of Tissues by Refrigeration, *Proc. Soc. Exp. Biol. and Med.* 71:196 (1949)
- Heidelberger, C., Chandury, N.K., Danenberg, P.V., Mooren, M., Griesbach, L., Duschinsky, R., Schnitzer, R.J., Plevin, E., Scheiner, T., Fluorinated Pyrimidines, a New Class of Tumor Inhibitory Compounds, *Nature* 179:663-666 (1957)
- Heidelberger, C., in *Antineoplastic and Immunosuppressive Agents*, eds Sarotelli, A.C. and Johns, A.G., Springer, New York, pt II, chp 41, pp 193-231 (1975)
- Heidelberger, C., Griesbach, L., Cruz, O., Schnitzer, R.J., Grunberg, E.G., Fluorinated Pyrimidines VI: Effect of 5-Fluorouridine and 5-Fluorodeoxy-uridine on Transplantable Tumors, *Proc. Soc. Exp. Biol.* 97:470-475 (1958)
- Hunt, C.A., Liposome Disposition in Vivo V. Liposome Stability in Plasma and Implications for Drug Carrier Function, *Bioch. Biophys. Acta* 719:450-463 (1982)
- Hunt, C.A., Tsang, S.,  $\alpha$ -Tocopherol Retards Autoxidation and Prolongs the Shelf-life of Liposomes,

Internat. J. Pharmaceutics 8:101-110 (1981)

Jackson, A.J., The Effect of Route of Administration on the Disposition of Inulin Encapsulated in Multilamellar Liposomes, Res. Commun. Chem. Pathol. Pharmacol. 27:293-304 (1980)

James, T.L., Pagolotti, A.L., Ivanetich, K.M., Wataya, Y., Lam, S.S.M., Santi, D.V., Thymidylate Synthetase: Fluorine-19-NMR Characterization of the Active Site Peptide Covalently Bound to 5-Fluoro-2'-deoxyuridilate and 5,10-Methylenetetrahydrofolate, Bioch. Bioph. Res. Commun. 72:404-410 (1976)

Jandle, J.H., Files, N.M., Barnet, S.B., MacDonald, R.A., Proliferative Response of the Spleen and Liver to Hemolysis, J. Exp. Med. 122:299 (1965)

Jones, A.L., Schmucker, D.L., Current Concepts of Liver Structure as Related to Function, Gastroenterology 73:833-851 (1977)

Jost, P.C., Griffith, O.H., Capaldi, R.A., Vanderkooj, G., Evidence for Boundary Lipid in Membranes, Proc. Acad. Nat. Sci. USA 70:480-484 (1973)

Juliano, R.L., Stamp, D., The Effect on Particle Size and Charge on the Clearance Rates of Liposomes and Liposome Encapsulated Drugs, Bioch. Bioph. Res. Commun. 63: 651-658 (1975)

Jung, W., Gebhardt, R., Mecke, D., Alteration in Activity and Ultrastructural Localization of Several Phosphatases on the Surface of Adult Rat Hepatocytes in Primary Monolayer Culture, Eur. J. Cell Biolog. 27:230-241 (1982)

Kimelberg, H.K., Protein Liposome Interactions and their Relevance to the Structure and Function of Cell Membranes, Mol. Cell Biochem. 10:171-190 (1976)

Kimelberg, H.K., Differential Distribution of Liposome-Entrapped Methotrexate and Labeled Lipids after i.v. Injection in a Primate, Biolph. Bioch. Acta 448:531 (1976)

Kimelberg H.K., Mayhew, E., Properties and Biological Effects of Liposomes and Their Use in Pharmacology and Toxicology, Crit. Rev. Toxic. 6:25-79 (1978)

Kinsky, S.C., Nicolloti, R.A., Immunological Properties of Model Membranes, Ann. Rev. Biochem. 46:49-68 (1977)

Kirby, C., Clarke, J., Gregoriadis, G., Effect of Cholesterol Content of Small Unilamellar Liposomes on their Stability In Vivo and In Vitro, Biochem. J. 186:591-598 (1980)

- Knight, C.G., Liposomes: From Physical Structure to Therapeutic Application, in: Cell and Tissue Physiology, eds Dingle, J.T., Gordon, J.L., Elsevier/North Holland Biomedical Press, (1981)
- Knox, W.E., in Enzyme Pattern in Fetal, Adult and Neoplastic Rat Tissues, Karger, Basel, pp 256 (1972)
- Krebs H.A., Henseleit K., Untersuchungen uber die Harnstoffbildung im Tierkorper, Hoppe Seyler's Z. Physiol. Chem. 210:33 (1932)
- Kornberg, R.D., McConnell, H.M., Inside-Outside Transition of Phospholipid Vesicle Membranes, Biochemistry 10:1111-1120 (1971)
- Labow, R., Maley, F., The Effect of Methotrexate on Enzymes Induced Following Partial Hepatectomy, Cancer Res. 29:366-372 (1969)
- Langenbach, R.J., Danenberg, P.V., Heidelberger, C., Thymidylate Synthetase. Mechanism of Inhibition by 5-Fluoro-2'-deoxyuridilate, Bioch. Bioph. Res. Commun. 48:1565-1571 (1972)
- Lazar, G., The Reticuloendothelial-Blocking Effect of Rare Earth Elements in Rats, J. Ret. Soc. 13:231-237 (1973)
- Lehninger A.L., Biosynthesis of DNA, in Biochemistry, 2nd edition, pg 738 (1975)
- Lorenson, M.Y., Maley, G.F., Maley, F., The Purification and Properties of Thymidylate Synthetase from Chick Embryo Extracts, J. Biol. Chem. 242:3332-3344 (1967)
- Lowry, O.H., Rosebrough, N.J., Farr, A.L., Randall, R.J., Protein Measurements with the Folin Phenol Reagent, J. Biol. Chem. 193:265-275 (1959)
- Ludwig, J., Tomas, Z.J., Preparation of 5-Fluoro- and 5-Alkyl-2'-deoxyuridine-5'-phosphates free of 3'-Phosphates via Phosphorodiamidates, Synthesis (Jan 1982) :32-34 (1982)
- Maley, F., Maley, G.F., Nucleotide Interconversion IV. Activities of Deoxycytidilate Deaminase and Thymidylate Synthetase in Normal Rat Liver and Hepatomas, Cancer Res. 21:1421 (1961)
- Markwell, M.A.K., Haas, S.M., Bieber, L.L., Tolbert, N.E., A Modification of the Lowry Procedure to Simplify Protein Determination in Membrane and Lipoprotein Samples, Anal. Biochem. 87:206-210 (1978)
- Mauk, M.R., Gamble, R.C., Stability of Lipid Vesicles in Tissues of the Mouse: A Gamma Ray Perturbed Angular Correlation Study, Proc. Nat. Acad. Sci. USA 76:765-769

(1979)

Mayhew, E., Rustum, Y.M., Szoka, F., Papahadjopoulos, D., Role of Cholesterol in Enhancing the Antitumor Activity of Cytosine Arabinoside Entrapped in Liposomes, *Cancer Treat. Rep.* 63:1923-1928 (1979)

McIntyre, P., The Reticuloendothelial System: Organization and Physiology, *John Hopkins Medic. J.* 130:61-68 (1972)

v.Moellendorf, W., in *Die Milz*, Springer Verlag, New York, Vol 6:6, p 136 (1969)

Motta, P., Muto, M., Fujita, T., *The Liver, An Atlas of Scanning Electron Microscopy*, Igaku Shoin Publ., Tokyo, 1978

Munthe-Kaas, A.C., Mass Isolation und Culture of Rat Kupffer Cells, *J. Exp. Med.* 141:1-10 (1975)

Myers, C.E., Young, R.C., Chabner, B.A., Biochemical Determinants of 5-Fluorouracil Response In Vivo: The Role of Deoxyuridilate Pool Expansion, *J. Clin. Invest.* 56:1231-1238 (1975)

Myers, C.E., Diasio, R., Eliot, H.M., Chabner, B.A., Pharmacokinetics of Fluoropyrimidines: Implications of their Clinical Use, *Cancer Treatment Rep.* 3:175-183 (1976)

Okasaki, R., Kornberg, A., Deoxythymidine Kinase of *Escherichia Coli*, *J. Biol. Chem.*, 239:269-274 (1964)

Pagano, R.E., Weinstein, J.N., Interactions of Liposomes with Mammalian Cells, *Ann. Rev. Biophys. Bioeng.* 7:435-468 (1978)

Papahadjopoulos, D., Studies on the Mechanism of Action of Local Anesthetics with Phospholipid Model Membranes, *Bioph. Bioch. Acta* 265:169-186 (1972)

Papahadjopoulos, D., Poste, G., Mayhew, E., Cellular Uptake of Cyclic AMP Captured within Phospholipid Vesicles and Effect on Cell-Growth Behavior, *Bioph. Bioch. Acta* 323:404 (1974)

Paterson, A.R.P., Naik, S.R., Cass, C.E., Inhibition of Uridine Uptake in HeLa Cells by Nitrobenzylthioinosine and Related Compounds, *Mol. Pharmacol.* 13:1014-1023 (1977)

Paterson, A.R.P., Lau, E.Y., Dahlig, E., Cass, C.E., A Common Basis for Inhibition of Nucleoside Transport by Dipyridamol and Nitrobenzylthioinosine, *Mol. Pharmacol.* 18:40-44 (1980)

Poste, G., Liposome Targetting In Vivo: Problems and Opportunities, *Biol. Cell* 47:19-38 (1983)

- Priest, D.G., Doig, M.T., Hynes, J.B., Purification of Mouse Liver Thymidylate Synthetase by Affinity Chromatography Using 10-Methylene-5,8-dideazafolate as the Affinant, *Experientia* 37:119-120 (1981)
- Priest, D.G., Alford, C.W., Batson, K.K., Doig, M.T., A Centrifugal Column Assay for Thymidylate Synthetase Using the Active Site Titrant 5-Fluoro-deoxyuridilate, *Anal. Biochem.* 103:51-54 (1980)
- Rahman, Y.E., Lau, E.H., Wright, B.J., Application of Liposomes to Metal Chelating Therapy, in *Liposomes and Immunobiology*, ed. Tom, B.H., and Six, H.R., Elsevier/North Holland Biomedical Press, pp 285-299 (1980)
- Rahman, Y.E., Cerny, E.A., Patel, K.R., Lau, E.H., Wright, B.J., Differential Uptake of Liposomes Varying in Size and Lipid Composition by Parenchymal and Kupffer Cells in Mouse Liver, *Life Sci.* 31:2061-2071 (1982)
- Rahman, Y.E., Cerny, E.A., Lau, E.H., Carnes, B.A., Enhanced Iron Removal From Liver Parenchymal Cells in Experimental Iron Overload, *Blood* 62:209-213 (1983)
- Reyes, P., Heidelberger, C., Fluorinated Pyrimidines XXVI. Mammalian Thymidylate Synthetase: Its Mechanism of Action and Inhibition by Fluorinated Nucleotides, *Mol. Pharmacol.* 1:14-30 (1965)
- Ritchie H.D. and Hardcastle J.D., in 'Isolated Organ Perfusion' (1973)
- Roerdink, F.H., Hoekstra, D., Damen, J., Scherphof, G.L., Wisse, E., Introduction of Enzymes into Liver Cells by Means of Liposomes, ed. Schiewe, T., and Rapaport S., in *FEBS*, Vol. 56, pp 89-98 (1979)
- Roerdink, F., Dijkstra, J., Hartman, G., Bolscher, B., Scherphof, G., The Involvement of Parenchymal, Kupffer and Endothelial Cells in the Hepatic Uptake of Intravenously Injected Liposomes, *Bioch. Bioph. Acta* 677:79-89 (1981)
- Ross B.D., in *Perfusion Techniques in Biochemistry*, Clarendon Press, Oxford (1972)
- Rowley, G.L., Kenyon, G.L., PEI-Cellulose Thin Layer Chromatography Product Study of the Creatinine Kinase and Pyruvate Kinase Reaction, *Anal. Biochem.* 58:525-533 (1975)
- Rustum, Y.M., Schwartz, H.S., Methods for the Separation and Identification of Ribosenucleotides on DEAE-Cellulose, *Biochem.* 53:411-419 (1973)
- Rutman, R.J., Cantorow, A., Paschkis, K.E., Studies in 2-acetylaminofluorene carcinogenesis III: The

- Utilization of Uracil-2-<sup>14</sup>C by Preneoplastic Rat Liver Hepatoma, *Cancer Res.* 14:119-134 (1954)
- Ryman, B.E., Tyrell, D.A., Liposomes - Bags of Potential, *Assay in Biochem.* 16:49-98 (1980)
- Saba, T.M., Physiology and Physiopathology of the Reticuloendothelial System, *Arch. Intern. Med.* 126:1031-1052 (1970)
- Santi, D.V., McHenry, C.S., 5-Fluoro-2'-deoxyuridilate: Covalent Complex with Thymidylate Synthetase, *Proc. Nat. Acad. Sci. USA* 69:1855-1857 (1972)
- Santi, D.V., McHenry, C.S., Sommer, H., Mechanism of Interaction of Thymidylate Synthetase with 5-Fluorodeoxyuridilate, *Biochemistry* 13:471-480 (1974)
- Scherphof, G., Interaction of Liposomes with Biological Fluids and Fate of Liposomes In Vivo, *Liposome Methodology, Inserm*, 107:80-92 (1982)
- Scherphof, G., Roerdink, F., Dijkstra, J., Ellens, H., Zanger, R., Wisse, E., Uptake of Liposomes by Rat and Mouse Hepatocytes and Kupffer Cells, *Biol. Cell* 47:47-58 (1983)
- Schreier, H., Raeder-Schikorr, M., Liposomen - Ein Neuartiger Arzneistofftrager, *Pharmazie In Unserer Zeit* 11:103-108 (1982)
- Scow, R.O., Blanchette-Mackie, E.J., Smith, L.G., Role of Lipoprotein Lipase and Capillary Endothelium in the Clearance of Chylomycrons from Blood: A Model for Lipid Transport by Lateral Diffusion in Cell Membranes, in *Cholesterol Metabolism and Lipolytic Enzymes*, ed Polonovski, J., Masson Publ. Inc., N.Y. pp 143-164 (1977)
- Segal, A.W., Wills, E.J., Richmond, J.F., Slavin, G., Black, D.V., Gregoriadis, G., Morphological Observations on the Cellular and Subcellular Destination of Intravenous Administrated Liposomes, *Br. J. Exp. Pathol.* 55:320-327 (1974)
- Seglen, P.O., Preparation of Isolated Rat Liver Cells, *Methods in Cell Biology*, 13:29-83 (1975)
- Senior, J., Gregoriadis, G., Stability of Small Unilamellar Liposomes in Serum and Clearance From the Circulation: The Effect of the Phospholipid and Cholesterol Content, *Life Science*, 30:2123-2136 (1982)
- Sherrill B.C., Innerarity T.L., Mahley, R.W., Rapid Hepatic Clearance of the Canine Lipoproteins Containing Only the E Apoprotein by a High Affinity Receptor, *J. Biol. Chem.* 255:1804-1807 (1980)
- Sommer H., Santi, D.V., Purification and Amino Acid Analysis of an Active Site Peptide from Thymidylate

Synthetase Containing Covalently Bound 5-Fluoro-2'-deoxyuridilate and Methylenetetrahydrofolate, *Bioch. Bioph. Res. Commun.* 57:689-695 (1974)

Shohami, E., Kanner, N., Koren, R., S-Substituted Derivatives of 6-Mercaptopurine Ribosides Interact Both With the Transport and Metabolic Phosphorylation of Uridine by Virus-Transformed Hamster Fibroblasts. *Bioch. Bioph. Acta* 601:206-219 (1980)

Speiser, P., Ultrafine Solid Compartments as Carriers for Drug Delivery, in *Optimization of Drug Delivery*, eds. Bundgaard, H., Bagger-Hansen, A., Kofod, H., Munksgaard Copenhagen, pp305-313 (1981)

Spencer, R.P., Pearson, H.A., Evaluation of the Spleen, in *Radionuclide Studies of the Spleen*, CRC Press, Chp.2 pp 5-10 (1975)

Stein, O., Stein, Y., Eisenberg, S., A Radioautographic Study of the Transport of <sup>125</sup>I-Labeled Serum Lipoproteins in Rat Aorta, *Z. Zellforschung*, 138:223-237 (1973)

Steinman, R.M., Mellman, J.S., Muller, W.A., Cohn, Z.A., Endocytosis and the Recycling of Plasma Membranes, *J. Cell. Biol.* 96:1-27 (1983)

Stockton, G.W., Johnson, K.G., Butler, K.W., Polnaszek, C.F., Cyr, R., Smith, I.C.P., Molecular Order in *Acholeplasma Laidlawii* Membranes as Determined by Deuterium Magnetic Resonance of Biosynthetically-Incorporated Specifically-Labeled Lipids, *Bioch. Acta* 401:535-539 (1975)

Straubinger, R.M., Hong, K., Friend, D.S., Papahadjopoulos, D., Endocytosis of Liposomes and Intracellular Fate of Encapsulated Molecules, *Cell* 32:1069-1079 (1983)

Szoka, F.C., Jacobson, K., Derzko, Z., Papahadjopoulos, D., Fluorescence Studies on the Mechanism of Liposome-Cell Interactions In Vitro, *Bioch. Bioph. Acta*, 600:1-18 (1980)

Szoka, F.C., Magnusson, K-E., Wojcieszyn, J., Hou, Y., Derzko, Z., Jacobson, K., Use of Lectins and Polyethylene Glycol for Fusion of Glycolipid Containing Liposomes with Eukaryotic Cells, *Proc. Nat. Acad. Sci. USA*, 78:1685-1689 (1981)

Tanaka, T., Taneda, K., Kobayashi, H., Katsuhiko, O., Muranishi, S., Sezaki, H., Application of Liposomes to the Pharmaceutical Modification of the Distribution Characteristics of Drugs in Rat, *Chem. Pharm. Bull.* 23:3069-3074 (1975)

- Tanaka, H., Saba, T.M., Mayron, L.W., Kaplan, E., Phagocytosis of Gelatinized "RE Test Lipid Emulsions" by Kupffer Cells, *Exp. Mol. Pathol.* 25:189 (1976)
- Thomas, P., Birbeck, M.S.C., Cartwright, P., A Radioautographic Study of the Hepatic Uptake of Circulating Carcinoembryonic Antigen by the Mouse, *Biochem. Soc. Trans.* 5:312-313 (1977)
- Thomas, P., Summers, J.W., The Biliary Excretion of Circulating Asialoglycoproteins in the Rat, *Bioch. Bioph. Res. Commun.* 80:335-339 (1978)
- Tryfiates, G.P., Activation and Protection from 5-Fluorodeoxyuridilate Inactivation of Mammalian Thymidylate Synthetase by Pyridoxal 5'-Phosphate, *Enzyme* 25:356-360 (1980)
- Tyrell, D.A., Heath, T.D., Colley, C.M., Ryman, B.E., New Aspects of Liposomes, *Bioch. Bioph. Acta*, 457:259 (1976)
- Vannotti, A., The Role of the Reticuloendothelial System in Iron Metabolism, in: *Physiopathology of the RES*, ed. Halpern, B.N., Charles Thomas Publ., Springfield, Ill. (1957)
- Washlien, W., Santi, D.V., Assay of Intracellular Free and Macromolecular-Bound Metabolites of 5-Fluorodeoxyuridine and 5-Fluorouracil, *Cancer Research*, 39:3397-3404 (1979)
- Wataya, J., Santi, D.V., Active Site Labeling of Thymidylate Synthetase with 5-Fluoro-2'-deoxy-uridilate, *Methods in Enzymology* 46:307-312 (1972)
- Wataya, Y., Hayatsu, H., Effect of Amines on the Bisulfite-Catalyzed Hydrogen Isotope Exchange at the 5 Position of Uridine, *Biochemistry* 11:3583-3588 (1972)
- Weibel, E.R., Straubli, W., Gnagi, H.R., Hess, E.A., Correlated Morphometric and Biochemical Studies on the Liver Cell: Morphometric Model, Stereologic Methods and Normal Morphometric Data for the Rat Liver, *J. Cell Biol.* 42:68 (1969)
- Windler, E., Chao, Y., Havel, R.J., Regulation of the Hepatic Uptake of Triglyceride-Rich Lipoproteins in the Rat, *J. Biol. Chem.* 255:8303-8307 (1980)
- Wisse, E., An Electron Microscopic Study of the Fenestrated Endothelial Lining of Rat Liver Sinusoids, *J. Ultrastruct. Res.* 31:125-150 (1970)
- Wisse, E., Gregoriadis, G., Daems, W.T., Electron Microscopic Cytochemical Localization of Intravenously Injected Liposomes Encapsulating Horseradish Peroxidase in Rat Liver Cells, in *The Reticuloendothelial System in Health and Disease*, ed Reichard, S.M., Escobar,

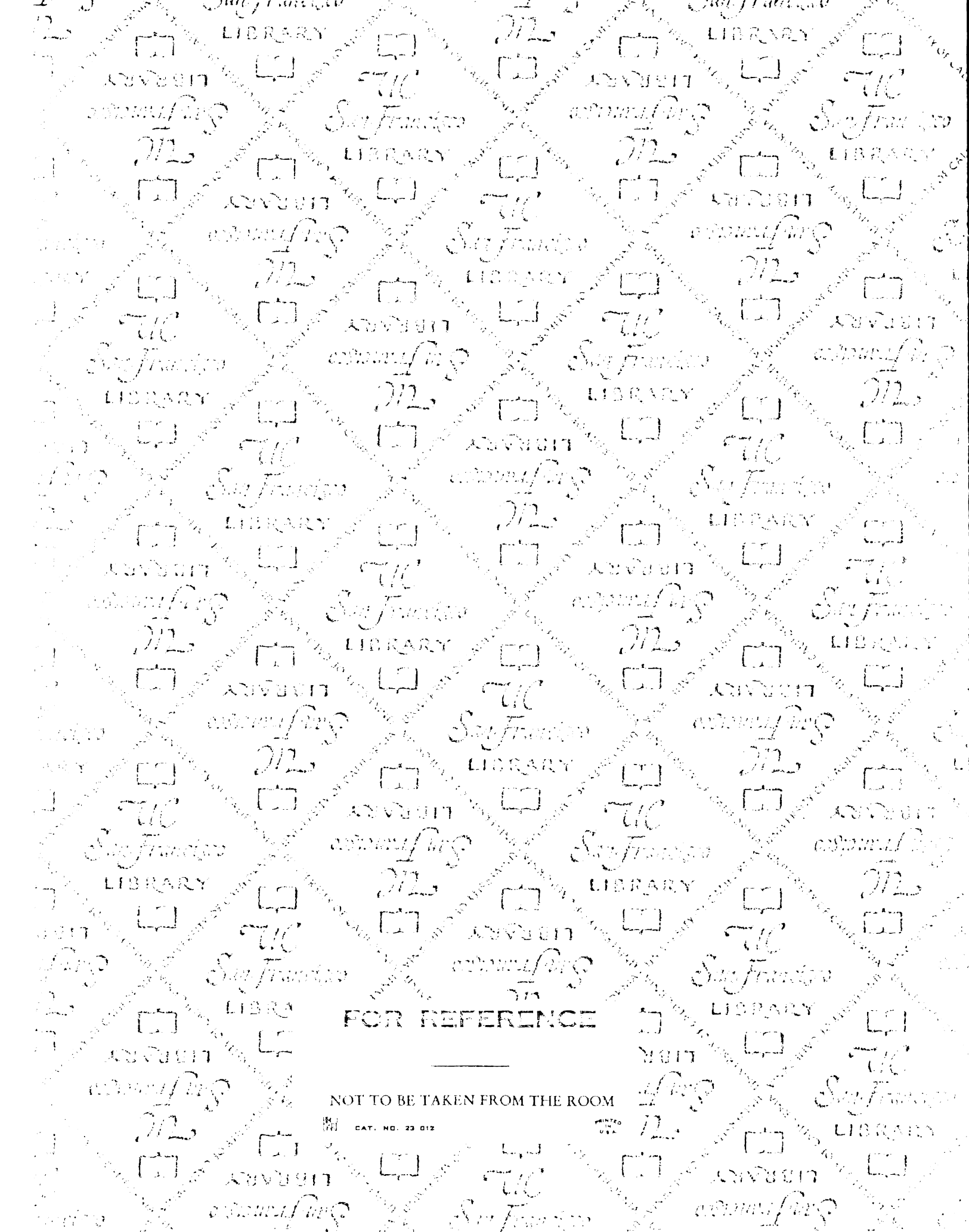


M.R., Friedman, H., Plenum Press, N.Y. pp 237-245  
(1976)

Wisse, E., in Kupffer Cells and Other Liver Sinusoidal  
Cells, ed. Wisse, E., Elsevier/North Holland Biomedical  
Press, pp 33-60 (1977)

Yatwin, M.B., Clinical Prospects for Liposomes, Med.  
Phys. 9:149-175 (1982)





FOR REFERENCE

NOT TO BE TAKEN FROM THE ROOM

CAT. NO. 23 012

